

MANEUVER REGULATION, TRANSVERSE FEEDBACK LINEARIZATION
AND ZERO DYNAMICS

by

Christopher Nielsen

A thesis submitted in conformity with the requirements
for the degree of Masters of Applied Science
Graduate Department of Electrical and Computer Engineering
University of Toronto

Copyright © 2004 by Christopher Nielsen

Abstract

Maneuver Regulation, Transverse Feedback Linearization and Zero Dynamics

Christopher Nielsen

Masters of Applied Science

Graduate Department of Electrical and Computer Engineering

University of Toronto

2004

The maneuver regulation (or path following) problem has received considerable attention in the control literature where feedback linearization has proven an effective approach to solving the problem. This thesis presents a general synthesis method for designing path following controllers for a class of systems using the concept of transverse feedback linearization. The relationship between maneuver regulation, transverse feedback linearization, and zero dynamics is explored. An output stabilization problem is solved, which under suitable conditions, also solves a maneuver regulation problem.

Dedication

This work is dedicated to my loving and supportive family. Thank you all so much, you continue to inspire and motivate me even after all these years. I would be nowhere without all of you.

I'd especially like to dedicate this work to my newborn nephew Tristan. I hope to someday share the beauty of the subject contained in these pages with you.

Acknowledgements

I would like to thank first and foremost, Dr. Manfredi Maggiore, my supervisor, for his many suggestions and constant support during this research. I would also like to thank him for giving me the opportunity to work with him and be a part of the Systems Control Group at the University of Toronto. Dr. Maggiore's enthusiasm for control theory is infectious and inspiring.

I must acknowledge the influential and significant contributions to my understanding of the maneuver regulation problem provided by the work of Dr. John Hauser and Dr. Andrzej Banaszuk. The results presented in this document were inspired by their work, for this I am indebted to them.

I would be remiss if I did not acknowledge the various people who have helped me reach this point in my research. Dr. Mireille Broucke and Dr. Bruce Francis for providing valuable insight. Dr. Raymond Kwong and Dr. Raviraj Adve, who along with Dr. Francis form my thesis committee. Dr. Dwight Aplevich for introducing me to control systems research in my undergraduate days at the University of Waterloo. Finally, the various students and visiting scholars in the systems control group with whom I've had a chance to share ideas and interact in a most meaningful way during this year and a half.

Contents

Contents	vi
Introduction	1
1 Literature Review	5
1.1 Inversion Based Controllers	5
1.2 Path Coordinates	6
1.3 Path Following from Trajectory Tracking	10
1.4 Partial Feedback Linearization and Output Regulation	11
1.5 Implementations of Maneuver Regulation Controllers	13
2 Problem Formulation	15
2.1 Required assumptions and framework	16
2.2 Problem Statement	23
2.3 Single output systems	25
2.4 Zero dynamics algorithm	26
3 Main Results	29
3.1 Solution to Problem 2	29
3.2 Linear Time Invariant Systems	38
3.3 Solution to Problem 3	42
3.4 State Maneuvers	47

3.5	On Relative Degree	50
3.5.1	The case $p = 2$	50
3.5.2	The case $p > 2$	53
4	Applied Transverse Feedback Linearization	57
4.1	Kinematic Unicycle	58
4.1.1	Following a circular path	58
4.1.2	Following arbitrary paths	61
4.2	Rear-wheel driving car-like robot	65
4.2.1	Following arbitrary paths	66
4.2.2	Following paths generated by 4 th order splines	68
4.3	Kinematic Hovercraft	70
4.3.1	Following arbitrary paths	72
4.3.2	Following paths generated by 4 th order splines	74
4.4	1-trailer Systems	75
4.4.1	Following a sinusoid	76
4.4.2	Characterizing Γ^*	77
4.4.3	Checking Relative Degree	85
4.4.4	Involutivity	85
	A Basic Concepts	90
	Bibliography	96

List of Figures

1.1	Frennet-Serret Frames	8
2.1	Example of a curve which is not regular	17
2.2	Example of a curve which is not proper	17
2.3	Example of a curve which is not injective	17
2.4	Schematic representation of single input, multiple output systems	19
2.5	Example 2.1.2: phase curves in the state space.	22
2.6	Valid neighborhood of Γ^* for global tranverse feedback linearization	25
2.7	Valid neighborhoods of Γ^* for local transverse feedback linearization	25
3.1	Transverse linear controllability when $n^* = 2$	33
3.2	Depiction of the proof of Theorem 3.1.4	36
3.3	Example 3.1.1: phase curves in output coordinates.	38
4.1	Unicycle coordinates	58
4.2	Kinematic Unicycle: Phase curves in output coordinates of a unicycle system following a circle	60
4.3	Maneuver regulation for the unicycle with forward velocity $v = 1$	62
4.4	Geometric interpretation of condition (4.5).	64
4.5	Kinematic state space variables of a car-like robot	65
4.6	A typical spline curve in \mathbb{R}^2	69
4.7	Example 4.2: Phase curves in output coordinates of Car-like vehicle following a 4 th order (C^3) curve	71
4.8	Kinematic Model of a Hovercraft.	72

4.9	Hovercraft output trajectories following an approximation of the Lake Ontario coast line near	
4.10	Kinematic model of the Standard 1-trailer.	76
4.11	Gridding a two dimensional manifold.	81
4.12	The value of $L_g L_f H_0$ over a uniform 2-dimensional grid of M_1^c	82
4.13	The value of the functions defining $H_2(x)$ generated by a uniform gridding of Γ^*	83
4.14	The value of $L_g L_f^2 h$ along a uniform gridding of Γ^*	84
4.15	Output of the trailer system (4.13) generated by a uniform gridding of Γ^*	84
4.16	Numerically checking transverse linear controllability in a neighborhood of Γ^*	86
A.1	An n -dimensional slice of $U \subset M$	91
A.2	An example of the tangent space at a point $p \in M$	91
A.3	Example of an integral manifold in \mathbb{R}^3	94
A.4	A foliation by integral submanifolds.	95

Introduction

The subject of this thesis is output maneuver regulation. Maneuver regulation is also known as 'path following' and as such, the two terms will be used interchangeably throughout this work. The output maneuver regulation problem can be stated as: given a system, find, if possible, a feedback making the system's *output* approach and move along a given curve (path or maneuver) with no associated timing law from an initial condition on or off the path. State maneuvers are a special case of output maneuvers where the desired maneuver is defined in the state space. In this work, the term maneuver regulation will be used with the understanding that output maneuver regulation is implied.

Given a path to be followed, a maneuver regulation controller forces output trajectories of the system to approach and slide along the path. The maneuver regulation controller does not have a timing law it must adhere to. The controller's main task is to steer the system along the path at some speed (bounded from away zero), chosen according to a set of specifications, or imposed by system dynamics.

In this setting, the maneuver regulation problem is more general than the trajectory tracking problem. In a trajectory tracking problem, the path to be followed is given a *specific time parametrization*. The tracking controller tries to make the system's state keep up with a reference point along the path whose time parametrization is usually imposed. On the other hand, a maneuver regulation controller drives the trajectories of a system to a maneuver *up to time re-parametrization*. Thus a single maneuver gives rise

to an infinite set of trajectories [24].

The difference between trajectory tracking and maneuver regulation is crucial for many robotics and aerospace applications where system dynamics impose constraints on the time parametrization of feasible maneuvers. For these systems, cases exist where a trajectory tracking problem is unsolvable yet the associated maneuver regulation problem does admit a solution (consider, for instance, the problem of maneuvering a wheeled vehicle with bounded maximum translational speed by means of steering). A trajectory tracking controller does not make the desired path an invariant set. This has practical implications for applications in which it is more important to faithfully re-create a motion in the state or output space than it is to track a timed reference trajectory. For these situations, a maneuver regulation controller is better suited. In order to further motivate the study of maneuver regulation we now present a pair of relevant application examples. The purpose of these examples is to illustrate situations where maneuver regulation is preferable to trajectory tracking.

Example : Cutting Tool

Consider the application of maneuver regulation controllers to an industrial cutting tool. In this application, it is desirable to approach the cutting area as quickly as possible. In the frame work of maneuver regulation, this is the task of approaching the path. Once on the surface to be machined, it is desirable to control the speed of cutting depending on the material being cut and to ensure quality edges. In the framework of maneuver regulation, this is the task of traversing the path. In other words, the task of controlling the dynamics on the path. Maneuver regulation controllers allow us to decouple these tasks and design controllers that meet both the approach specifications and the cutting specifications. This decoupling is harder to accomplish with trajectory tracking controllers.

Example : Intelligent Wheelchair

Consider the application of maneuver regulation controllers to an automated wheelchair. It is not difficult to imagine a situation where the wheelchair user enters a tightly confined

space, for example to use a wash room. In this situation a maneuver regulation controller based on the approach presented in this thesis could be quite effective. In this case, the intelligent wheelchair could simply remember the path the user followed to enter the wash room. Then, in order to leave the confined area the controller presented here would be used (it could be difficult to manually re-trace ones path *backwards*). Since the wheelchair is, by construction, starting on the path, a great advantage of our controller is that it guarantees the wheelchair remains on the path as it maneuvers backwards out of the tight area thus avoiding possibly harmful collisions. Tracking controllers do not make the desired path invariant, thus, in the situation described above, a tracking controller may lead to collisions in tight areas.

This work treats the maneuver regulation problem as an output stabilization problem. We solve an output stabilization problem, which with some extra conditions, solves the maneuver regulation problem. This approach admits a synthesis method for designing path following controllers for a class of systems and was inspired by the work of Banaszuk and Hauser [8]. It is based on the well-known concept of feedback linearization modified for the purposes of path following. The specific problem studied in this thesis is a special case of the following more general problem.

Problem 1: *Consider a control system with state defined on a manifold M and output defined on a manifold N*

$$\begin{aligned} \dot{x} &= f(x, u) \\ y &= h(x) \end{aligned} \tag{1}$$

where $f : M \times \mathbb{R}^m \rightarrow TM$ is a C^∞ vector field and the mapping $h : M \rightarrow N$.

Given a parameterized path $\sigma : \mathbb{D} \rightarrow N$, where \mathbb{D} is either \mathbb{R} or S^1 , find a smooth feedback control law $\bar{u} : M \rightarrow \mathbb{R}$ such that the controlled system (1) enjoys the following properties:

(i.) $y(t) \rightarrow \sigma(\mathbb{D})$ as $t \rightarrow \infty$.

(ii.) $\|\dot{y}\| \geq d > 0$.

(iii.) Let $x^0 = x(0)$

$$\left(\begin{array}{l} y(0) = h(x^0) \in \sigma(\mathbb{D}) \\ \dot{y}(0) \in T_{h(x^0)}\sigma(\mathbb{D}) \end{array} \right) \Rightarrow (\forall t \geq 0) y(t) \in \sigma(\mathbb{D}).$$

Condition (i.) guarantees the output trajectories approach the desired path. Condition (ii.) ensures path traversal and condition (iii.) asks that the path be invariant under (1). The focus of this thesis is on solving Problem 1 for the case when the system to be controlled is a nonlinear, control affine, time invariant system with $m = 1$.

More specifically, the problem considered here investigates systems with outputs and extends the results of Banaszuk and Hauser [8] to the case of non-periodic maneuvers defined in the output space (rather than periodic maneuvers in the state space). The main challenge here lies in finding conditions for feedback linearization of dynamics transverse to an embedded submanifold of the state space whose dimension is not restricted to be one. A natural way to study this problem is to use the notion of zero dynamics.

This thesis is organized as follows. Chapter 1 contains a brief literature review. Chapter 2 establishes the framework of this thesis, various required assumptions are introduced. Once the appropriate assumptions have been established, we are ready to formally introduce Problems 2 and 3, which are the main focus this work. This structure aids in understanding that solving Problems 2 and 3, under the appropriate assumptions, solves Problem 1.

Chapter 3 presents necessary and sufficient conditions for solving Problems 2 and 3 in Theorems 3.1.1 and 3.3.1 respectively. More constructive results, useful for controller design, are presented in Theorems 3.1.4 and 3.3.3. Chapter 4 applies the results of Chapter 3 to solve the maneuver regulation problem for various kinematic systems.

Chapter 1

Literature Review

The preceding decade has seen considerable effort and attention paid to motion control problems, specifically with regards to autonomous vehicles. The problems of motion control addressed in the literature may be broadly classified into three groups : a) point stabilization b) trajectory tracking c) maneuver regulation [30]. Of these three, maneuver regulation has received comparatively less attention than stabilization and tracking. This chapter presents a sampling of some of the more significant works recently published. The aim is to give a global overview of some existing techniques used to solve the maneuver regulation problem and point out some advantages and drawbacks for each.

1.1 Inversion Based Controllers

Motion (path) planning and open-loop control are equivalent in the context of maneuver regulation. These terms imply open-loop or feed-forward controllers. These techniques have been referred to as *dynamic inversion* by Hauser and Hindman [25] and Consolini *et al.* [16, 15] or the *Problem of Reproducing the Reference Output* by Isidori [26]. In this approach, the set of desired trajectories in the output space are used to determine the precise inputs which allows for perfect reproduction.

This is a particularly useful approach for systems which are differentially flat. Fliess

et al. define a system to be differentially flat if its entire state and control signals can be expressed in terms of the output and a finite number of its derivatives [21]. The flatness property means that the desired maneuver in the output space completely specifies the desired states and control inputs required to follow the path.

The obvious drawback of a pure motion planning solution is that it requires that the initial state of the system be compatible with the desired path and it is not robust against disturbances or uncertainties. Due to these concerns the majority of control schemes which employ motion planning also include feedback in order to improve robustness of the closed loop system. Not surprisingly, De Luca *et al.* observed that integration of path planning and feedback control design yields better tracking performance [32].

The controller proposed by Sørдалen and de Wit [40] is not based on dynamic inversion, yet employs both path planning and feedback in its design. Sørдалen and de Wit investigate the control of a nonholonomic unicycle. In their approach, a piecewise continuous feedback controller is designed which stabilizes the unicycle to an arbitrary position and posture in the state space. The stabilizing controller is then combined with a path planner which solves the maneuver regulation problem as a series of point stabilizations. This approach only works for paths which can be constructed using circles and straight lines. The result of this design is a switching or hybrid controller. Aicardi *et al.* [2] use a similar approach on a unicycle represented in polar coordinates, solving the path following problem as a series of point stabilizations.

1.2 Path Coordinates

One of the most common approaches to solving the maneuver regulation problem is the use of Frenet-Serret frames, often referred to as path coordinates. Path coordinates are used to transform the path following problem into a stabilization problem. Like trajectory tracking, this approach entails the convergence of a system's state to a prescribed state.

Instead of being a pre-assigned function of time, the desired state is a function of the configuration of the vehicle with respect to the path.

A Frenet - Serret frame is an orthonormal basis for \mathbb{R}^3 which moves along the path. Its evolution, as a function of the path parametrization, is completely determined by the curvature and torsion of the path via the Frenet-Serret formulas. Given a regular curve $t \mapsto x(t)$, $x : \mathbb{R} \rightarrow \mathbb{R}^3$, we next show how to construct the associated Frenet-Serret frame.

We begin by defining the arc length of the curve from a fixed point $x_0 = x(t_0)$,

$$s = \int_{t_0}^t \|\dot{x}(t)\| dt \quad (1.1)$$

where $\|\cdot\|$ denotes Euclidean norm. By definition, a regular curve is such that $\forall t \in \mathbb{R}$, $\|\dot{x}(t)\| \neq 0$. It can be shown that this condition implies that the mapping $t \mapsto s$ defined by (1.1) is a diffeomorphism of \mathbb{R} onto its image. Its inverse $s \mapsto t$ can be used to define an arc length (or unit speed) reparametrization for the curve, $s \mapsto x(s)$. After such a re-parametrization, one has that

$$s = \int_0^s \|\dot{x}(s)\| ds$$

which implies that $\|\dot{x}(s)\| = 1$ for all s . In other words, the tangent vector, $T(s) := \dot{x}(s)$, to a unit speed curve, is a unit vector. By differentiating the expression

$$\langle T(s), T(s) \rangle = 1$$

with respect to s , one immediately gets that $\langle \frac{dT(s)}{ds}, T(s) \rangle = 0$. It can be shown that $\left\| \frac{dT(s)}{ds} \right\| = k(s)$ where $k(s)$ denotes the unsigned curvature of the curve. A necessary and sufficient condition for a plane curve to be a straight line is that $\forall s \in \mathbb{R}$, $k(s) = 0$. Assuming $k(s) \neq 0$, let $N(s) := \frac{1}{k(s)} \frac{dT}{ds}$, and $B(s) = T(s) \times N(s)$. The resulting orthonormal frame $\{T, N, B\}$ is the Frenet-Serret frame associated to the curve in question, see Figure 1.1.

For vehicle systems, the maneuver regulation problem can be solved by finding a coordinate transformation which represents a system's dynamics in terms of a Frenet-Serret

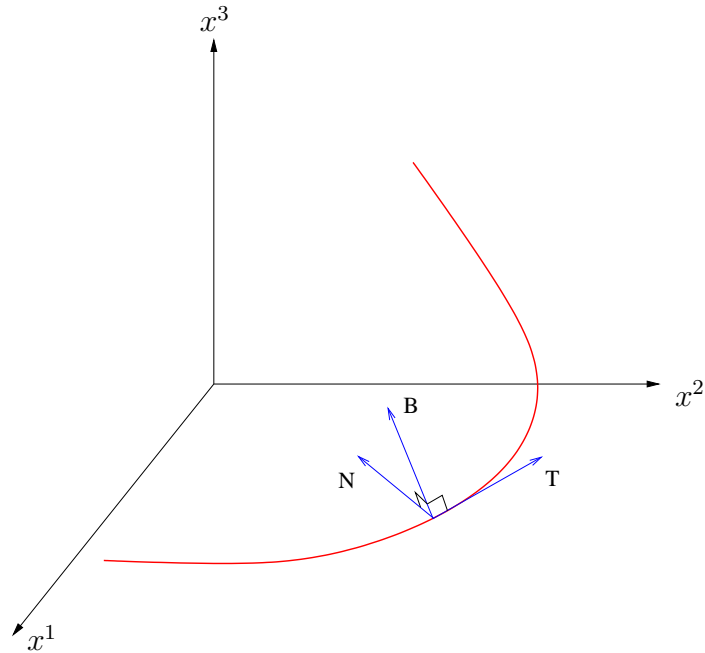


Figure 1.1: Frennet-Serret Frames

frame. The transformation gives the arc length parameter s of the curve to be followed as a function of the system's position relative to the curve. The arc length parameter s describes the *unique* location on the desired path which minimizes the distance from the system to the path. Once in path coordinates, the controller's objective is to stabilize to zero the system's dynamics in the direction of the vector $N(s)$ and $B(s)$.

There are a wide variety of works which employ path coordinates in order to solve the path following problem. DeSantis [18] employs path coordinates to solve a path following problem for a trailer system following circular paths and straight lines. Even though Frenet-Serret frames are defined only in \mathbb{R}^3 , the author is able to apply them to higher dimensional systems by considering $n - 1$ simultaneous frames, one for each trailer. This is possible since the desired path lies in \mathbb{R}^2 where Frenet - Serret frames are defined.

Canudas de Wit *et al.* use path coordinates to solve the maneuver regulation problem for the unicycle [17]. Encarnação and Pascoal [19] apply path coordinates to a three dimensional path. They are interested in path following for autonomous underwater

vehicles. When the path is 3-D, a higher dimensional subsystem must be stabilized.

Samson combines the use of path coordinates with the chain form for nonholonomic systems [43]. He applies this approach to the control of a trailer system. A general nonholonomic control system, expressed in kinematic form, is given by

$$\dot{x} = \sum_{i=1}^m g_i(x)u_i.$$

When $m = 2$, the chain form is given by

$$\begin{aligned}\dot{z}_1 &= y_1 u_2 \\ \dot{z}_2 &= z_1 u_2 \\ &\vdots \\ \dot{z}_{n-2} &= z_{n-3} u_2 \\ \dot{y}_1 &= u_1 \\ \dot{y}_2 &= u_2\end{aligned}$$

The trailer system which Samson considers falls under this class, however extensions exist for the case $m > 2$. The approach of Samson is to represent the trailer system in path coordinates and then apply a second state and control transformation to put the trailer into chained form.

Chain form does not alter the essential properties of path coordinates. The maneuver regulation problem still reduces to a stabilization problem except that the chain form simplifies the control design. This approach requires that both inputs be used and no degrees of freedom left to assign path dynamics.

Finally a more recent result from Astolfi *et al.* [7] considers the problem of making a lead trailer follow circular and rectilinear paths. They follow the approach of DeSantis [18] decoupling longitudinal velocity control and steering control. This differs from Samson's approach of using the chain form where both inputs were required. Astolfi *et al.* use a Lyapunov based control law which allows for maneuver regulation solution in the forward, backward direction and a precise characterization of the region of convergence.

Path coordinates represent a natural approach to path following. This approach is suitable for situations in which the desired path is embedded in \mathbb{R}^3 and thus it is popular in automotive applications. For more general paths embedded in higher dimensional space, this approach is not suitable. Path coordinate solutions demonstrate that the maneuver regulation problem is simplified by the appropriate choice of coordinate system. This partially motivates the solution presented in this thesis.

1.3 Path Following from Trajectory Tracking

The maneuver regulation problem has been greatly influenced by a paper by Hauser and Hindman [24]. In this work, the authors present a constructive and analytical method for properly selecting a time re-parametrization for tracking control laws to solve the maneuver regulation problem. Hauser and Hindman find a mapping which converts a trajectory tracking control law into a maneuver regulation control law.

The novel idea presented is to take an existing tracking law, and redefine the trajectory time to be the value obtained from the mapping. The redefined time corresponds to the point on the maneuver closest to the current state. The authors present a solution for systems which are *feedback linearizable*. They focus on feedback linearizable systems since these are systems for which the tracking problem can be solved using a static feedback control law.

In addition to formally proving the existence of such a mapping, Hauser and Hindman provide an algorithmic and numerically robust method for calculating the value of the mapping which is suitable for real-time implementation. This paper gives theoretical insight into the relationship between trajectory tracking and maneuver regulation. Although initially unheralded, the results of [24] has recently spurred much new work in the area of maneuver regulation.

Encarnaç o and Pascoal [20] use the ideas of Hauser and Hindman to solve the ma-

maneuver regulation problem for *fully actuated* autonomous underwater vehicles. The main extension provided by the work of Encarnação and Pascoal is to apply the results from [24] for dynamic models by using backstepping. That is, they work with system models which are not purely kinematic. Al-Hiddabi and McClamroch [3] design tracking controllers for nonlinear non-minimum phase systems and then apply the results from [24] to convert their tracking control law into a maneuver regulation control law. They apply the results to a planar vertical takeoff and landing (PVTOL) aircraft.

More recently, work by Skjente *et al.* [44] uses the results of [24] to solve the output maneuver regulation problem. The work of Skjente *et al.* approaches the maneuver regulation problem from a general perspective for a class of systems. In this regard, their work is similar to the work presented here. The authors in [44] divide the maneuver regulation problem into two tasks, geometric and dynamic. The geometric task is to approach the desired path. The dynamic task consists of satisfying a time, speed or acceleration requirement *on* the desired maneuver. This is an interesting and novel way of looking at the path following problem. This two-task view of the problem is useful when considering the practical implementation of maneuver regulation controllers.

Since Skjente *et al.* are using the results of [24], it follows that the main drawback of this approach is that it requires the system be feedback linearizable. The authors consider uncertain models, but nevertheless require that system have a vector relative degree of n . In general, this may be quite restrictive.

1.4 Partial Feedback Linearization and Output Regulation

Partial feedback linearization (or input - output linearization) as presented by Isidori [26] represents a natural framework for solving the maneuver regulation problem. This is evidenced by the body of work on path following which employs this method (see for

example Altafini [5, 6], Coelho and Nunes [14], Bolzern *et al.* [11] and Banaszuk and Hauser [8, 9]). The work of this thesis is based on the results of Banaszuk and Hauser [8] and so it falls within this category.

Banaszuk and Hauser [8] approach the maneuver regulation problem from a general viewpoint thus representing an attractive starting point for this work. Banaszuk and Hauser solve the state maneuver regulation problem for periodic orbits. They provided necessary and sufficient conditions for generating a coordinate and feedback transformation which linearizes the dynamics transverse to the desired maneuver. This is useful in facilitating a simple solution to the geometric task of the path following problem.

Bolzern *et al.* [11] work with the n -body trailer system. They solve a maneuver regulation problem when the output of the system is the mid-point of the front vehicle's axle. The trailer system they consider has off-axle hitching and so it is not differentially flat as in [21]. Bolzern *et al.* generate a so-called 'offset model' of the trailer system similar to path coordinates. They show that by using lateral offset (i.e. the lateral distance from guide point to path) as an output, they can stabilize these dynamics and solve the path following problem. This is a specific application of the general framework in which we solve the path following problem. The work of Bolzern *et al.* is important with regards to the work presented here. These types of works help motivate the need to generalize and formalize the use of input - output linearization for path following.

We conclude this section by discussing an interesting approach to solving the maneuver regulation problem presented by Altafini [5]. Altafini casts the maneuver regulation problem as an output regulation problem. He considers the general n -trailer and models it in path coordinates. In path coordinates, the trailer is input - output linearized and then the regulation problem is solved on the partially linearized system. The regulation controller tries to asymptotically stabilize the trailer to paths whose curvature is regarded as a *persistent disturbance* produced by an exosystem. Note that the position of each trailer is embedded in \mathbb{R}^2 . As such, the curvature function completely specifies

the desired path up to congruence [12].

The main drawback of Altafini's solution is his reliance on path coordinates. As pointed out earlier, if the desired path is embedded in \mathbb{R}^4 path coordinates do not apply. In addition, the curvature function of the desired path must be neutrally stable [26]. This requirement restricts the class of maneuvers which can be followed using this technique. Despite these problems, this approach is very appealing for its theoretical and practical significance. Although beyond the scope of this thesis, it would be fruitful to investigate this approach for a more general class of systems.

1.5 Implementations of Maneuver Regulation Controllers

Here we discuss some experimental results published in the area of path following. The aim is to give the reader an idea of the methodology used in implementing path following controllers and highlight some fascinating application examples.

Nelson and Cox [34] discuss an early implementation for industrial car-like robots. Position is sensed using odometry, i.e., by knowing the starting point (initial conditions) relative to a known workspace, the system is able to extrapolate its location. This implementation is based on a path planner and feedback similar to [2, 40]. The path is traversed as a series of point stabilizations.

Sampei *et al.* [42] report an experimental implementation of a path following controller for a trailer system. This implementation relies on path coordinates and only works for desired paths which are straight lines, but it works in both forward and reverse directions. Sampei *et al.* work with the standard trailer system of Fliess *et al.* and so it is possible to apply dynamic feedback linearization to the system.

We conclude this chapter by discussing the RABBIT bipedal robot [13, 37]. The RABBIT testbed represents one of the most elaborate experimental implementations

utilizing path following controllers. The path following controller is vital in ensuring a stable walking motion. This is a prime example of a situation where tracking controllers are not appropriate in order to remain in a desired region of operation. Since stability of the walking motion is the overriding concern in this application, path following controllers are better suited. Specifically, a path following controller is designed which guarantees that all of the phases of the walking motion are executed in *sequential order*. A tracking controller in the presence of an obstacle could lead to a phase being skipped and the entire walking motion becoming unstable. Specifically, if the motion of the robot becomes retarded in the presence of the obstacle, a tracking controller would try to catch up to its reference trajectory to regain synchrony which could lead to crashes. In this case it is more important to faithfully follow the maneuver than some time parametrization associated with a tracking law.

RABBIT's path following controller is based on converting a tracking law into a maneuver regulation law. The time scaling of the tracking law is parameterized by the bipedal robot's state and thus the controller bears some resemblance to the ideas of Hauser and Hindman [24]. The result is that when a disturbance affects the walking motion, the feedback controller focuses on maintaining the appropriate speed and limb position based on the current walking phase, and *not* time.

Chapter 2

Problem Formulation

This chapter contains the appropriate assumptions and formal problem statements which this thesis solves. The main purpose of this chapter is to describe the class of systems and class of paths under consideration and present Problems 2 and 3. We show that under the appropriate assumptions, solving these problems also solves a general maneuver regulation problem, Problem 1. The problem statements considered in this chapter are inspired by the work of Banaszuk and Hauser [8]. There, the authors consider periodic maneuvers in the state space and present necessary and sufficient conditions for feedback linearization of the associated transverse dynamics.

Section 2.1 defines the required assumptions and presents the class of system and path under consideration. Problems 2 and 3 are introduced in Section 2.2. Section 2.3 explains why systems with one dimensional outputs are not considered. Finally, Section 2.4 discusses the application of the zero dynamics algorithm to maneuver regulation.

2.1 Required assumptions and framework

Consider the smooth dynamical system

$$\begin{aligned} \dot{x} &= f(x) + g(x)u \\ y &= h(x) \end{aligned} \tag{2.1}$$

defined on \mathbb{R}^n , with $h : \mathbb{R}^n \rightarrow \mathbb{R}^p$ ($p \geq 2$) of class C^∞ , and $u \in \mathbb{R}$. We are given a smooth parameterized curve to follow, $\sigma : \mathbb{D} \rightarrow \mathbb{R}^p$, where \mathbb{D} is either \mathbb{R} or S^1 . When $\mathbb{D} = S^1$, σ is a periodic function with constant period $T_0 > 0$. Specifically, $(\forall t) \gamma(t) = \gamma(t + T_0)$. We impose geometric restrictions on the class of curves $\sigma(\cdot)$.

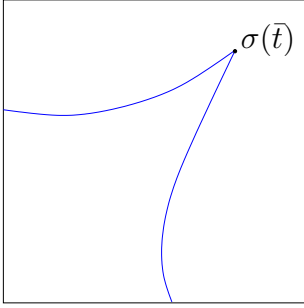
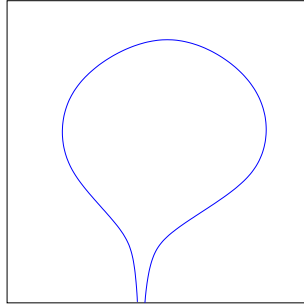
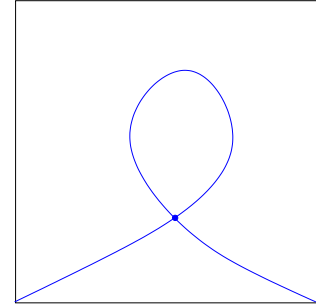
Assumption 1: The curve $\sigma : \mathbb{D} \rightarrow \mathbb{R}^p$ enjoys the following properties:

- (i) σ is C^r , ($r \geq 1$)
- (ii) σ is regular, i.e., $\|\dot{\sigma}\| \neq 0$
- (iii) $\sigma : \mathbb{D} \rightarrow \sigma(\mathbb{D})$ is injective (when $\mathbb{D} = S^1$ we instead require $\sigma(\mathbb{D})$ to be a Jordan curve)
- (iv) σ is proper, i.e. for any compact $K \subset \mathbb{R}^p$, $\sigma^{-1}(K)$ is compact (automatically satisfied when $\mathbb{D} = S^1$)

Assumption 1 guarantees that $\sigma(\mathbb{D})$ is a submanifold of \mathbb{R}^p with dimension 1. It should be noted that although this is a required assumption, it is not very restrictive. Assumption 1 precludes curves which have the properties depicted in Figures 2.1, 2.2, 2.3.

Assumption 2: There exists a C^1 map $\gamma : \mathbb{R}^p \rightarrow \mathbb{R}^{p-1}$ such that 0 is a regular value of γ and $\sigma(\mathbb{D}) = \gamma^{-1}(0)$. Moreover, the *lift* of $\gamma^{-1}(0)$ to \mathbb{R}^n , $\Gamma := (\gamma \circ h)^{-1}(0)$, is a submanifold of \mathbb{R}^n .

Since the path σ is given as a parameterized curve, the first part of Assumption 2 can always be satisfied locally. The assumption requires that the *entire* path can be

Figure 2.1: $\dot{\sigma}(\bar{t}) = 0$ Figure 2.2: Improper σ Figure 2.3: σ not injective

represented as the zero level set of the function γ . With regards to the second part of Assumption 2, a sufficient condition for

$$\Gamma = \{x : \gamma_1(h(x)) = \dots = \gamma_{p-1}(h(x)) = 0\} \quad (2.2)$$

to be a submanifold of \mathbb{R}^n is that h be *transversal* to $\gamma^{-1}(0)$, i.e., [1, 23]

$$(\forall x \in \Gamma) \quad \text{Im}(dh)_x + T_{h(x)}\gamma^{-1}(0) = \mathbb{R}^p. \quad (2.3)$$

We have $\dim \Gamma = n - p + 1$ [15]. The problem of maneuvering y to $\gamma^{-1}(0)$ is thus equivalent to maneuvering x to Γ . Thus, the problem of maneuvering x to Γ has been cast as an output stabilization problem for the system

$$\begin{aligned} \dot{x} &= f(x) + g(x)u \\ y' &= (\gamma \circ h)(x). \end{aligned} \quad (2.4)$$

In general one may only be able to maneuver x to the subset of Γ which can be made invariant by a suitable choice of the control input. Accordingly, let Γ^* be the largest controlled invariant submanifold of Γ under (2.1) and let $n^* = \dim \Gamma^*$ ($n^* \leq \dim \Gamma = n - p + 1$). Further, let u^* be a smooth feedback rendering Γ^* invariant and define $f^* := (f + gu^*)|_{\Gamma^*}$. The following assumption, if satisfied, guarantees that by stabilizing the output of (2.4), the original system (2.1) will traverse a portion of the path and the

maneuver regulation problem is solved.

Assumption 3: Γ^* is a globally well defined, connected, parallelizable, closed submanifold (with $n^* \geq 1$) and the following conditions hold

- (i) $(\exists \epsilon > 0)(\forall x \in \Gamma^*) \quad \|L_{f^*}h(x)\| > \epsilon.$
- (ii) $f^* : \Gamma^* \rightarrow T\Gamma^*$ is complete.

In [8], $\Gamma^* = \Gamma = \sigma(S^1)$, and it is assumed that $f(x) = f^*(x) \neq 0$ on Γ^* . Thus in that work Assumption 3 is automatically satisfied. The completeness of f^* follows from the periodicity of $\sigma(S^1)$ which implies that Γ^* is compact [12, Corollary IV.5.6].

We first focus on the assumption that Γ^* be well defined. In order to derive conditions guaranteeing that Γ^* is well defined, associate with each constraint in (2.2) the single input, single output (SISO) system $\{f, g, \gamma_k \circ h\}$ where $k \in \{1, \dots, p-1\}$ and a corresponding zero dynamics manifold Γ_k^* .

Lemma 2.1.1. *If $\bigcap_k \Gamma_k^*$ is a closed, controlled invariant submanifold, then Γ^* exists and it is given by $\Gamma^* = \bigcap_k \Gamma_k^*$.*

Proof. (C) Choose any point $x \in \Gamma^*$. Since $\Gamma^* \subset \Gamma$,

$$(\forall k \in \{1, \dots, p-1\}) \quad \gamma_k(h(x)) = 0.$$

This, together with the fact that, by definition, Γ^* is locally invariant around x , implies that

$$(\forall k \in \{1, \dots, p-1\}) \quad x \in \Gamma_k^*$$

or $x \in \bigcap_k \Gamma_k^*$.

(D) Since $\bigcap_k \Gamma_k^*$ is controlled invariant and output zeroing, and since $\Gamma^* \subset \bigcap_k \Gamma_k^*$, one has that, by the maximality of Γ^* , $\Gamma^* = \bigcap_k \Gamma_k^*$. \square

Lemma 2.1.1 can be used to highlight a few important concepts regarding this framework. Consider the single input single output systems $\{f, g, \gamma_i \circ h\}$ with $i \in \{1, \dots, p-1\}$,

as introduced above. Although we consider each system separately, they are in fact related by having the same input. Figure 2.4 gives a schematic representation of the interaction between the outputs of the SISO systems and the lone input. By Assumption 2,

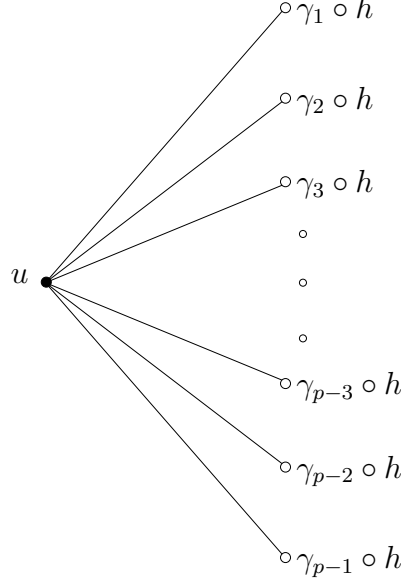


Figure 2.4: Schematic representation of single input, multiple output systems

Γ is the intersection of $p - 1$ zero level sets corresponding to simultaneous stabilization of the output of (2.4). Lemma 2.1.1 formalizes the intuition that it is insufficient to stabilize a subset of the outputs in order to be on Γ .

Let r_i be the relative degree of system $\{f, g, \gamma_i \circ h\}$ and define $\mathcal{H}_i : x \mapsto \text{col}(\gamma_i \circ h(x), L_f(\gamma_i \circ h(x)), \dots, L_f^{r_i-1}(\gamma_i \circ h(x)))$. If $\{r_1, \dots, r_{p-1}\}$ is well-defined (uniform) on \mathbb{R}^n , one has that each Γ_i^* is globally defined and given by $\Gamma_i^* = \mathcal{H}_i^{-1}(0)$. Even if $\bigcap_k \Gamma_k^*$ is nonempty, it may not be a submanifold. A sufficient condition for the intersection $\Gamma_i^* \cap \Gamma_j^*$, $i \neq j$, to be a submanifold is that [23]

$$(\forall x \in \Gamma_i^* \cap \Gamma_j^*) \quad T_x \Gamma_i^* + T_x \Gamma_j^* = \mathbb{R}^n$$

or, equivalently, $\ker(d\mathcal{H}_i)_x + \ker(d\mathcal{H}_j)_x = \mathbb{R}^n$. Using the fact that $T_x(\Gamma_i^* \cap \Gamma_j^*) = T_x \Gamma_i^* \cap T_x \Gamma_j^*$ one easily arrives at the following result.

Corollary 2.1.2. *Γ^* is a globally well defined closed submanifold if there exists a point*

$x_0 \in \Gamma$ around which each system $\{f, g, \gamma_i \circ h\}$, $i \in \{1 \dots p-1\}$ has a uniform relative degree r_i and, if $p > 2$, the following conditions are satisfied for $k = 1, \dots, p-2$.

(i) For $k = 1, \dots, p-2$,

$$\left(\forall x \in \bigcap_{j=1}^{k+1} \Gamma_j^* \right) H_x^k + \ker(d\mathcal{H}_{k+1})_x = \mathbb{R}^n,$$

where H_x^k is defined recursively as

$$H_x^1 := \ker(d\mathcal{H}_1)_x, \quad k = 1$$

$$H_x^k := H_x^{k-1} \cap \ker(d\mathcal{H}_k)_x, \quad k > 1.$$

(ii) Letting $u_k^* := -\frac{L_f^{r_k}(\gamma_k \circ h)}{L_g L_f^{r_k-1}(\gamma_k \circ h)}$, $1 \leq k \leq p-1$,

$$(u_1^*)|_{\cap_i \Gamma_i^*} = \dots = (u_{p-1}^*)|_{\cap_i \Gamma_i^*}.$$

In this case, $n^* = n - \sum_{i=1}^{p-1} r_i$.

Remark 2.1.1. Rather than using transversality to derive the sufficient conditions of Corollary 2.1.2, one can employ a slight modification of the zero dynamics algorithm of [27] (see also [26]) or the constrained dynamics algorithm presented in [36]. In both cases a feasible initial condition for the algorithm should be defined to be any point $x_0 \in \Gamma^*$ such that $f(x_0) + g(x_0)u_0 \in T_{x_0}\Gamma^*$ for some $u_0 \in \mathbb{R}$. If the sufficient conditions of Corollary 2.1.2 are not satisfied, the zero dynamics algorithm may still find a *locally* maximal controlled invariant submanifold of Γ . See Section 2.4 for more discussion on the zero dynamics algorithm.

The technical requirement that Γ^* be connected and parallelizable is needed in order to be able to generate a *global* basis for the tangent space of Γ^* . This assumption guarantees the existence of non-vanishing vector fields v_1, \dots, v_{n^*} , $v_i : \Gamma^* \rightarrow T\Gamma^*$, which span $T_x\Gamma^*$ at each $x \in \Gamma^*$ [12]. This is needed in some proofs of Chapter 3.

The condition, in Assumption 3, that $\|L_{f^*}h(x)\| > \epsilon$ on Γ^* implies that there are no equilibria on Γ^* and that, whenever $x \in \Gamma^*$, $\|y\| > \epsilon$. The result is an assurance that the

output of (2.1) traverses the curve $\sigma(\mathbb{D})$. The next example illustrates that this condition is not strictly necessary for the feasibility of the maneuver regulation problem.

Example 2.1.1. Consider the dynamical system and path

$$\dot{x} = \begin{bmatrix} x_2 \\ 0 \\ x_3 \end{bmatrix} + \begin{bmatrix} 0 \\ 1 \\ 0 \end{bmatrix} u$$

$$y = \text{col}(x_1, x_2), \quad \sigma : \lambda \in \mathbb{R} \mapsto \text{col}(\lambda, \lambda)$$

Here $\mathbb{D} = \mathbb{R}$ and $\sigma(\mathbb{D}) = \{y : y_1 - y_2 = 0\}$. The lift Γ is given by $\Gamma = \{x : x_1 - x_2 = 0\}$ and it is readily seen that $\Gamma^* = \Gamma$ and a smooth feedback rendering Γ^* invariant is $u^* = x_1$. Assumption 3 is not satisfied since there exists a single point on Γ^* where $L_{f^*}h(x) = \text{col}(x_2, x_1)$ is zero. Yet, almost all initial conditions on Γ^* result in path traversal. Specifically, the only case where the path is *not* traversed is when $x_1(0) = x_2(0) = 0$.

△

Example 2.1.1 shows that even if Assumption 3 is violated, it may still be possible to traverse the path. Example 2.1.1 also highlights the fact in the case of a linear time invariant system, Assumption 3 is always violated. This fact is shown in Chapter 3. If Assumption 3 is violated, i.e., if $L_{f^*}h(x) = 0$ for some $x \in \Gamma^*$, then the situation becomes problematic from the maneuver regulation point of view.

Example 2.1.2. Consider the dynamical system and path

$$\dot{x} = \begin{bmatrix} x_1 x_3 \\ \frac{-2x_1^2 x_3}{(x_1^2 + 1)^2} \\ x_3 \end{bmatrix} + \begin{bmatrix} 0 \\ 1 \\ 0 \end{bmatrix} u$$

$$y = \text{col}(x_1, x_2), \quad \sigma : \lambda \in \mathbb{R} \mapsto \text{col}\left(\lambda, \frac{1}{\lambda^2 + 1}\right)$$

Here $\mathbb{D} = \mathbb{R}$, $\Gamma = \Gamma^* = \{x : x_2 - \frac{1}{x_1^2+1} = 0\}$, and $u^* = 0$. Assumption 3 is not satisfied since

$$L_f h(x) = \text{col} \left(x_1 x_3, \frac{-2x_1^2 x_3}{(x_1^2 + 1)^2} \right)$$

is zero on the set $\{x : x_1 x_3 = 0\}$. Let $u = -x_2 + \frac{1}{x_1^2+1}$. The result is a closed-loop system where any initial condition

$$x^0 = \text{col}(\delta, *, \epsilon)$$

where $\epsilon\delta = 0$ will not result in path traversal. However, initial conditions where $\epsilon\delta \neq$

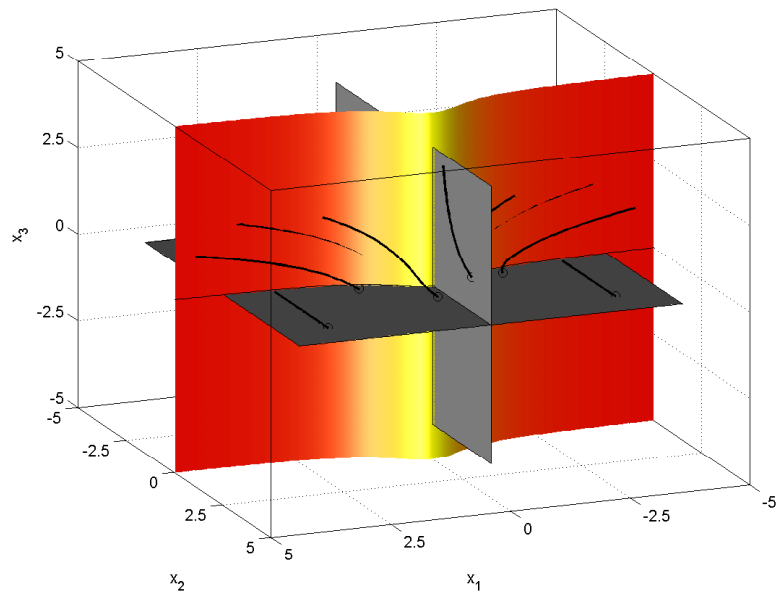


Figure 2.5: Example 2.1.2: phase curves in the state space.

0 will result in path traversal, see Figure 2.5. This example illustrates the fact that Assumption 3(i) avoids pathological situations whereby some phase curves originating outside of Γ^* may approach points of Γ^* where $L_{f^*}h = 0$, thus not traversing the path $\sigma(\mathbb{D})$.

2.2 Problem Statement

We are now ready to formulate the main problems investigated in this thesis. The following are a direct generalization of analogous problem statements found in [8].

Problem 2: *Find, if possible, a single coordinate transformation $T : x \mapsto (z, \xi) \in \Gamma^* \times \mathbb{R}^{n-n^*}$ valid in a neighborhood \mathcal{N} of Γ^* such that in (z, ξ) coordinates*

$$(i) \Gamma^* = \{(z, \xi) \in \Gamma^* \times \mathbb{R}^{n-n^*} : \xi = 0\}$$

(ii) *The dynamics of system (2.1) take the form*

$$\begin{aligned} \dot{z} &= f_0(z, \xi) \\ \dot{\xi}_1 &= \xi_2 \\ &\vdots \\ \dot{\xi}_{n-n^*-1} &= \xi_{n-n^*} \\ \dot{\xi}_{n-n^*} &= b(z, \xi) + a(z, \xi)u \end{aligned} \tag{2.5}$$

where $a(z, \xi) \neq 0$ in \mathcal{N} .

The following is the local version of Problem 2.

Problem 3: *For some $x^0 \in \Gamma^*$, find, if possible, a transformation $T^0 : x \mapsto (z^0, \xi^0) \in \Gamma^* \times \mathbb{R}^{n-n^*}$ valid in a neighborhood U^0 of $x^0 \in \Gamma^*$ such that in (z^0, ξ^0) coordinates properties (i) and (ii) of Problem 2 are satisfied in U^0 .*

Banaszuk and Hauser [8] provide a solution to these problems in the special case when $\mathbb{D} = S^1$ and $h(x) = x$ in (2.1).

Remark 2.2.1. It is clear that if one can solve Problem 2 or 3, then by choosing a feedback matrix K such that linear portion of (2.5) is Hurwitz, the smooth feedback

$$u = -\frac{1}{a(z, \xi)}(b(z, \xi) + K\xi). \tag{2.6}$$

achieves local stabilization to Γ^* and makes Γ^* invariant. However, (2.6) does not prevent the closed-loop system from exhibiting finite escape time (i.e., the entire $\sigma(\mathbb{D})$ is traversed

in finite time), even though the vector field of the closed-loop system is complete on Γ^* . A similar problem is encountered in feedback linearization when stabilizing a minimum phase system in normal form. There are various ways to modify (2.6) to avoid finite escape time. Discussing them is beyond the scope of this thesis.

The great advantage in linearizing the dynamics transversal to the desired set lies in our ability to use linear control techniques. Since we are essentially stabilizing a linear system, it becomes possible to, for example, stabilize to the set in optimal time.

We show that solving Problems 2 and 3, also solves Problem 1. We restate the specifications of Problem 1 under the current assumptions:

(i.) $y(t) \rightarrow \sigma(\mathbb{D})$ as $t \rightarrow \infty$.

(ii.) $\liminf_{t \rightarrow \infty} \|\dot{y}\| \neq 0$.

(iii.)

$$\left(\begin{array}{l} y'(0) = \gamma \circ h(x^0) = 0 \\ L_f(\gamma \circ h)(x^0) = 0 \end{array} \right) \Rightarrow (\forall t \geq 0) (\gamma \circ h)(x(t)) = 0.$$

Assume that a solution has been obtained to Problem 2 or Problem 3. We immediately obtain that part (i.) of Problem 1 can be satisfied since, as already noted, the controller (2.6) achieves output stabilization of (2.4), or, equivalently, stabilization of y to $\sigma(\mathbb{D})$. Note that y asymptotically approaches $\sigma(\mathbb{D})$, but never actually reaches it.

Part (ii.) is satisfied by Assumption 3. Finally, we show that a controller solving Problems 2 or 3 satisfies (iii.). If $(\gamma \circ h)(x^0) = 0$ and $(L_f(\gamma \circ h))(x^0) = 0$, then $x^0 \in \Gamma^*$. This is because $(\gamma \circ h)(x^0) = 0$ implies $x^0 \in \Gamma$, $(L_f(\gamma \circ h))(x^0) = 0$ implies $f(x^0) \in T_{x^0}\Gamma$ and thus $x^0 \in \Gamma^*$. Controller (2.6) makes Γ^* invariant, i.e., $(\forall t \geq 0), (\gamma \circ h)(x(t)) = 0$.

Remark 2.2.2. If Assumption 3(i) does not hold, then we have that the path is not traversed and the path following problem cannot be solved in this manner. Specifically, Problem 1, condition (ii.) is violated. In these cases, solving Problems 2 and 3 results in the solution to an output stabilization problem.

We refer to Problem 2 as global transverse feedback linearization (TFL). We seek a *single* coordinate and feedback transformation which is valid in a tubular neighborhood of Γ^* , not necessarily in all of \mathbb{R}^n . We refer to Problem 3 as *local* transverse feedback linearization. Here we seek several coordinate and feedback transformations, each valid over a neighborhood of a point on Γ^* , such that the union of a finite number of such neighborhoods contains Γ^* . See Figures 2.6 and 2.7.

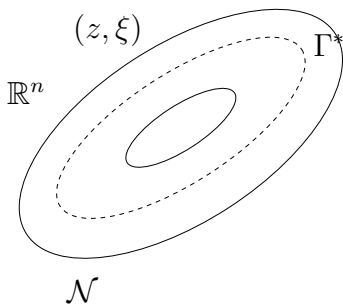


Figure 2.6: Global TFL

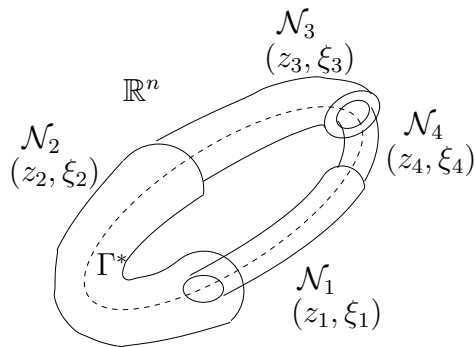


Figure 2.7: Local TFL

Problems 2 and 3 differ from standard input-output feedback linearization. Here we are interested in *designing* a suitable output map, α , so that the associated zero dynamics manifold coincides with Γ^* . The requirement of path traversal gives rise to a unique situation where unstable zero dynamics become not only desirable, but necessary. The maneuver regulation problem is solved by stabilizing the output of (2.4) which can be accomplished using input - output linearization. However, we will show that one may still be able to solve Problems 2 and 3 even in the case when (2.4) is not input-output linearizable.

2.3 Single output systems

Here we briefly discuss the case when $p = 1$ in (2.1) and justify why we do not consider this case in Problems 2 and 3. When $p = 1$, the output space is the real line, \mathbb{R} . Recall that we only consider smooth paths $\sigma : \mathbb{D} \rightarrow \mathbb{R}^p$ which are either of infinite extent $\mathbb{D} = \mathbb{R}$

or otherwise periodic $\mathbb{D} = S^1$. This implies that when $\mathbb{D} = \mathbb{R}$, the desired path is *the entire* output space. On the other hand, when $p = 1$, one cannot have $\mathbb{D} = S^1$ because S^1 cannot be embedded in \mathbb{R} . As a result, the only class of curve compatible with this framework for the case $p = 1$ are curves of infinite extent.

In this scenario, we have that $\sigma(\mathbb{D}) = \mathbb{R}$ and *any* point in the state space is actually on the path. This case is degenerate since the problem of getting on the path is trivially solved.

2.4 Zero dynamics algorithm

It is useful to review the zero dynamics algorithm (ZDA) since it is used prominently in this work. Consider the system

$$\begin{aligned} \dot{x} &= f(x) + g(x)u \\ y &= h(x) \end{aligned} \tag{2.7}$$

with the same number of inputs as outputs, m . The ZDA is initialized at a regular point x_0 in state space of (2.7). A regular point is a point for which $f(x_0) = 0$ and $h(x_0) = 0$. With this initialization the user of the algorithm has a priori knowledge that there exists at least one point which zeros the output and is controlled invariant. In other words, the initialization guarantees the existence of at least one point where if $x(0) = x_0$ and for all $t \geq 0$ $u(t) = 0$, then $y(t) = 0$. We now introduce the zero dynamics algorithm as presented in [26]:

Step 0: Set

$$M_0 = h^{-1}(0)$$

Step k: Find a neighborhood U_{k-1} of x_0 such that $M_{k-1} \cap U_{k-1}$ is an embedded submanifold.

Let M_{k-1}^c denote the connected component of $M_{k-1} \cap U_{k-1}$ containing x_0 . Then set

$$M_k = \{x \in M_{k-1}^c : f(x) \in \text{span} \{g_1(x), \dots, g_m(x)\} + T_x M_{k-1}^c\}.$$

The following proposition describes the conditions under which the ZDA converges to a maximal output zeroing submanifold.

Proposition 2.4.1 ([26], 6.1.1). *Suppose that, for each $k \geq 0$ there exists a neighborhood U_k of x_0 such that $M_k \cap U_k$ is a smooth submanifold. Then, for some $k^* > 0$ and some neighborhood U_{k^*} of x_0 , $M_{k^*+1} = M_{k^*}^c$.*

Moreover, if

$$\dim(\text{span}\{g_1(x_0), \dots, g_m(x_0)\}) = m \quad (2.8)$$

and the subspace

$$\text{span}\{g_1(x), \dots, g_m(x)\} \cap T_x M_{k^*}^c \quad (2.9)$$

has constant dimension for all $x \in M_{k^*}^c$, then $\mathcal{Z}^* = M_{k^*}^c$ is a locally maximal output zeroing submanifold.

In applying the zero dynamics algorithm to the maneuver regulation problem, we see that by Assumption 2, M_0 is a globally defined submanifold. This implies that $U_0 = \mathbb{R}^n$ and $M_0 \cap U_0 = M_0$. In the notation of this work, we have that $\mathcal{Z}^* = \Gamma^*$. Next we note that expressions (2.8) and (2.9) reduce to

$$\dim(\text{span}\{g_1(x_0)\}) = 1 \quad (2.10)$$

and

$$\dim(\text{span}\{g_1(x)\} \cap T_x \Gamma^*) = c, c \in \mathbb{Z} \quad \forall x \in \Gamma^* \quad (2.11)$$

respectively.

Isidori shows that when $c = 0$ the control u^* which makes \mathcal{Z}^* (Γ^*) invariant under (2.7) is unique. The condition for the uniqueness of u^* is implied by the notion of *transverse linear controllability* presented in Chapter 3.

We require that that Γ^* be globally well defined. This ensures feasibility of the path with respect to the system to be controlled. The algorithm generates the *maximal* output

zeroing submanifold. If only a portion of the path can be followed, then Γ^* will represent the feasible part of the path in a neighborhood of $h(x_0)$ [15]. Local feasibility of the path is assured by initializing the algorithm at an $x_0 \in \Gamma^*$ such that $f(x_0) + g(x_0)u_0 \in T_{x_0}\Gamma^*$ for some real number u_0 .

Chapter 3

Main Results

This chapter presents the main results obtained in this thesis. Necessary and sufficient conditions are presented for solving Problem 2 and Problem 3. It is shown that in the special case when $\mathbb{D} = S^1$ and $y = x$ for the class of system under consideration, the conditions presented in this chapter are equivalent to those presented by Banaszuk and Hauser [8]. It is also shown that when specialized to the linear time invariant case, the results obtained recover some results on output stabilization by Wonham [47].

3.1 Solution to Problem 2

Theorem 3.1.1. *Problem 2 is solvable if and only if there exists a function $\alpha : \mathbb{R}^n \rightarrow \mathbb{R}$ such that*

1. $\Gamma^* \subset \{x \in \mathbb{R}^n : \alpha(x) = 0\}$
2. α yields a uniform relative degree $n - n^*$ over Γ^* .

Proof. (\Rightarrow) Consider system (2.5) and let $\alpha = \xi_1$. Conditions (i) and (ii) follow immediately.

(\Leftarrow) From a slight modification¹ of the proof of [26, Proposition 9.1.1] one obtains a coordinate transformation $T : \mathbb{R}^n \rightarrow \mathcal{Z}^* \times \mathbb{R}^{n-n^*}$, valid in a neighborhood of \mathcal{Z}^* , yielding the normal form (2.5), where $\mathcal{Z}^* := \{(z, \xi) : \xi = 0\}$ is the zero dynamics manifold associated with the output function α . We are left to show that $\mathcal{Z}^* = \Gamma^*$. First notice that $\Gamma^* \subset \mathcal{Z}^*$ for if $\bar{x} \in \Gamma^*$ then $\alpha(\bar{x}) = 0$. Since through \bar{x} there passes a controlled invariant submanifold, Γ^* , and \bar{x} is output zeroing, it follows that $\bar{x} \in \mathcal{Z}^*$ as well. Finally, since Γ^* and \mathcal{Z}^* are two connected, closed submanifolds of the same dimension and $\Gamma^* \subset \mathcal{Z}^*$, one has that $\Gamma^* = \mathcal{Z}^*$. \square

Here we explicitly show the transformation one obtains from the proof of Theorem 3.1.1. Let

$$a(x) = \frac{-L_f^{n-n^*} \alpha(x)}{L_g L_f^{n-n^*-1} \alpha(x)}, \quad b(x) = \frac{1}{L_g L_f^{n-n^*-1} \alpha(x)}$$

and consider the following vector fields defined in a neighborhood of Γ^*

$$\tilde{f}(x) = f(x) + g(x)a(x), \quad \tilde{g}(x) = g(x)b(x).$$

Let

$$\tau_i(x) = (-1)^{i-1} \text{ad}_{\tilde{f}}^{i-1} \tilde{g}(x), \quad 1 \leq i \leq n - n^*$$

and

$$\lambda_i(x) = L_{\tilde{f}}^{i-1} \alpha(x), \quad 1 \leq i \leq n - n^*.$$

Finally, consider the mapping $\varphi : x \mapsto \Gamma^*$ (for x sufficiently close to Γ^*) given by

$$\varphi(x) = \Phi_{-\lambda_1(x)}^{\tau_{n-n^*}} \circ \Phi_{-\lambda_2(x)}^{\tau_{n-n^*-1}} \circ \dots \circ \Phi_{\lambda_{n-n^*}}^{\tau_1}.$$

Then the coordinate transformation yielding the normal form (2.5) is given by

$$T : x \mapsto (\varphi(x), (\lambda_1(x), \lambda_2(x), \dots, \lambda_{n-n^*}(x))). \quad (3.1)$$

¹Here the main difference is that we do not require that the vector fields $\{\tau_i\}_{i \in \{1 \dots n-n^*\}}$ in [26, Proposition 9.1.1] be complete. This implies that the normal form (2.5) is valid over a neighborhood \mathcal{N} of Γ^* , rather than \mathbb{R}^n . If the vector fields τ_i $i \in \{1 \dots n - n^*\}$ are complete, then the transformation is globally valid on \mathbb{R}^n .

The conditions in Theorem 3.1.1, although rather intuitive, are difficult to check in practice. In what follows we present sufficient conditions for the existence of a solution to Problem 2 which are easier to check.

Corollary 3.1.2. *If one of the constraints in (2.2), $\gamma_{\bar{k}} \circ h$, yields a relative degree $n - n^*$ then Problem 2 is solved by setting $\alpha = \gamma_{\bar{k}} \circ h$.*

Remark 3.1.1. The smooth feedback

$$u^* := \frac{-L_f^{n-n^*} \alpha}{L_g L_f^{n-n^*-1} \alpha}$$

makes Γ^* an invariant submanifold of (2.1).

Lemma 3.1.3. *If there exists a function $\alpha : \mathbb{R}^n \rightarrow \mathbb{R}$ which satisfies the conditions of Theorem 3.1.1, then for all $x \in \Gamma^*$*

$$T_x \Gamma^* + \text{span}\{g, \dots, \text{ad}_f^{n-n^*-1} g\}(x) = \mathbb{R}^n. \quad (3.2)$$

Proof. The existence of α implies that one can transform the system dynamics into the form (2.5) and specifically that Γ^* is controlled invariant. Let $f^* := (f + gu^*)|_{\Gamma^*}$, with u^* defined as in Remark 3.1.1. Then, for all $x \in \Gamma^*$, $f^*(x) \in T_x \Gamma^*$. Also, $\text{span}\{f^*\}$ is a one dimensional, hence involutive, distribution. These facts imply that, on Γ^* ,

$$(\text{span}\{f^*\})^\perp = (T_x \Gamma^*)^\perp + \text{span}\{d\phi_2 \dots d\phi_{n^*}\}.$$

By Assumption 3, $f^* \neq 0$ and f^* is complete. Fix $x^0 \in \Gamma^*$, define the map $t \mapsto \Phi_t^{f^*}(x^0)$ and its inverse $\phi_1 : \Gamma^* \rightarrow \phi_1(\Gamma^*)$. The map $\Phi_t^{f^*}(x^0)$ is a diffeomorphism of $\phi_1(\Gamma^*)$ onto Γ^* . By construction $L_{f^*} \phi_1 = 1$ on Γ^* , implying that $d\phi_1(x) \notin (\text{span}\{f^*(x)\})^\perp$ and thus that, on Γ^* ,

$$(\mathbb{R}^n)^* = (\text{span}\{f^*\})^\perp + \text{span}\{d\phi_1\}.$$

or, equivalently,

$$\mathbb{R}^n = T_x \Gamma^* + \text{span}\{d\phi_1 \ d\phi_2 \dots d\phi_{n^*}\}^\perp. \quad (3.3)$$

For each $x \in \Gamma^*$, consider a set of linearly independent vectors $\{v_1, \dots, v_{n^*}\}$ spanning $T_x\Gamma^*$. Locally this can always be done, globally, by Assumption 3 this can be done since Γ^* is parallelizable. Let $V = [v_1 \ \cdots \ v_{n^*}]$ and define a matrix S as follows [8]

$$S(x) = \begin{bmatrix} d\phi_1 \\ d\phi_2 \\ \vdots \\ d\phi_{n^*} \\ dL_f^{n-n^*-1}\alpha \\ \vdots \\ \alpha \end{bmatrix} \begin{bmatrix} V & g & \cdots & ad_f^{n-n^*-1}g \end{bmatrix} \\ = \begin{bmatrix} L_V\phi & * \\ 0 & \Delta \end{bmatrix}$$

where $\{L_V\phi\}_{ij} = L_{v_j}\phi_i$, $i, j = 1, \dots, n^*$, and $\Delta \in \mathbb{R}^{n-n^* \times n-n^*}$ is upper triangular with non-zero diagonal (this follows from condition (2) in Theorem 3.1.1). It is clear that if the matrix $L_V\phi$ is nonsingular then S is nonsingular as well, implying that $\text{Im}([V \ g(x) \ \cdots \ ad_f^{n-n^*-1}g(x)]) = T_x\Gamma^* + \text{span}\{g, \dots, ad_f^{n-n^*-1}g\}(x) = \mathbb{R}^n$ and the proof is complete. To prove that $L_V\phi$ is nonsingular, we use the fact that the product of two matrices AB (where AB is a square matrix) is full rank if and only if $\text{Im } B \cap \ker A = 0$. In this case we must show that

$$\text{Im } V \cap \ker (\text{col}(d\phi_1(x), \dots, d\phi_{n^*}(x))) = 0$$

or, equivalently,

$$T_x\Gamma^* \cap \ker (\text{col}(d\phi_1(x), \dots, d\phi_{n^*}(x))) = 0,$$

and this follows directly from (3.3). \square

Remark 3.1.2. Condition (3.2) is a generalization of the notion of transverse linear controllability to the case of controlled invariant submanifolds of any dimension. It

is useful in deriving checkable sufficient conditions for the existence of a solution to Problem 2. The notion of transverse linear controllability was originally introduced in [33] and later used in [8] for transverse feedback linearization. In both papers, $n^* = 1$, $\mathbb{D} = S^1$, and $T_x\Gamma^* = \text{span}\{f^*(x)\}$. Figure 3.1 illustrates the situation where transverse linear controllability holds for the case $n^* = 2$.

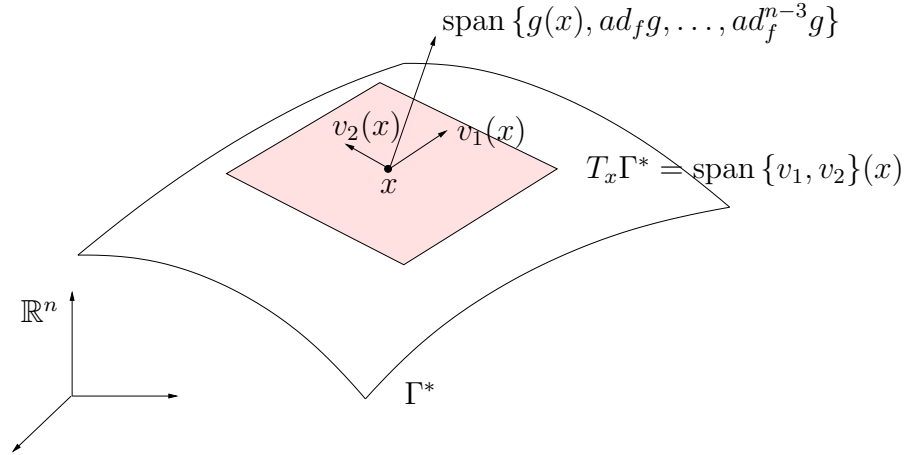


Figure 3.1: Transverse linear controllability when $n^* = 2$

Theorem 3.1.4. *Problem 1 is solvable if*

1. $T_x\Gamma^* + \text{span}\{g \dots ad_f^{n-n^*-1}g\}(x) = \mathbb{R}^n$ on Γ^*
2. *The distribution $\text{span}\{g \dots ad_f^{n-n^*-2}g\}$ is involutive.*

Proof. We will show that if the above conditions hold, then a function α can be constructed satisfying the conditions of Theorem 3.1.1. Let $\{v_1, \dots, v_{n^*}\}$ be a set of independent vector fields defined on Γ^* such that $T_x\Gamma^* = \text{span}\{v_1, \dots, v_{n^*}\}(x)$. As noted in the proof of Lemma 3.1.3, global existence of these vector fields is guaranteed by the fact

that, in Assumption 3, Γ^* is parallelizable. Condition (1) can be rewritten as

$$\text{span}\{v_1, \dots, v_{n^*}, g, \dots, ad_f^{n-n^*-1}g\}(x) = \mathbb{R}^n.$$

We use the flows of these vector fields to generate s-coordinates [45]. Choose any point $x^0 \in \Gamma^*$ and consider the mapping F defined as

$$s \mapsto \Phi_{s_n}^g \circ \dots \circ \Phi_{s_{n^*+1}}^{ad_f^{n-n^*-1}g} \circ \Phi_{s_{n^*}}^{v_{n^*}} \circ \dots \circ \Phi_{s_1}^{v_1}(x^0). \quad (3.4)$$

The map $F : F^{-1}(\mathcal{N}) \rightarrow \mathcal{N}$, where \mathcal{N} is a neighborhood of Γ^* , is a diffeomorphism. Let

$$\alpha(x) = s_{n^*+1}(x). \quad (3.5)$$

By construction, any point $x \in \Gamma^*$ can be reached by flowing along v_1, \dots, v_{n^*} . Therefore, in s-coordinates, any point $x \in \Gamma^*$ is represented as

$$F^{-1}(x) = \begin{bmatrix} * \\ \vdots \\ * \\ 0 \\ \vdots \\ 0 \end{bmatrix} \leftarrow \text{row } n^*$$

thus in particular $\alpha(x) = 0$, which proves that condition (1) of Theorem 3.1.1 is satisfied.

To complete the proof, notice that, by construction

$$L_{ad_f^{n-n^*-1}g}\alpha = 1$$

on \mathcal{N} . By the assumption of involutivity, the vector fields $ad_f^i g$, $i \in \{0 \dots n - n^* - 2\}$, in

s-coordinates have the form [45, Lemma 4]:

$$ad_f^i g = \begin{bmatrix} 0 \\ \vdots \\ 0 \\ * \\ \vdots \\ * \end{bmatrix} \leftarrow \text{row } n^* + 2.$$

It readily follows that, on \mathcal{N} , $L_{ad_f^i g} \alpha(x) = 0$, $i = 0, \dots, n - n^* - 2$. Thus α has a uniform relative degree $n - n^*$ on Γ^* . \square

Remark 3.1.3. Theorem 3.1.4 has a nice geometric interpretation, refer to Figure 3.2. In its proof, we use the flows of the vector fields spanning $T_x \Gamma^*$ to reach any point on Γ^* . Then, using the flow of the vector field $ad_f^{n-n^*-1} g$ we are able to make the system's state leave the surface Γ^* . At that point, the remaining vector fields of the mapping (3.4) span an involutive distribution. By Frobenius' Theorem [12, 26, 36], this means that through every point in a neighborhood of Γ^* there passes an integral manifold of such distribution. Let S_x denote the integral submanifold passing through x . We have that

$$T_x S_x = \text{span} \{g \dots ad_f^{n-n^*-2} g\}(x).$$

Hence, flowing along the $g, ad_f g, \dots, ad_f^{n-n^*-2} g$ does not take the system's state off of S_x . This is the key feature that allows us to conclude that the time, s_{n^*+1} , one flows along $ad_f^{n-n^*-1} g$ does not change while flowing along $g, ad_f g, \dots, ad_f^{n-n^*-2} g$.

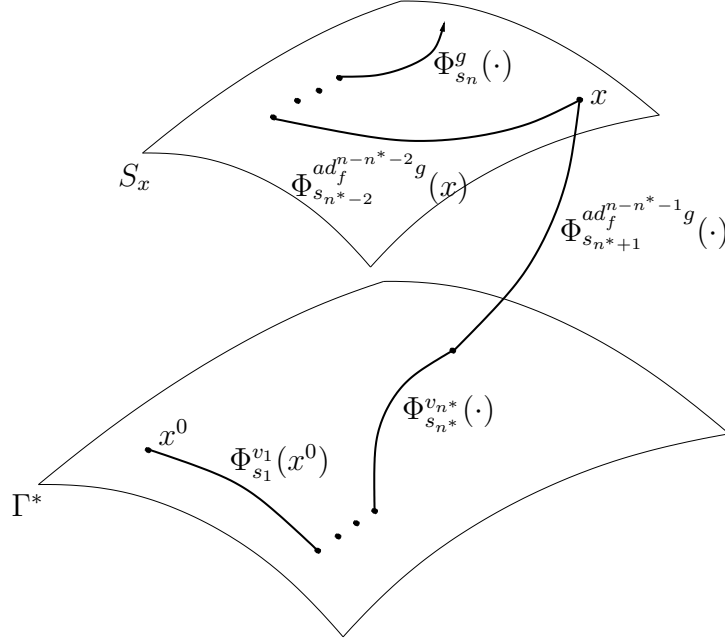


Figure 3.2: Depiction of the proof of Theorem 3.1.4

Example 3.1.1. Consider the following dynamical system and path to be followed.

$$\dot{x} = \begin{bmatrix} 3 \\ 6x_1 + x_3 \\ 0 \end{bmatrix} + \begin{bmatrix} 0 \\ 0 \\ 1 \end{bmatrix} u \quad (3.6)$$

$$y = \text{col}(x_1, x_2), \quad \sigma : \lambda \in \mathbb{R} \mapsto \text{col}(\lambda, (\lambda + 1)^2).$$

The path satisfies Assumption 1 with $\mathbb{D} = \mathbb{R}$. The first part of Assumption 2 is satisfied since

$$\sigma(\mathbb{D}) = \{y \in \mathbb{R}^2 : y_2 - (y_1 + 1)^2 = 0\}$$

One immediately has that

$$\Gamma = \{x \in \mathbb{R}^3 : x_2 - (x_1 + 1)^2 = 0\}.$$

Using Lemma 2.1.1 and Corollary 2.1.2 we obtain

$$\Gamma^* = \{x \in \Gamma : x_3 - 2 = 0\}.$$

Therefore, we have that $n^* = 1$. Since Γ is defined by one constraint which yields a uniform relative degree 2 on Γ^* , Corollary 3.1.2 trivially applies so that setting

$$\alpha(x) = x_2 - (x_1 + 1)^2$$

one can define a coordinate transformation $T : x \mapsto \text{col}(\varphi(x), \alpha(x), L_f\alpha(x))$ yielding the normal form (2.5). In this example we have

$$T(x) = \begin{bmatrix} \varphi(x) \\ x_2 - (x_1 + 1)^2 \\ x_3 - 2 \end{bmatrix}$$

As is customary in feedback linearization, one can define a smooth linearizing feedback solving the maneuver regulation problem without actually computing the function $\varphi(x)$.

This is given by

$$u = \frac{-L_f^2\alpha - k_1\alpha - k_2L_f\alpha}{L_gL_f\alpha}, \quad k_1, k_2 > 0$$

In this example we have that $L_f^2\alpha = 0$ and $L_gL_f\alpha = 1$ and so the controller reduces to

$$u = -k_1(x_2 - (x_1 + 1)^2) - k_2x_3.$$

The zero dynamics f^* in local coordinates are represented by

$$\dot{x}_1 = 3,$$

hence f^* is complete. Also, for all $x \in \Gamma^*$, $L_f h(x) = \text{col}(3, 6x_1)$ is bounded away from zero, and thus in particular Assumption 3 is satisfied. A plot of output curves of the closed-loop system is presented in Figure 3.3 with $k_1 = 6$ and $k_2 = 7$. This example illustrates that input-output linearization of 2.4 is a sufficient condition for Problem 2 to have a solution. We show in Section 3.5 that this condition is not necessary.

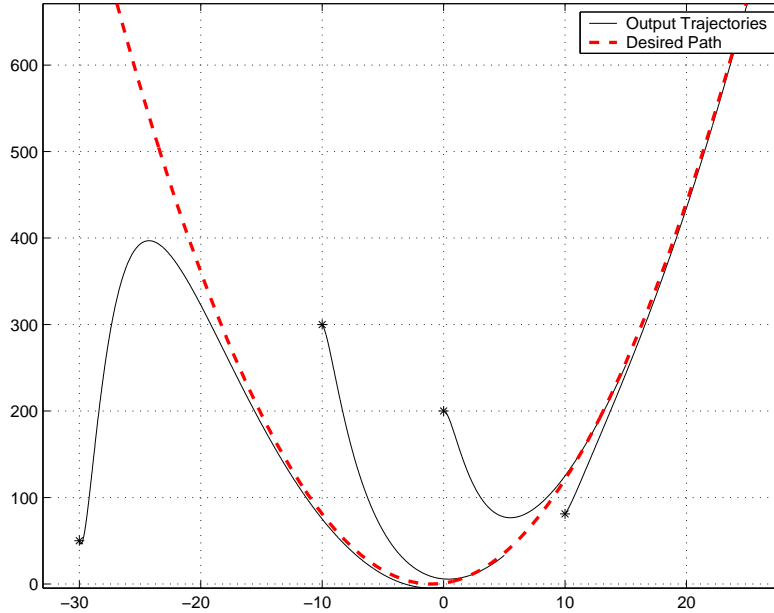


Figure 3.3: Example 3.1.1: phase curves in output coordinates.

3.2 Linear Time Invariant Systems

In this section we specialize our results to the case of LTI systems with paths given by straight curves passing through the origin (i.e., one dimensional subspaces). This specialization places a restriction on the class of paths considered in Problem 2. The value in this analysis is that it better illustrates some of the ideas of this thesis, and shows how our solution recovers a well-known necessary and sufficient condition for output stabilizability of LTI systems.

Consider the following n -dimensional single input linear system

$$\begin{aligned} \dot{x} &= Ax + bu \\ y &= Cx, \end{aligned} \tag{3.7}$$

(with $y \in \mathbb{R}^p$) and, given a full rank $D \in \mathbb{R}^{(p-1) \times p}$, define the path as $\sigma(\mathbb{R}) := \ker(D)$. In the LTI case, we do not require that the path be given as a parameterized curve. It is readily seen that $\sigma(\mathbb{R})$ satisfies Assumption 1. The lift of the path to the state space is

$$\Gamma = \ker(DC),$$

and hence Assumption 2 is satisfied and in particular, when C is full rank, $\dim \ker(DC) = n - p + 1$ still holds. In the linear setting, Γ^* becomes the largest (A, b) -invariant subspace contained in $\ker(DC)$. Let F be a *friend* of Γ^* , i.e., a feedback matrix that makes Γ^* an invariant subspace for $(A + bF)$. Then, we have $f^*(x) = (A + bF)x$, which is a complete vector field, and so Assumption 3(ii) is satisfied. Notice, however, that Assumption 3(i) is not satisfied in this simplified setup because

$$L_{f^*}h(x) = C(A + bF)x$$

is always zero at the origin. Because of this (see Remark 2.2.2), we focus our attention on just the stabilization problem. We thus seek to stabilize the output of the LTI system

$$\begin{aligned} \dot{x} &= Ax + bu \\ y' &= C'x := DCx. \end{aligned} \tag{3.8}$$

by means of state feedback. Following [47], we refer to this as the *output stabilization problem (OSP)*. In Problem 2, we require that the ξ dynamics be in Brunovsky normal form. Thus in the spirit of Problem 2, we further require that the rate of decay of the output to zero can be arbitrarily assigned (another way to say this is that the observable modes of (A, b, C') can be pole-shifted). We refer to this as the *output stabilization with controllability problem (OSCP)*.

Following [47], partition \mathbb{C} to distinguish between regions of the complex plane where “good” (stable) eigenvalues and “bad” (unstable) eigenvalues lie,

$$\mathbb{C} = \mathbb{C}^g \amalg \mathbb{C}^b,$$

(where the symbol \amalg is used to indicate *disjoint union*). Let $m(\lambda)$ denote the minimal polynomial of A and factor $m(\lambda)$ as

$$m(\lambda) = m_g(\lambda)m_b(\lambda),$$

where the zeros of m_g and m_b are in \mathbb{C}^g and \mathbb{C}^b , respectively. Let $V_g(A) = \ker(m_g(A))$ and $V_b(A) = \ker(m_b(A))$ be the associated “good” and “bad” modal subspaces of A .

Then, $\mathbb{R}^n = V_g(A) \oplus V_b(A)$. Theorem 4.4 in [47] gives a necessary and sufficient condition for output stabilizability of (3.8).

Theorem 3.2.1. *OSP is solvable if and only if*

$$V_b(A) \subset \Gamma^* + \text{Im}([b \ Ab \ \dots \ A^{n-1}b]).$$

The theorem can be rephrased as follows ([47]): OSP is solvable if and only if the bad modes of A can be made unobservable at the output or they can pole-shifted. The following is an obvious consequence of Theorem 3.2.1.

Corollary 3.2.2. *OSCP is solvable if and only if*

$$\mathbb{R}^n = \Gamma^* + \text{Im}([b \ Ab \ \dots \ A^{n-1}b]). \quad (3.9)$$

Intuitively (3.9) states that all modes of A can be made unobservable at the output or they can be pole-shifted.

We next seek to modify (3.9) to yield a decomposition of \mathbb{R}^n which can be related to transverse linear controllability (3.2). Recall that $n^* = \dim(\Gamma^*)$. Then we have

Lemma 3.2.3. *Condition (3.9) is equivalent to*

$$\mathbb{R}^n = \Gamma^* \oplus \text{Im}([b \ Ab \ \dots \ A^{n-n^*-1}b]). \quad (3.10)$$

For LTI systems, $f(x) = Ax$ and $g(x) = b$. Therefore, the Lie brackets $ad_f^i g$ are computed in the following manner

$$\begin{aligned} ad_f g &= [Ax, b] = \frac{\partial b}{\partial x} Ax - \frac{\partial Ax}{\partial x} b = -Ab \\ ad_f^2 g &= [f, ad_f g] = [Ax, -Ab] = A^2 b. \end{aligned}$$

Continuing in this way and noting that $\text{Im}(-Ab) = \text{Im}(Ab)$, we conclude that in the LTI case, transverse linear controllability (3.2) reduces to (3.10). This result gives

Corollary 3.2.4. *(OSCP) is solvable if and only if the system is transverse linearly controllable.*

Proof of Lemma 3.2.3. Sufficiency is obvious. We prove necessity. Assume that (3.9) holds and recall that Γ^* is (A, b) -invariant by construction. Γ^* is (A, b) -invariant if and only if

$$A\Gamma^* \subset \Gamma^* + \mathcal{B}, \quad \mathcal{B} := \text{Im}(b).$$

We proceed via contradiction. Choose any $0 \leq k \leq n - n^* - 1$ and assume that $A^k b \in \Gamma^*$, then

$$A^{k+1}b \in A\Gamma^* \subset \Gamma^* + \mathcal{B}.$$

$$A(A^{k+1}b) \subset \Gamma^* + \mathcal{B} + \text{Im}(Ab).$$

Repeating this argument one concludes that

$$\text{Im}([A^k b \ \cdots \ A^{n-1} b]) \subset \Gamma^* + \text{Im}([b \ Ab \ \cdots \ A^{k-1} b]),$$

and hence

$$\dim(\Gamma^* + \text{Im}([b \ Ab \ \cdots \ A^{n-1} b])) \leq n^* + k < n,$$

contradicting the assumption that (3.9) holds. Thus (3.9) holds only if

$$\text{Im}([b \ \cdots \ A^{n-n^*-1} b]) \cap \Gamma^* = 0. \quad (3.11)$$

Further, (3.9) implies

$$\dim(\text{Im}([b \ \cdots \ A^{n-n^*-1} b])) = n - n^*.$$

In other words, it implies that for all $1 \leq k \leq n - n^* - 1$

$$A^k b \notin \text{Im}([b \ \cdots \ A^{k-1} b])$$

for, if not, then $A^i b \in \text{Im}([b \ \cdots \ A^{k-1} b])$, $k \leq i \leq n - 1$, contradicting (3.9). This shows that $b, \dots, A^{n-n^*-1} b$ are linearly independent which, together with (3.11), yields (3.10), as required. \square

On the other hand, we have the following

Lemma 3.2.5. *Problem 2 is solvable if and only if (3.7) is transversally linearly controllable.*

Proof. We apply Theorem 3.1.4 to (3.7). First, notice that condition 2 is *always* satisfied for LTI systems because in the LTI setting, $f(x) = Ax$ and $g(x) = b$. We have

$$\text{span}\{g \dots ad_f^{n-n^*-2}g\} = \text{Im}([b \dots A^{n-n^*-2}b])$$

which, being a constant distribution, is involutive. Explicitly

$$[A^i b, A^j b] = \frac{\partial A^j b}{\partial x} A^i b - \frac{\partial A^i b}{\partial x} A^j b = 0$$

for all $0 \leq i, j \leq n - n^* - 2$ and involutivity follows. Theorem 3.1.4 states that a sufficient condition for Problem 2 to be solvable is that (3.7) be transverse linearly controllable. By Lemma 3.1.3, this condition is also necessary. \square

We conclude that

Corollary 3.2.6. *In the LTI case, Problem 2 is equivalent to (OSCP).*

3.3 Solution to Problem 3

The following is an obvious result in the light of Theorem 3.1.1.

Theorem 3.3.1. *Problem 3 is solvable if and only if there exists a function $\alpha : \mathbb{R}^n \rightarrow \mathbb{R}$ defined in a neighborhood U^0 of some $x^0 \in \Gamma^*$ such that*

1. $\Gamma^* \cap U^0 \subset \{x \in U^0 : \alpha(x) = 0\}$
2. α yields a relative degree $n - n^*$ at x^0 .

Proof. (\Rightarrow) Let $\alpha = \xi_1^0$, conditions (1) and (2) follow.

(\Leftarrow) Let $\xi_1^0 = \alpha(x)$. A partial coordinate transformation on U^0 is given by

$$\xi_k^0 = L_f^{k-1}\alpha, \quad k \in \{1 \dots n - n^*\}.$$

We seek n^* more independent functions to complete the transformation and yield the correct form. This can always be done [26, Proposition 4.1.3]. From the proof of Theorem 3.1.1 we have that the zero dynamics of the resulting normal form coincide, on U^0 , with Γ^* . \square

We now explicitly show the coordinate transformation one obtains from the proof of Theorem 3.3.1. By definition of relative degree, the distribution $G = \text{span}\{g\}$ is nonsingular around x^0 and thus involutive. By Frobenius' Theorem, there exists $n - 1$ real-valued function $\lambda_1^0(x), \dots, \lambda_{n-1}^0(x)$, such that

$$\text{span}\{d\lambda_1^0(x), \dots, d\lambda_{n-1}^0(x)\} = G^\perp.$$

In the set $\{\lambda_1^0(x), \dots, \lambda_{n-1}^0(x)\}$ there exists n^* functions (without loss of generality $\lambda_1^0(x), \dots, \lambda_{n^*}^0(x)$) with the property that the n differentials $d\alpha, dL_f\alpha, \dots, dL_f^{n-n^*-1}\alpha, d\lambda_1^0, \dots, d\lambda_{n^*}^0$ are linearly independent. The coordinate transformation yielding the normal form 2.5 in a neighborhood of x^0 is given by

$$T^0 : x \mapsto (\lambda_1^0(x), \dots, \lambda_{n^*}^0(x), \xi_1^0(x), \dots, \xi_{n-n^*}^0(x)).$$

Lemma 3.3.2. *If there exists a function $\alpha : \mathbb{R}^n \rightarrow \mathbb{R}$ which satisfied the conditions of Theorem 3.3.1, then*

$$T_x\Gamma^* + \text{span}\{g, \dots, ad_f^{n-n^*-1}g\}(x^0) = \mathbb{R}^n.$$

Proof. See the proof of Lemma 3.1.3. \square

Let

$$D = \text{span} \{g \dots ad_f^{m-n^*-2}g\}. \quad (3.12)$$

Theorem 3.1.4 proves that involutivity of D , together with transverse linear controllability, are sufficient conditions for the existence of a function α satisfying conditions (1) and (2) in Theorem 3.1.1 and hence solving Problem 2. When the involutive closure of D , $\text{inv}(D)$, is regular at $x^0 \in \Gamma^*$ (has constant dimension around x^0 , see Chapter A), the next result provides necessary and sufficient conditions to solve Problem 3. These conditions are easier to check than those in Theorem 3.3.1.

Theorem 3.3.3. *Assume that $\text{inv}(D)$ is regular at $x^0 \in \Gamma^*$. Then Problem 3 is solvable if and only if*

1. $T_{x^0}\Gamma^* + \text{span}\{g, \dots, ad_f^{m-n^*-1}g\}(x^0) = \mathbb{R}^n$
2. $ad_f^{m-n^*-1}g(x^0) \notin \text{inv}(D)(x^0)$.

Proof. (\Rightarrow) Assume that the conditions of Theorem 3.3.1 hold. By Lemma 3.3.2, (1) holds. By definition of relative degree, in a neighborhood $\Gamma^* \cap U^0$, $d\alpha \in D^\perp$ and $L_{ad_f^{m-n^*-1}g}\alpha \neq 0$. Recall that $d\alpha \in D^\perp$ implies $d\alpha \in (\text{inv } D)^\perp$. Since $L_{ad_f^{m-n^*-1}g}\alpha \neq 0$, one has that $ad_f^{m-n^*-1}g \notin \text{span}\{d\alpha\}^\perp$ and thus also $ad_f^{m-n^*-1}g \notin \text{inv}(D)$, showing that (2) holds.

(\Leftarrow) Assume $\text{inv}(D)$ is regular at x^0 and conditions (1) and (2) hold. This part of the proof closely follows the idea of the proof of Theorem 2.3 in [8]. Notice that $n - n^* - 2 \leq \dim(\text{inv } D) \leq n - 1$. If $\dim(\text{inv } D) = n - n^* - 2$ then essentially the same proof of Theorem 3.1.4 applies and we are done. Hence, we focus on the case $n - n^* - 1 \leq \dim(\text{inv } D) \leq n - 1$. As in the proof of Theorem 3.1.4, let $\{v_1, \dots, v_{n^*}\}$ be a set of vector fields defined on Γ^* such that $T_x\Gamma^* = \text{span}\{v_1, \dots, v_{n^*}\}(x)$, and generate s -coordinates by flowing along the vector fields $v_1, \dots, v_{n^*}, ad_f^{m-n^*-1}g, \dots, g$ with times s_1, \dots, s_n , respectively. By condition (1), there exists a neighborhood U of x^0 such that

the map F defined as

$$s \mapsto \Phi_{s_n}^g \circ \dots \circ \Phi_{s_{n^*+1}}^{ad_f^{n-n^*-1}g} \circ \Phi_{s_{n^*}}^{v_{n^*}} \circ \dots \circ \Phi_{s_1}^{v_1}(x^0),$$

is a diffeomorphism of $F^{-1}(U)$ onto U . Define the set

$$M := \{x \in U : s_{n^*+2}(x) = \dots = s_n(x) = 0\}$$

which is an embedded submanifold of U containing $\Gamma^* \cap U$ of dimension $n^* + 1$. The submanifold M is the set of points reachable from Γ^* by flowing along $ad_f^{n-n^*-1}g$. Since, by assumption, $\text{inv}(D)$ is regular at x^0 , it follows that $\text{inv}(D)$ generates a foliation by integral submanifolds, \mathcal{S} , in a neighborhood of x^0 which, without loss of generality, we can take to be U . Let S_x denote a leaf of the foliation passing through $x \in \Gamma^* \cap U$. On $\Gamma^* \cap U$, $T_x M = T_x \Gamma^* + \text{span}\{ad_f^{n-n^*-1}g\}$. By condition (1) $T_x M + D = \mathbb{R}^n$, implying that $T_x M + \text{inv}(D) = \mathbb{R}^n$ or, equivalently, $T_x M + T_x S_x = \mathbb{R}^n$. This shows that, on $\Gamma^* \cap U$, M is transversal to \mathcal{S} and $T_x M \cap T_x S_x = T_x \Gamma^* \cap \text{inv}(D)(x)$ is a regular distribution. Let \hat{n} be its dimension. Since we are considering the case $n - n^* - 1 \leq \dim(\text{inv } D) \leq n - 1$, we have that $1 \leq \hat{n} \leq n^*$. Making, if needed, $M \cap U$ smaller, let $\{\hat{v}_1, \dots, \hat{v}_{\hat{n}}\}$ be a set of vector fields defined on $M \cap U$ spanning $T_x M \cap \text{inv}(D)$ on $M \cap U$. Choose additional $n^* - \hat{n}$ vector fields $\{\hat{v}_{\hat{n}+1}, \dots, \hat{v}_{n^*}\}$ defined on $\Gamma^* \cap U$ such that $T_x \Gamma^* = \text{span}\{\hat{v}_1, \dots, \hat{v}_{n^*}\}(x) \quad \forall x \in \Gamma^* \cap U$. Then, by condition (1),

$$\{\hat{v}_1, \dots, \hat{v}_{\hat{n}}, \hat{v}_{\hat{n}+1}, \dots, \hat{v}_{n^*}, g, \dots, ad_f^{n-n^*-1}g\}$$

is a set of independent vector fields on $\Gamma^* \cap U$. Moreover, $\text{inv}(D) = \text{span}\{\hat{v}_1, \dots, \hat{v}_{\hat{n}}\} + D$. By making, if necessary, $M \cap U$ smaller we can assume that the vector fields $\{\hat{v}_1, \dots, \hat{v}_{\hat{n}}, g, \dots, ad_f^{n-n^*-1}g\}$ are independent on $M \cap U$. The domain of definition of the vector fields involved in our construction is summarized as:

$$\{\hat{v}_{\hat{n}+1}, \dots, \hat{v}_{n^*}\} \text{ on } \Gamma^* \cap U$$

$$\{\hat{v}_1, \dots, \hat{v}_{\hat{n}}\} \text{ on } M \cap U$$

$$\{g, \dots, ad_f^{n-n^*-1}g\} \text{ on } U.$$

We use these vector fields to define the map $G : G^{-1}(U^0) \rightarrow U^0$ ($U^0 \subset U$ is a neighborhood of x^0),

$$\begin{aligned} p \mapsto & \Phi_{p_n}^g \circ \cdots \circ \Phi_{p_{n^*-2}}^{ad_f^{n-n^*-2}} \circ \Phi_{p_{n^*-1}}^{\hat{v}_{\hat{n}}} \circ \cdots \circ \Phi_{p_{n^*-\hat{n}+2}}^{\hat{v}_1} \\ & \circ \Phi_{p_{n^*-\hat{n}+1}}^{ad_f^{n-n^*-1}g} \circ \Phi_{p_{n^*-\hat{n}}}^{\hat{v}_{n^*}} \circ \cdots \circ \Phi_{p_1}^{\hat{v}_{\hat{n}+1}}(x^0). \end{aligned}$$

Let $P_1 = (p_1, \dots, p_{n^*-\hat{n}})$, $P_2 = (p_{n^*-\hat{n}+1}, \dots, p_{n^*+1})$, $P_3 = (p_{n^*+2}, \dots, p_n)$, and define

$$\begin{aligned} G_1^{P_1}(x^0) &:= \Phi_{p_{n^*-\hat{n}}}^{\hat{v}_{n^*}} \circ \cdots \circ \Phi_{p_1}^{\hat{v}_{\hat{n}+1}}(x^0) \\ G_2^{P_2}(x^1) &:= \Phi_{p_{n^*+1}}^{\hat{v}_{\hat{n}}} \circ \cdots \circ \Phi_{p_{n^*-\hat{n}+2}}^{\hat{v}_1} \circ \Phi_{p_{n^*-\hat{n}+1}}^{ad_f^{n-n^*-1}g}(x^1) \\ G_3^{P_3}(x^2) &:= \Phi_{p_n}^g \circ \cdots \circ \Phi_{p_{n^*+2}}^{ad_f^{n-n^*-2}}(x^2), \end{aligned}$$

so that $G(p) = G_3^{P_3} \circ G_2^{P_2} \circ G_1^{P_1}(x^0)$. For a fixed x^0 , $x^1 \in \Gamma^* \cap U^0$, and $x^2 \in M \cap U^0$, each $G_i^{P_i}$ is a diffeomorphism onto its image, thus G is a diffeomorphism onto U^0 . This can be most easily seen by examining the order in which the various flows are composed. In particular, since $\hat{v}_{\hat{n}+1}, \dots, \hat{v}_{n^*}$ are independent on Γ^* , the set of points reached by flowing along these vector fields is an embedded submanifold, \bar{S} , of dimension $n^* - \hat{n}$, contained in Γ^* . Next, since $ad_f^{n-n^*-1}g, \hat{v}_1, \dots, \hat{v}_{\hat{n}}$ are independent on $M \cap U^0$, the set of points reachable from \bar{S} by flowing along these vector fields is precisely $M \cap U^0$. Thus $M \cap U^0 = \{x \in U^0 : P_3(x) = 0\}$ and $\Gamma^* \cap U^0 = \{x \in U^0 : p_{n^*-\hat{n}+1}(x) = 0, P_3(x) = 0\}$. Finally, the set of points reachable from $M \cap U^0$ by flowing along $g, \dots, ad_f^{n-n^*-2}g$ is the entire U^0 .

Choose $\alpha(x) = p_{n^*-\hat{n}+1}(x)$. Then $\Gamma^* \cap U^0 \subset \{x \in U^0 : \alpha(x) = 0\}$ and thus condition (1) in Theorem 3.3.1 is satisfied. By the involutivity of $\text{inv}(D) = \text{span}\{\hat{v}_1, \dots, \hat{v}_{\hat{n}}\} + D$, the vector fields $ad_f^i g$, $i = 0, \dots, n - n^* - 2$, in s-coordinates have the form [45, Lemma

4]

$$ad_f^i g = \begin{bmatrix} 0 \\ \vdots \\ 0 \\ * \\ \vdots \\ * \end{bmatrix} \leftarrow \text{row } n^* - \hat{n} + 2,$$

and thus, on U^0 , $L_{ad_f^i g} \alpha = 0$, $i = 0, \dots, n - n^* - 2$. It is also clear that $L_{ad_f^{n-n^*-1} g} \alpha \neq 0$ on U^0 . Thus the assumptions of Theorem 3.3.1 are satisfied. \square

Corollary 3.3.4. *Assume that $\text{inv } D$ has constant dimension on Γ^* and that*

1. $T_x \Gamma^* + \text{span}\{g, \dots, ad_f^{n-n^*-1} g\}(x) = \mathbb{R}^n$ on Γ^*
2. $ad_f^{n-n^*-1} g(x) \notin \text{inv}(D)(x)$ on Γ^* .

Then there exists an open covering $\{U^{(i)}\}$ of Γ^* and a collection of transformations $\{T^{(i)}\}$, with $T^{(i)} : x \mapsto (z^{(i)}, \xi^{(i)}) \in \Gamma^* \cap U^{(i)} \times \mathbb{R}^{n-n^*}$ such that $\Gamma^* \cap U^{(i)} = \{\xi^{(i)} = 0\}$ and in $(z^{(i)}, \xi^{(i)})$ coordinates the systems has the form (2.5).

Corollary 3.3.5. *If $\text{inv } D$ is such that for any $x^0 \in \Gamma^*$*

$$\dim(\text{inv } D)(x^0) = n,$$

then Problems 2 and 3 are unsolvable.

3.4 State Maneuvers

In this section, we show that when $y = x$ in (2.1) and $\mathbb{D} = S^1$ the results obtained thus far are equivalent to the results presented in [8]. See also [35]. The conditions presented in [8, Theorem 2.1] for a global solution are

- (a) $\dim(\text{span}\{f^*, g, \dots, ad_{f^*}^{m-2} g\}) = n$ on Γ^*

(b) There exists a function $\alpha : \mathbb{R}^n \rightarrow \mathbb{R}$ such that

- (i) $d\alpha \neq 0$ on Γ^* .
- (ii) $\alpha = 0$ on Γ^*
- (iii) $L_{ad_{f^*}^i g} \alpha = 0$ near Γ^* for $i = 0 \dots n - 3$.

Lemma 3.4.1. *Conditions (a) and (b) above hold if and only if the conditions of Theorem 3.1.1 hold.*

Proof. (\Rightarrow) Assume conditions (a) and (b) hold. Condition (b.ii) is the same as condition (1) in Theorem 3.1.1. Next, since f^* is by definition tangent to Γ^* , condition (b.ii) implies that $L_{f^*} \alpha = 0$ on Γ^* . This, together with condition (b.iii), implies that, on Γ^* , $\text{span}\{d\alpha\}^\perp = \text{span}\{f^*, g, \dots, ad_{f^*}^{n-3} g\}$. By condition (a), necessarily $L_{ad_{f^*}^{n-3} g} \alpha \neq 0$ on Γ^* . This, together with condition (b.iii) shows that α yields a relative degree $n - 1$, which is precisely condition (2) in Theorem 3.1.1.

(\Leftarrow) Assume the conditions of Theorem 3.1.1 hold. Condition (a) holds by Lemma 3.1.3. Condition (b.ii) is identical to condition (1) in Theorem 3.1.1. Finally, since α yields a relative degree $n - 1$ (recall that here $n^* = 1$), conditions (b.i) and (b.iii) are satisfied. \square

In the local case, consider the distribution D , in (3.12), with $n^* = 1$. The conditions presented in [8, Theorem 2.4] are

- (a) $\dim(\text{span}\{f^*, g, \dots, ad_{f^*}^{m-2} g\}) = n$ on Γ^*
- (b) The distribution D is either
 - (i) involutive or
 - (ii) $\dim(\text{inv } D) = n - 1$ in a neighborhood of Γ^* and $f^* \in \text{inv } D$ on Γ^* .

Lemma 3.4.2. *Conditions (a) and (b) above hold if and only if the conditions of Corollary 3.3.4 hold.*

Proof. (\Rightarrow) Assume (a) and (b) above hold. Then we just have to show that condition (2) of Corollary 3.3.4 holds. If D is involutive then (a) immediately gives (2). Otherwise, since $f^* \in \text{inv } D$ on Γ^* , condition (a) implies condition (2).

(\Leftarrow) Obvious. □

A key difference between the normal form presented in this paper (2.5) and the one presented in [8] lies in the structure given to the vector field f_0 in (2.5). In the case $n^* = 1$ the following procedure illustrates how to obtain the normal form presented in [8]. Fix a point $x_0 \in \Gamma^*$ and define the map $t \mapsto \Phi_t^{f^*}(x_0)$ and its inverse $\varphi' : \Gamma^* \rightarrow \varphi'(\Gamma^*)$. Note that, by Assumption 3(ii), φ' is globally defined and that, when $\mathbb{D} = S^1$, $\varphi'(\Gamma^*) = S^1$. By construction $L_{f^*}\varphi' = 1$ on Γ^* . Let $z = \varphi'(x)$ and let $\xi_i = L_f^{i-1}\alpha$, $i = 1 \dots n-1$. With this transformation, together with the feedback

$$u = \frac{-L_f^{n-1}\alpha + v}{L_g L_f^{n-2}\alpha}$$

one obtains

$$\begin{aligned} \dot{z} &= 1 + f_1(z, \xi) + g_0(z, \xi)v \\ \dot{\xi}_1 &= \xi_2 \\ &\vdots \\ \dot{\xi}_{n-2} &= \xi_{n-1} \\ \dot{\xi}_{n-1} &= v, \end{aligned} \tag{3.13}$$

($f_1(z, 0) = 0$) which is the normal form as presented in [8]. It is interesting to note that the normal form of [8] is also valid when $\mathbb{D} = \mathbb{R}$ (in such a case, the domain of z is $\varphi'(\Gamma^*) = \mathbb{R}$ rather than S^1).

When $n^* > 1$, the normal form (3.13), could perhaps be generalized by finding a partial coordinate transformation $z = \varphi(x)$ yielding $\dot{z} = \text{col}(1, 0, \dots, 0)$ on Γ^* . This is always possible locally. Doing so globally amounts to finding a *global* rectification for a vector field on a manifold. We are not aware of a method to accomplish this.

3.5 On Relative Degree

Based on the results presented thus far, natural questions one may ask are:

- (i) If none of path constraints yield a well defined relative degree, can Problems 2 and 3 still be solved?
- (ii) If one of the constraints yields *some* well defined relative degree r , with $r \neq n - n^*$, can this constraint be used as α ?

In this section we show that the answer to (i) is yes, while the answer to (ii) is no. Recall, by assumption, the desired set Γ is represented as the zero level set of $p - 1$ functions

$$\Gamma = \{x : \gamma_1(h(x)) = \dots = \gamma_{p-1}(h(x)) = 0\}.$$

3.5.1 The case $p = 2$

The case when $p = 2$ deserves special attention because many important applications of path following to mobile vehicles have two dimensional output spaces (this is the case, e.g., for unicycles, cars, hovercraft's, and trailer systems). Furthermore, when $p = 2$, a curve in the output space is represented by just one constraint,

$$\sigma(\mathbb{D}) = \gamma^{-1}(0), \quad \text{where } \gamma : \mathbb{R}^p \rightarrow \mathbb{R}.$$

Thus, the problem of driving the system output to $\sigma(\mathbb{D})$ is equivalent to that of stabilizing the output of the following SISO system,

$$\begin{aligned} \dot{x} &= f(x) + g(x)u \\ y' &= \gamma \circ h(x). \end{aligned} \tag{3.14}$$

The typical approach to stabilizing the output of a SISO system is to check whether (3.14) has a well-defined relative degree and, if so, to perform input output linearization (this approach has been followed, e.g., in Example 3.1.1). It is easily seen that, in the case

$p = 2$, Corollary 3.1.2 states precisely that a sufficient condition for Problem 2 to have a solution is that (3.14) has a well-defined relative degree r . In fact, if (3.14) has a well-defined relative degree r , then necessarily $r = n - n^*$. For, the zero dynamics manifold of (3.14) is by definition the maximal output zeroing submanifold or, equivalently, the largest controlled invariant submanifold contained in $\Gamma = \gamma \circ h(x)$, and thus it coincides with Γ^* . Therefore, we conclude that, when $p = 2$, the answer to question (ii) is negative.

With regards to question (i), one may wonder whether the condition that (3.14) has a well-defined relative degree is also necessary. This is equivalent to asking whether, in the case $p = 2$, the class of systems for which Problem 2 is solvable is made by systems with output $\gamma \circ h$ which have a well-defined relative degree. We now show, by means of a counter-example, that the answer to this question is negative, and thus the class of systems for which Problem 2 is solvable is larger than the class of systems with a well-defined relative degree (from the output $\gamma \circ h$).

Example 3.5.1. Consider the system

$$\begin{aligned} \dot{x}_1 &= x_3 + x_1 u \\ \dot{x}_2 &= 1 & y &= \text{col}(x_1, x_2), \\ \dot{x}_3 &= u \end{aligned} \tag{3.15}$$

and the path $\sigma : \mathbb{R} \rightarrow \mathbb{R}^2$ defined by $\lambda \mapsto \text{col}(0, \lambda)$. Then $\sigma(\mathbb{R}) = \{y \in \mathbb{R}^2 : y_1 = 0\}$. Let $\gamma(y) := y_1$. Then, the lift of the path to the state space is

$$\Gamma = \gamma \circ h^{-1}(0) = \{x \in \mathbb{R}^3 : x_1 = 0\}.$$

The SISO system

$$\begin{aligned} \dot{x}_1 &= x_2 + x_1 u \\ \dot{x}_2 &= 1 & y' &= \gamma \circ h(x) := x_1, \\ \dot{x}_3 &= u \end{aligned} \tag{3.16}$$

does not have a well-defined relative degree anywhere on the set $\{x_1 = 0\}$ because $L_g(\gamma \circ h) = x_1$ changes sign in any neighborhood of $\{x_1 = 0\}$.

Application of the zero dynamics algorithm gives that the largest controlled invariant submanifold contained in Γ is

$$\Gamma^* = \{x : x_1 = x_3 = 0\}.$$

Thus $n^* = 1$ and the smooth feedback rendering Γ^* invariant is $u^* = 0$, yielding $f^* = \frac{\partial}{\partial x_2}$.

We now check the sufficient conditions of Theorem 3.1.4. We have

$$g = x_1 \frac{\partial}{\partial x_1} + \frac{\partial}{\partial x_3}, \quad ad_f g = (x_3 - 1) \frac{\partial}{\partial x_1}.$$

Thus, for all $x \in \Gamma^*$,

$$T_x \Gamma^* + \text{span}\{g, ad_f g\}(x) = \text{span}\left\{\frac{\partial}{\partial x_2}, \frac{\partial}{\partial x_3}, -\frac{\partial}{\partial x_1}\right\} = \mathbb{R}^3$$

showing that the system is transversely linearly controllable and condition (1) in Theorem 3.1.4 is satisfied. Condition (2) is also satisfied because $\text{span}\{g\}$, being one dimensional, is involutive. We conclude that, despite the fact that (3.16) does not have a well-defined relative degree, by Theorem 3.1.4 we know that there exists a solution to Problem 2. By following the semi-constructive procedure outlined in the proof of Theorem 3.1.4 we can actually compute an output function α solving the problem. To this end, we choose $x^0 = 0$ and construct the map

$$s \mapsto x := \Phi_{s_3}^g \circ \Phi_{s_2}^{ad_f g} \circ \Phi_{s_1}^{f^*}(0).$$

We have

$$s_1 \mapsto \Phi_{s_1}^{f^*}(0) = \text{col}(0, s_1, 0)$$

$$(s_2, p) \mapsto \Phi_{s_2}^{ad_f g}(p) = \text{col}((p_3 - 1)s_2 + p_1, p_2, p_3)$$

$$(s_3, q) \mapsto \Phi_{s_3}^g(q) = \text{col}(e^{s_3} q_1, q_2, s_3 + q_3).$$

The composition of the maps above gives

$$\Phi_{s_3}^g \circ \Phi_{s_2}^{ad_f g} \circ \Phi_{s_1}^{f^*}(0) = \text{col}(-s_2 e^{s_3}, s_1, s_3).$$

We next find the inverse $x \mapsto s$,

$$s_1(x) = x_2, \quad s_2(x) = -x_1 e^{-x_3}, \quad s_3(x) = x_3.$$

Finally, we pick $\alpha(x) = s_2(x) = -x_1 e^{-x_3}$. We indeed verify that this output meets the two necessary and sufficient conditions to solve Problem 2: (i) $\Gamma^* \subset \{x : \alpha(x) = 0\}$ (when $x_1 = x_3 = 0$ one has $\alpha = 0$) and, (ii), the system with output α has a well-defined relative degree $n - n^* = 2$ in a neighborhood of Γ^* :

$$\begin{aligned} L_g \alpha &= -x_1 e^{-x_3} + x_1 e^{-x_3} = 0 \\ L_g L_f \alpha &= -e^{-x_3} + x_3 e^{-x_3} \neq 0 \quad \forall x \in \Gamma^*. \end{aligned}$$

This example satisfies Assumption 3 since

$$L_{f^*} h = \left\langle dh, \frac{\partial}{\partial x_2} \right\rangle = 1.$$

This indicates that in stabilizing the auxiliary output $y = \gamma \circ h(x)$, the original system output $y = h(x)$ remains unstable and the result is that the path is traversed by this system.

△

3.5.2 The case $p > 2$

When $p > 2$, the problem of driving the system output to $\sigma(\mathbb{D})$ is equivalent to that of stabilizing the outputs of (2.4), rewritten below for convenience

$$\begin{aligned} \dot{x} &= f(x) + g(x)u \\ y'_1 &= \gamma_1 \circ h(x) \\ &\vdots \\ y'_{p-1} &= \gamma_{p-1} \circ h(x). \end{aligned}$$

In the case $p > 2$, we must stabilize *all* $p - 1$ outputs. This implies that, Problem 2 can only be solved using $\alpha = \gamma_{\bar{k}} \circ h$ if the relative degree associated with $\{f, g, \gamma_{\bar{k}} \circ h\}$ is precisely $n - n^*$.

As we did for the case $p = 2$, we now show, by means of a counter-example, that even if none of the constraints of a system with $p > 2$, yield the desired relative degree, Problem 2 may still be solvable.

Example 3.5.2. Consider the system

$$\begin{aligned} \dot{x}_1 &= x_3 + x_1 u \\ \dot{x}_2 &= 1 \\ \dot{x}_3 &= u \\ \dot{x}_4 &= x_1 + x_4 u \end{aligned} \quad y = \text{col}(x_1, x_2, x_4), \quad (3.17)$$

and the path $\sigma : \mathbb{R} \rightarrow \mathbb{R}^3$ defined by $\lambda \mapsto \text{col}(0, \lambda, 0)$. Then $\sigma(\mathbb{R}) = \{y \in \mathbb{R}^3 : y_1 = y_3 = 0\}$. Let $\gamma_1(y) := y_1$ and $\gamma_2(y) := y_2$. Then, the lift of the path to the state space is

$$\Gamma = \gamma \circ h^{-1}(0) = \{x \in \mathbb{R}^3 : x_1 = x_4 = 0\}.$$

The SIMO system

$$\begin{aligned} \dot{x}_1 &= x_3 + x_1 u \\ \dot{x}_2 &= 1 \\ \dot{x}_3 &= u \\ \dot{x}_4 &= x_1 + x_4 u \end{aligned} \quad y' = \gamma \circ h(x) := \text{col}(x_1, x_4), \quad (3.18)$$

does not have a well-defined relative degree associated with either output anywhere on the set $\{x_1 = x_4 = 0\}$ because $L_g(\gamma_1 \circ h) = x_1$ and $L_g(\gamma_2 \circ h) = x_4$ both change sign in any neighborhood of $\{x_1 = x_4 = 0\}$.

Application of the zero dynamics algorithm gives that the largest controlled invariant submanifold contained in Γ is

$$\Gamma^* = \{x : x_1 = x_3 = x_4 = 0\}.$$

Thus $n^* = 1$ and the smooth feedback rendering Γ^* invariant is $u^* = 0$, yielding $f^* = \frac{\partial}{\partial x_2}$.

We now check the sufficient conditions of Theorem 3.1.4. We have

$$g = x_1 \frac{\partial}{\partial x_1} + \frac{\partial}{\partial x_3} + x_4 \frac{\partial}{\partial x_4}, \quad ad_f g = (x_3 - 1) \frac{\partial}{\partial x_1}, \quad ad_f^2 g = (1 - x_3) \frac{\partial}{\partial x_4}.$$

Thus, for all $x \in \Gamma^*$,

$$T_x \Gamma^* + \text{span}\{g, ad_f g, ad_f^2 g\}(x) = \text{span} \left\{ \frac{\partial}{\partial x_2}, \frac{\partial}{\partial x_3}, -\frac{\partial}{\partial x_1}, \frac{\partial}{\partial x_4} \right\} = \mathbb{R}^4$$

showing that the system is transversely linearly controllable and condition (1) in Theorem 3.1.4 is satisfied. As for condition (2), we must check that $\text{span}\{g, ad_f g\}$ is involutive, which is the case since

$$[g, ad_f g] = (2 - x_3) \frac{\partial}{\partial x_1} = \frac{2 - x_3}{x_3 - 1} ad_f g \in \Delta.$$

We conclude that, despite the fact that none of the outputs of (3.18) has a well-defined relative degree, by Theorem 3.1.4 we know that there exists a solution to Problem 2. By following the semi-constructive procedure outlined in the proof of Theorem 3.1.4 we can compute an output function α solving the problem. To this end, we choose $x^0 = 0$ and construct the map

$$s \mapsto x := \Phi_{s_4}^g \circ \Phi_{s_3}^{ad_f g} \circ \Phi_{s_2}^{ad_f^2 g} \circ \Phi_{s_1}^{f^*}(0).$$

We have

$$\begin{aligned} s_1 &\mapsto \Phi_{s_1}^{f^*}(0) = \text{col}(0, s_1, 0, 0) \\ (s_2, p) &\mapsto \Phi_{s_2}^{ad_f^2 g}(p) = \text{col}(p_1, p_2, p_3, (1 - p_3)s_2 + p_4) \\ (s_3, q) &\mapsto \Phi_{s_3}^{ad_f g}(q) = \text{col}((q_3 - 1)s_3 + q_1, q_2, q_3, q_4) \\ (s_4, r) &\mapsto \Phi_{s_4}^g(r) = \text{col}(e^{s_4} r_1, r_2, s_4 + r_3, e^{s_4} r_4). \end{aligned}$$

The composition of the maps above gives

$$\Phi_{s_4}^g \circ \Phi_{s_3}^{ad_f g} \circ \Phi_{s_2}^{ad_f^2 g} \circ \Phi_{s_1}^{f^*}(0) = \text{col}(-s_3 e^{s_4}, s_1, s_4, s_2 e^{s_4}).$$

We next find the inverse $x \mapsto s$,

$$s_1(x) = x_2, \quad s_2(x) = x_4 e^{-x_3}, \quad s_3(x) = -x_1 e^{-x_3}, \quad s_4(x) = x_3.$$

Finally, we pick $\alpha(x) = s_2(x) = x_4e^{-x_3}$. To verify that this output meets the necessary and sufficient conditions to solve Problem 2: (i) $\Gamma^* \subset \{x : \alpha(x) = 0\}$ (when $x_1 = x_3 = x_4 = 0$ one has $\alpha = 0$) and, (ii), the system with output α has a well-defined relative degree $n - n^* = 3$ in a neighborhood of Γ^* :

$$L_g\alpha = -x_4e^{-x_3} + x_4e^{-x_3} = 0$$

$$L_gL_f\alpha = x_1e^{-x_3} - x_1e^{-x_3} = 0$$

$$L_gL_f^2\alpha = -e^{-x_3} + x_3e^{-x_3} \neq 0 \quad \forall x \in \Gamma^*$$

This example also satisfies Assumption 3 since

$$L_{f^*}h = \left\langle dh, \frac{\partial}{\partial x_2} \right\rangle = 1$$

again indicating that the path is traversed by this system.

△

Another such example for the case $p > 2$ can be found in [8, Example 3.1].

Chapter 4

Applied Transverse Feedback

Linearization

This chapter presents various application examples of the results presented in Chapter 3. In presenting these examples, the value and the limitations of our solution to the maneuver regulation will become apparent. In particular, it will be shown in some cases a simple procedure can be used to design a smooth feedback control solving the maneuver regulation problem. In other cases, we find that Problems 2 and 3 are unsolvable, even when a solution is known to exist to the general maneuver regulation problem, Problem 1.

4.1 Kinematic Unicycle

4.1.1 Following a circular path

Consider the kinematic model of a unicycle with fixed translational speed $v \neq 0$ and a circular path to follow of radius 1.

$$\dot{x} = \begin{bmatrix} v \cos x_3 \\ v \sin x_3 \\ 0 \end{bmatrix} + \begin{bmatrix} 0 \\ 0 \\ 1 \end{bmatrix} u \quad (4.1)$$

$$y = \text{col}(x_1, x_2), \quad \sigma : \lambda \in S^1 \mapsto \text{col}(\cos \lambda, \sin \lambda).$$

See Figure 4.1 for a depiction of the unicycle. For this system we have $n = 3$, $p = 2$ and h is of class C^∞ . First, we will show that the various assumptions introduced in Chapter 2

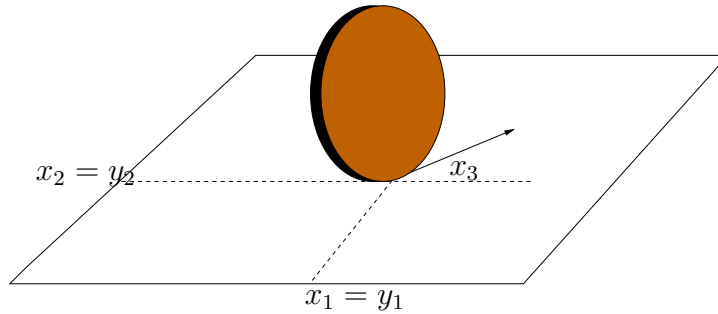


Figure 4.1: Unicycle coordinates

are indeed satisfied. Assumption 1 is clearly satisfied with $\mathbb{D} = S^1$ and furthermore, $\sigma(\mathbb{D})$ can be represented as the pre-image of a map $\gamma : \mathbb{R}^2 \rightarrow \mathbb{R}$

$$\sigma(\mathbb{D}) = \left\{ y \in \mathbb{R}^2 : \gamma(y) = y_1^2 + y_2^2 - 1 = 0 \right\}.$$

The lift

$$\Gamma = \{x : \gamma(h(x)) = 0\} = \{x : x_1^2 + x_2^2 - 1 = 0\}$$

is obviously a submanifold (a cylinder). Using Lemma 2.1.1 we obtain

$$\Gamma^* = \{x \in \Gamma : x_1 \cos x_3 + x_2 \sin x_3 = 0\},$$

therefore, $n^* = 1$. Since Γ is defined by one constraint which yields a uniform relative degree 2 on Γ^* , Corollary 3.1.2 trivially applies so that setting

$$\alpha(x) = x_1^2 + x_2^2 - 1$$

one can define a coordinate transformation $T : x \mapsto \text{col}(\varphi(x), \alpha(x), L_f\alpha(x))$ yielding the normal form (2.5). As is customary in feedback linearization, one can define a smooth linearizing feedback solving the maneuver regulation problem without actually computing the function $\varphi(x)$. This is given by

$$u = \frac{-L_f^2\alpha - k_1\alpha - k_2L_f\alpha}{L_gL_f\alpha}, \quad k_1, k_2 > 0$$

or in coordinates

$$u = \frac{-2v^2 - k_1(x_1^2 + x_2^2 - 1) - k_2(x_1 \cos x_3 + x_2 \sin x_3)}{2v(x_2 \cos x_3 - x_1 \sin x_3)}, \quad k_1, k_2 > 0.$$

The zero dynamics f^* , which correspond to the system dynamics when constrained to evolve on Γ^* , in local coordinates are represented by

$$\dot{x}_3 = v,$$

hence f^* is complete. Also, for all $x \in \mathbb{R}^3$, $L_f h(x) = \text{col}(v \cos x_3, v \sin x_3)$ is bounded away from zero, and thus in particular Assumption 3 is satisfied. A plot of output curves of the closed-loop system is presented in Figure 4.2 for the case $v = 1$ with $k_1 = k_2 = 1$.

Remark 4.1.1. A very interesting property of the solution presented above is the remaining degree of freedom in the control. Notice that the velocity control was not used to stabilize the system to Γ^* (the geometric task associated with maneuver regulation). Since the zero dynamics represents the dynamics *on* the path, we are free to assign dynamics while traversing the curve by choosing the appropriate velocity control. Therefore, this solution leaves an extra degree of freedom in the control (as opposed to say, chained form solutions) which can be used to solve the dynamic task associated with maneuver regulation.

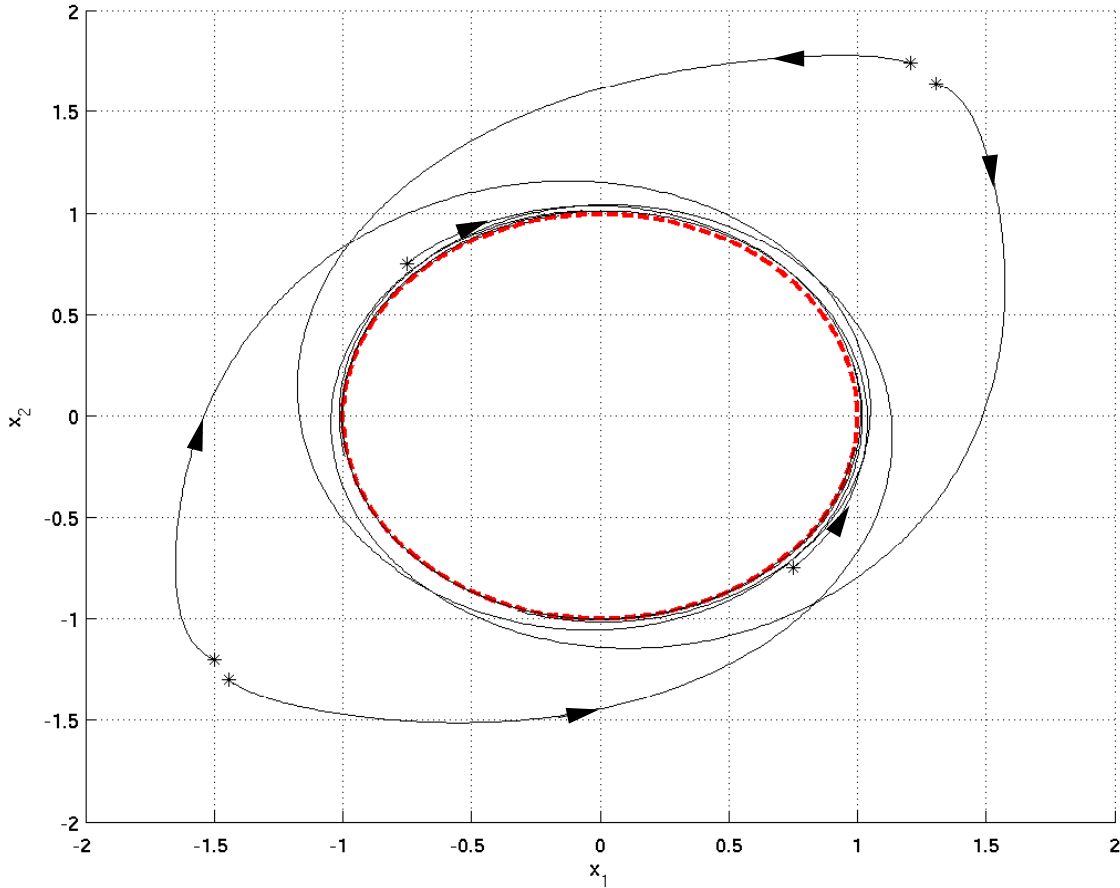


Figure 4.2: Kinematic Unicycle: Phase curves in output coordinates of a unicycle system following a circular path.

The unicycle example was easily solved by using the lone path constraint. We have shown that there exist cases where this approach will not work. In those cases, the results of Theorem 3.1.4 become relevant as seen in Examples 3.5.1 and 3.5.2. We now apply the semi-constructive procedure of Theorem 3.1.4 to the unicycle system (4.1). Use Lemma 2.1.1 to get the mapping $\Gamma^* = \mathcal{H}^{-1}(0)$. Solve $T_x\Gamma^* = \ker d\mathcal{H}$ and obtain

$$T_x\Gamma^* = \text{span} \left(-x_2 \frac{\partial}{\partial x_1} + x_1 \frac{\partial}{\partial x_2} + \frac{\partial}{\partial x_3} \right)$$

Choose $x^0 = \text{col}(1, 0, \frac{\pi}{2}) \in \Gamma^*$ and generate the the mapping F defined as

$$s \mapsto \Phi_{s_3}^g \circ \Phi_{s_2}^{ad_f g} \circ \Phi_{s_1}^X(x^0)$$

where $\text{span}\{X\}(x) = T_x\Gamma^*$. We get

$$x = F(s) = \begin{bmatrix} v \cos(s_1)s_2 + \cos(s_1) \\ v \sin(s_1)s_2 + \sin(s_1) \\ s_3 + s_1 + \frac{\pi}{2} \end{bmatrix}. \quad (4.2)$$

A function α satisfying the properties of Theorem 3.1.1 is found by inverting (4.2) and setting $\alpha(x) = s_2(x)$.

$$\alpha(x) = s_2(x) = \frac{1}{v} \left(\sqrt{x_1^2 + x_2^2} - 1 \right) \quad (4.3)$$

Theorem 3.1.4 actually recovers a function whose differential spans the same co-distribution as the α function obtained using one of the path constraints. Expression (4.3) is not differentiable at $(x_1, x_2) = (0, 0)$, so it should not be used directly.

4.1.2 Following arbitrary paths

More can be said about the unicycle with the aid of Theorem 3.1.4. Consider the problem of maneuvering the output of the unicycle to *any* curve $\sigma(\mathbb{D})$ satisfying Assumption 1 with $r \geq 2$. In this special case Assumption 2 is not needed. Specifically, we do not need to assume that there exists a submersion γ such that $\sigma(\mathbb{D}) = \gamma^{-1}(0)$ because the lift of $\sigma(\mathbb{D})$, Γ , is always an embedded submanifold of dimension 2 (a generalized cylinder $\Gamma = \sigma(\mathbb{D}) \times \mathbb{R}$) and Assumption 3 is always satisfied. To see why the latter is true, refer to Figure 4.3 and observe that the nonholonomic constraint of the unicycle yields $\Gamma^* = \{x \in \mathbb{R}^3 : x = (\sigma(t), \arctan2(\dot{\sigma}(t))), t \in \mathbb{D}\}$, where $\arctan2 : \mathbb{R} \times \mathbb{R} \rightarrow \mathbb{R}$ denotes the smooth arctangent function. Hence, Γ^* is a well defined closed submanifold of dimension 1. To show that f^* is complete, assume without loss of generality that σ is unit speed, i.e., $\|\dot{\sigma}\| = 1$. Then, the flow of f^* , $t \mapsto \Phi_t^{f^*} = (\sigma(vt), \arctan(v\dot{\sigma}(vt)))$ is well defined for all $t \in \mathbb{D}$. Next, the conditions of Theorem 3.1.4 reduce to

$$T_x\Gamma^* + \text{span}\{g, \text{ad}_f g\} = \mathbb{R}^3 \text{ on } \Gamma^*,$$

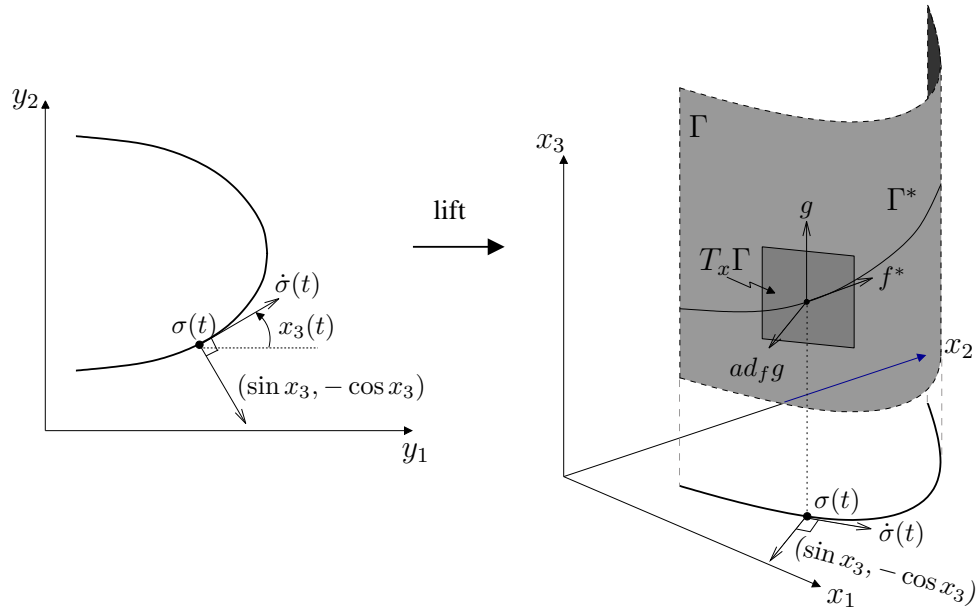


Figure 4.3: Maneuver regulation for the unicycle with forward velocity $v = 1$.

where $ad_f g = \text{col}(v \sin x_3, -v \cos x_3, 0)$. Simple geometric considerations (see Figure 4.3) show that, for all $x \in \Gamma^*$,

$$T_x \Gamma = \text{span}\{f^*, g\}(x) = T_x \Gamma^* + \text{span}\{g\}(x)$$

and

$$\text{span}\{ad_f g\}(x) = (T_x \Gamma)^\perp.$$

Theorem 3.1.4 can thus be applied to conclude that Problem 2 has a solution. Here Theorem 3.1.4 allows us to recover the well known fact that unicycles with constant forward velocity can follow any smooth regular curve on the plane.¹

The unicycle example demonstrates that in practice, when $p = 2$, and $\sigma \in C^r$, $r \geq 2$, it is natural and more fruitful to try to use the sole constraint defining the submersion γ as the desired function α .

Consider a kinematic model of a unicycle with fixed translational speed $v \neq 0$ and an

¹Actually, Theorem 3.1.4 *partially* recovers this well-known property of unicycles in that it requires that the curve σ has no self-intersections (see Assumption 1(iii)).

arbitrary parameterized path to follow.

$$\dot{x} = \begin{bmatrix} v \cos x_3 \\ v \sin x_3 \\ 0 \end{bmatrix} + \begin{bmatrix} 0 \\ 0 \\ 1 \end{bmatrix} u \quad (4.4)$$

$$y = \text{col}(x_1, x_2), \quad \sigma : \lambda \in \mathbb{D} \mapsto \text{col}(\sigma_1(\lambda), \sigma_2(\lambda)).$$

Lemma 4.1.1. *If the curve σ in (4.4) satisfies assumptions 1 with $r \geq 2$ then Corollary 3.1.2 applies to the unicycle system.*

Proof. Assume σ satisfies Assumptions 1 with $r \geq 2$. We have already seen that Assumption 2 and part of Assumption 3 are automatically satisfied. Then there exists a map $\gamma : \mathbb{R}^2 \rightarrow \mathbb{R}$ such that $\sigma(\mathbb{D}) = \gamma^{-1}(0)$. The lift of this path is a generalized cylinder given by

$$\Gamma = \{x : \gamma \circ h = 0\}.$$

The linear output of the unicycle ensures that γ will solely be a function of the position coordinates x_1 and x_2 . Check the conditions of Corollary 3.1.2 using the standard definition of relative degree for SISO systems [26].

$$\begin{aligned} \alpha &= \gamma(x_1, x_2) \\ \dot{\alpha} &= L_f \gamma + L_g \gamma u = v \cos x_3 \frac{\partial \gamma}{\partial x_1} + v \sin x_3 \frac{\partial \gamma}{\partial x_2} \\ \ddot{\alpha} &= L_f^2 \gamma + L_g L_f \gamma u = v^2 \cos^2 x_3 \frac{\partial^2 \gamma}{\partial x_1^2} + v^2 \sin^2 x_3 \frac{\partial^2 \gamma}{\partial x_2^2} + \\ &\quad 2 \sin x_3 \cos x_3 \frac{\partial^2 \gamma}{\partial(x_1, x_2)} + \left(v \cos x_3 \frac{\partial \gamma}{\partial x_2} - v \sin x_3 \frac{\partial \gamma}{\partial x_1} \right) u \end{aligned}$$

We fail to achieve the desired relative degree of 2 at any $x \in \mathbb{R}^3$ where

$$x_3 = \arctan \left(\frac{\frac{\partial \gamma}{\partial x_2}}{\frac{\partial \gamma}{\partial x_1}} \right), \quad (4.5)$$

which cannot occur $\forall x \in \Gamma^*$. □

Expression (4.5) has a geometric interpretation at points where relative degree is not well defined. Relative degree is lost at points where the unicycle's heading coincides with

the normal direction to the curve, see Figure 4.4. Clearly, this cannot happen when $x \in \Gamma^*$.

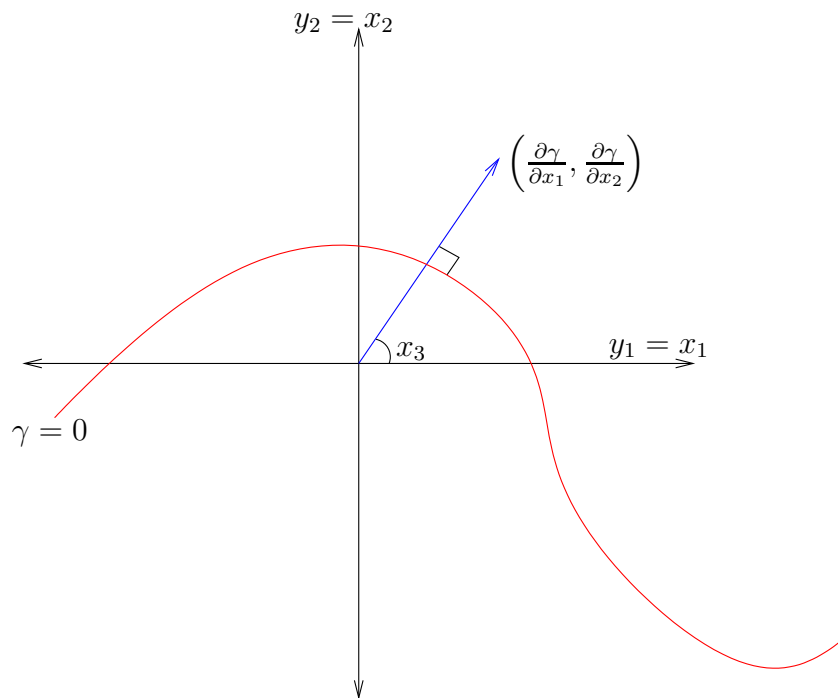


Figure 4.4: Geometric interpretation of condition (4.5).

4.2 Rear-wheel driving car-like robot

Consider the kinematic model of a rear-wheel drive car-like robot with fixed translational speed $v \neq 0$ and unrestricted steering angle.

$$\dot{x} = \begin{bmatrix} v \cos x_3 \\ v \sin x_3 \\ \frac{v}{\ell} \tan x_4 \\ 0 \end{bmatrix} + \begin{bmatrix} 0 \\ 0 \\ 0 \\ 1 \end{bmatrix} u \quad (4.6)$$

$$y = \text{col}(x_1, x_2).$$

In this example, we assume that $x \in \mathbb{R}^4$ when in fact $x \in \mathbb{R}^2 \times S^1 \times (-\frac{\pi}{2}, \frac{\pi}{2})$. See Figure 4.5 for a description of these coordinates. First we investigate some of the general properties of this system with the aid of the results from Chapter 3 and then present a specific example.

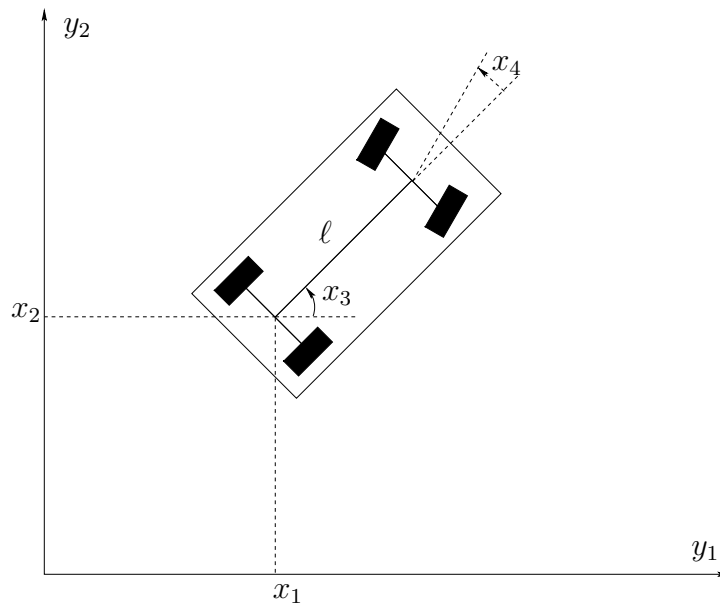


Figure 4.5: Kinematic state space variables of a car-like robot

4.2.1 Following arbitrary paths

Consider the problem of maneuvering the output of the car-like robot (hereafter referred to as simply the 'car') to an arbitrary curve $\sigma(\mathbb{D})$ satisfying Assumption 1 with $r \geq 3$. As in the case of the unicycle, we have that the second part of Assumption 2 is unnecessary. The lift of $\sigma(\mathbb{D})$ is always an embedded submanifold of dimension 3 ($\Gamma = \sigma(\mathbb{D}) \times \mathbb{R}^2$). Unlike the unicycle, the car has a model singularity when $x_4 = \pm\frac{\pi}{2} + 2k\pi$. This may constrain the class of curve which can be followed. Observe that the nonholonomic constraint of rolling without slipping implies that

$$\Gamma^* = \left\{ x \in \mathbb{R}^4 : x = (\sigma(s), \varphi(s), \arctan\left(\frac{\ell}{v}\dot{\varphi}(s)\right), s \in \mathbb{D}) \right\}$$

where $\varphi = \arctan2(\dot{\sigma}(s))$ is the angle of $\dot{\sigma}(s)$ with respect to the positive y_1 axis, and $\arctan2 : \mathbb{R} \times \mathbb{R} \rightarrow \mathbb{R}$ denotes the smooth arctangent function. Assume, without loss of generality, that $\|\dot{\sigma}\| = 1$, then $\dot{\varphi}(s)$ is precisely the signed curvature of σ . Therefore, on the path, the steering angle x_4 is constrained to be a function of the signed curvature of σ . Admissible curves are ones for which the curvature does not cause the model to become singular. Since the model singularity occurs as $\dot{\varphi} \rightarrow \infty$, we conclude that Γ^* is indeed a well defined closed submanifold of dimension 1 for any *smooth* curve σ . A constraint on the steering angle of (4.6) would appear as a restriction on the maximum allowable curvature, k_{max} , of the path, i.e., $|\dot{\varphi}(s)| \leq k_{max}$. Assumption 3(i) holds since $\|L_{f^*}h\| = \|\text{col}(v \cos x_3, v \sin x_3)\| = |v|$ is bounded away from zero.

The second part of Assumption 3 deals with the completeness of f^* . Assume, without loss of generality, that $\|\dot{\sigma}\| = 1$. Following the path $\sigma(\mathbb{D})$ generates a map $t \mapsto \Phi_t^{f^*} = (\sigma(vt), \varphi_v(t), \arctan(\frac{\ell}{v}\dot{\varphi}_v(t)))$, where $\varphi_v(t) = \arctan2(v\dot{\sigma}(vt))$ and $\arctan2 : \mathbb{R} \times \mathbb{R} \rightarrow \mathbb{R}$ denotes the smooth arctangent function. This map is well defined for all $t \in \mathbb{D}$ and so we conclude that f^* is indeed complete.

Checking the conditions of Theorem 3.1.4, we require that

$$T_x\Gamma^* + \text{span}\{g, \text{ad}_f g, \text{ad}_f^2 g\} = \mathbb{R}^4,$$

where

$$ad_f g = -\frac{v}{\ell} (1 + \tan^2 x_4) \frac{\partial}{\partial x_3}$$

$$ad_f^2 g = -\frac{v^2}{\ell} \sin x_3 (1 + \tan^2 x_4) + \frac{\partial}{\partial x_1} + \frac{v^2}{\ell} \cos x_3 (1 + \tan^2 x_4) \frac{\partial}{\partial x_2}.$$

Since $\Gamma = \sigma(\mathbb{D}) \times \mathbb{R}^2$, we immediately see that $T_x \Gamma = T_x \Gamma^* + \text{span}\{g, ad_f g\}$. This is an immediate consequence of the fact that both g and $ad_f g$ are orthogonal to $\frac{\partial}{\partial x_1}$ and $\frac{\partial}{\partial x_2}$. Then, since $\text{span}\{ad_f^2 g\} \perp \Gamma$ provided $x_4 \neq \pm\frac{\pi}{2} + 2k\pi$, we conclude that transverse linear controllability holds at points where $x_4 \neq \pm\frac{\pi}{2} + 2k\pi$.

Since $n^* = 1$, we check if the distribution $\text{span}\{g, ad_f g\}$ is involutive. For the car system (4.6), involutivity holds since

$$[g, ad_f g] = \left(-\frac{2v}{L} (1 + \tan^2 x_4) \tan x_4 \right) \frac{\partial}{\partial x_3} \in \text{span}\{g, ad_f g\}.$$

The conditions of Theorem 3.1.4 are satisfied and therefore we conclude that Problem 2 has a solution.

Lemma 4.2.1. *If the curve σ in (4.6) satisfies assumptions 1 with $r \geq 3$ then Corollary 3.1.2 applies to the car system (4.6).*

Proof. This proof is identical to the the proof of Lemma 4.1.1. The difference being that we require a higher class of smoothness from γ since Γ^* is now embedded in a higher dimensional ambient space.

The desired relative degree of 3 fails at points for which

$$\left(-\frac{v^2}{\ell} \frac{\partial \gamma}{\partial x_1} \sin x_3 + \frac{v^2}{\ell} \frac{\partial \gamma}{\partial x_2} \cos x_3 \right) \sec^2 x_4 = 0 \quad (4.7)$$

which cannot occur $\forall x \in \Gamma^*$. □

We fail to achieve the required relative degree of 3 at points in the state space where (4.7) holds. This has the same geometric interpretation as for the case of the unicycle. The second interesting aspect of the expression (4.7) is that it allows us to

recover the model singularity. If relative degree is well defined, then the control

$$u^* = -\frac{L_f^3 \gamma}{L_g L_f^2 \gamma} = -\frac{L_f^3 \gamma}{\frac{v^2}{L} \left(\frac{\partial \gamma}{\partial x_2} \cos x_3 - \frac{\partial \gamma}{\partial x_2} \sin x_3 \right) \sec^2 x_4}$$

makes Γ^* invariant. When the model singularity is encountered, we have that $\sec x_4 \rightarrow \infty$. Thus, the relative degree remains well defined, however, the feedback u^* vanishes. Therefore, the x_4 dynamics vanish and the system gets 'jammed' at $|x_4| = \frac{\pi}{2} + 2k\pi$ and the car stops traversing the path (the differential model of the car becomes singular).

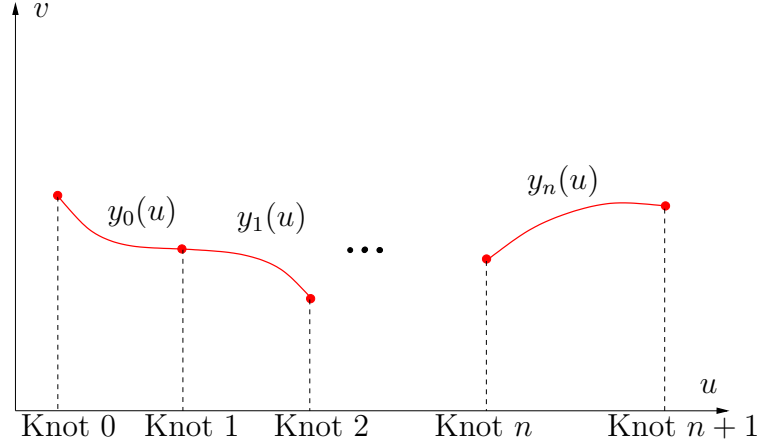
4.2.2 Following paths generated by 4th order splines

Let us now look at more specific and useful application example. Again, consider the kinematic model of a rear-wheel drive car-like robot with fixed translational speed $v \neq 0$ and unrestricted steering angle (4.6). We attempt to follow a path generated by 4th order splines. Splines are useful in path generation since they can be utilized to model arbitrary paths by connecting splines to create a piecewise smooth polynomial. The final spline can be made arbitrarily accurate by increasing the number of polynomials and can be made arbitrarily smooth by increasing the order the polynomials. In general, we can enforce that n^{th} order splines belong to the class C^{n-1} . In this example, we are using 4th order splines and so the best we can achieve are C^3 curves. Note that each polynomial is C^∞ , it is only when we join them that we lose smoothness.

Recall [10] that the knots of a spline are a set of real numbers representing the values of the dependent variable where one polynomial ends and the next begins. Let K represent an ordered collection of knots and let I represent an index set of all piecewise polynomials. Introduce the following notation to represent the spline we wish to follow, which may have an arbitrary number of knots

$$\sigma : \lambda \in \mathbb{R} \mapsto \left(\lambda, \sum_{i \in I} \sum_{j=0}^4 (a_j^i (\lambda - K_i)^j) (1(\lambda - K_i) - 1(\lambda - K_{i+1})) \right) \quad (4.8)$$

where $1(t)$ is the unit step function. Figure 4.6 shows a typical spline curve. We enforce

Figure 4.6: A typical spline curve in \mathbb{R}^2

that the spline be the graph of a function in \mathbb{R}^2 . This guarantees injectivity and properness and therefore this class of curves satisfy Assumption 1. Let σ_i represent a single segment of the spline. Then, Assumption 2 is also satisfied since for each segment of the spline we have that

$$\sigma_i(\mathbb{D}) = \left\{ y \in (K_i, K_{i+1}) \times \mathbb{R} : y_2 - \sum_{j=0}^4 a_j^i (y_1 - K_i)^j = 0 \right\}$$

which yields

$$\sigma(\mathbb{D}) = \bigcup_{i \in I} \sigma_i(\mathbb{D}).$$

We have seen that for any σ satisfying Assumption 1, Γ is a well defined regular submanifold.

$$\Gamma = \bigcup_{i \in I} \left\{ x \in (K_i, K_{i+1}) \times \mathbb{R}^3 : x_2 - \sum_{j=1}^4 a_j^i (x_1 - K_i)^j = 0 \right\}. \quad (4.9)$$

Using Lemma 2.1.1 we can obtain a characterization of Γ^* . By Lemma 4.2.1, in each knot interval we can use the sole constraint defining Γ and apply Corollary 3.1.2

$$\alpha_i(x) = x_2 - \sum_{j=1}^4 a_j^i (x_1 - K_i)^j.$$

Define a coordinate transformation in each knot interval (K_i, K_{i+1}) ,

$$T_i : x \mapsto \text{col}(\varphi_i(x), \alpha_i(x), L_f \alpha_i(x), L_f^2 \alpha_i(x))$$

yielding the normal form (2.5). The smooth linearizing feedback solving the maneuver regulation problem is

$$u_i = \frac{-L_f^3 \alpha_i - k_1 \alpha_i - k_2 L_f \alpha_i - k_3 L_f^2 \alpha_i}{L_g L_f \alpha_i}, \quad k_1, k_2, k_3 > 0.$$

In order to traverse the entire path, the controller must switch from u_i to u_{i+1} when x_1 switches from knot interval (K_i, K_{i+1}) to (K_{i+1}, K_{i+2}) . The controller u_i is a function of the path constraint and its first 3 derivatives. Thus, in order for the *switching* to be bumpless, we require a 4th order or higher spline. Figure 4.5 presents various simulation results on the car system following a 4th order spline consisting of 38 knots. In this simulation the linear gains were chosen to be $[k_1, k_2, k_3] = [6, 7, 8]$ with $v = 50$ and $\ell = 15$. This particular spline represents an approximation of the Toronto Indy race track.

4.3 Kinematic Hovercraft

We investigate the maneuver regulation problem for a kinematic hovercraft system model derived from the basis of an underactuated ship. The complete model, as taken from [39], is

$$\dot{x} = \begin{bmatrix} x_4 \cos x_3 - x_5 \sin x_3 \\ x_4 \sin x_3 + x_5 \cos x_3 \\ x_6 \\ \frac{m_{22}}{m_{11}} x_4 x_5 - \frac{d_{11}}{m_{11}} x_4 \\ -\frac{m_{11}}{m_{22}} x_4 x_5 - \frac{d_{22}}{m_{22}} x_5 \\ \frac{m_{11}}{m_{22}} x_4 x_5 - \frac{m_{22}}{m_{33}} x_4 x_5 - \frac{d_{33}}{m_{33}} x_6 \end{bmatrix} + \begin{bmatrix} 0 \\ 0 \\ 0 \\ \frac{1}{m_{11}} \\ 0 \\ 0 \end{bmatrix} u_1 + \begin{bmatrix} 0 \\ 0 \\ 0 \\ 0 \\ \frac{1}{m_{22}} \\ 0 \end{bmatrix} u_2 + \begin{bmatrix} 0 \\ 0 \\ 0 \\ 0 \\ 0 \\ \frac{1}{m_{33}} \end{bmatrix} u_3 \quad (4.10)$$

$$y = \text{col}(x_1, x_2).$$

Note that model (4.10) is kinematically equivalent to a spherical underwater vehicle moving in a plane [28]. See figure (4.8) for a picture of the hovercraft's state variables.

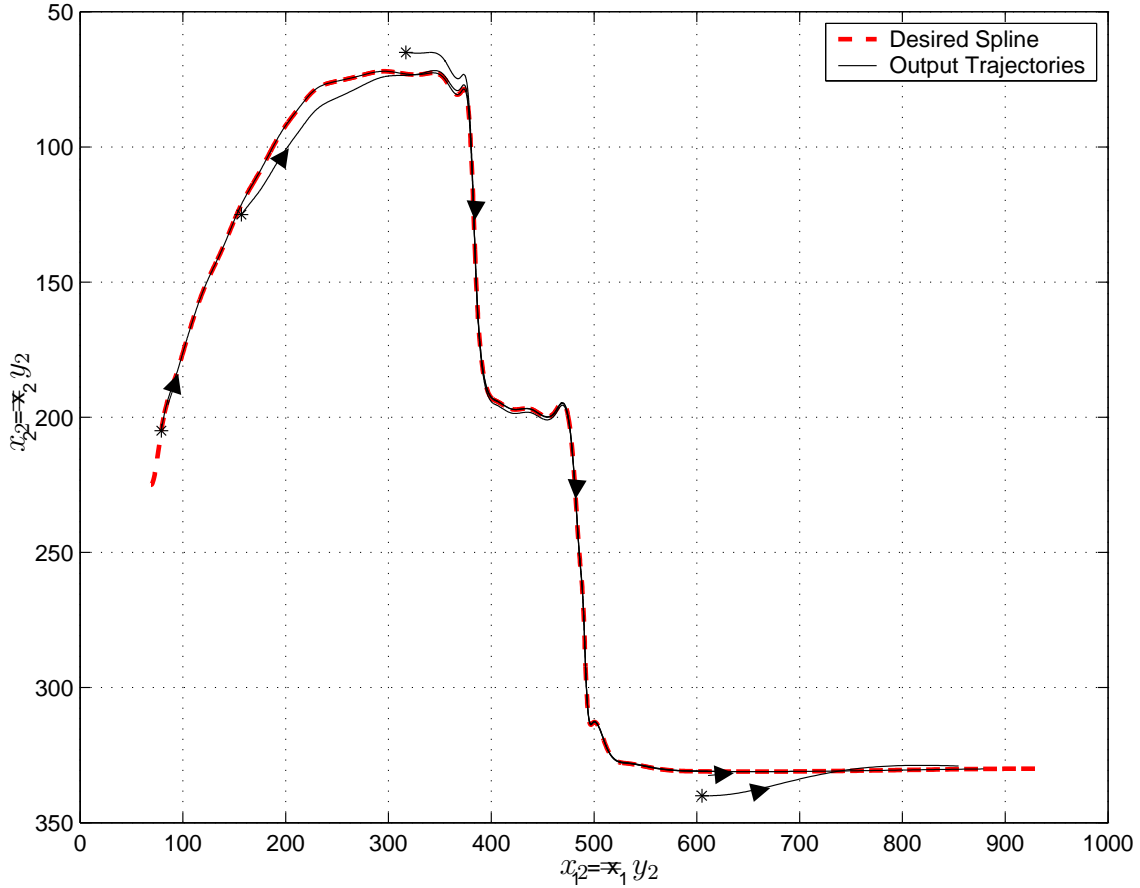


Figure 4.7: Example 4.2: Phase curves in output coordinates of Car-like vehicle following a 4th order (C^3) spline.

In order to put the hovercraft (4.10) into the current framework, we design the following preliminary feedbacks in order to get constant surge and sway velocities $x_4 = x_5 = v$.

$$u_1(x) = m_{11} \left(\frac{d_{11}}{m_{11}} x_4 - \frac{m_{22}}{m_{11}} x_4 x_5 + k_1 (x_4 - v) \right)$$

$$u_2(x) = m_{22} \left(\frac{m_{11}}{m_{22}} x_4 x_5 + \frac{d_{22}}{m_{22}} x_5 + k_2 (x_5 - v) \right)$$

with $k_1, k_2 > 0$. We can eliminate the x_4 and x_5 dynamics from (4.10). Furthermore, we adopt the reasonable simplifying assumptions from [39] and let $m_{11} = m_{22}$, $d_{33} = 0$ and $m_{33} = 1$. The assumption that $m_{11} = m_{22}$ corresponds to assuming that the vessel is symmetric with respect to the x_4 and x_5 axes. The d_{ii} terms represent hydrodynamic damping coefficients which we ignore. There is no loss of generality in assuming $d_{33} = 0$

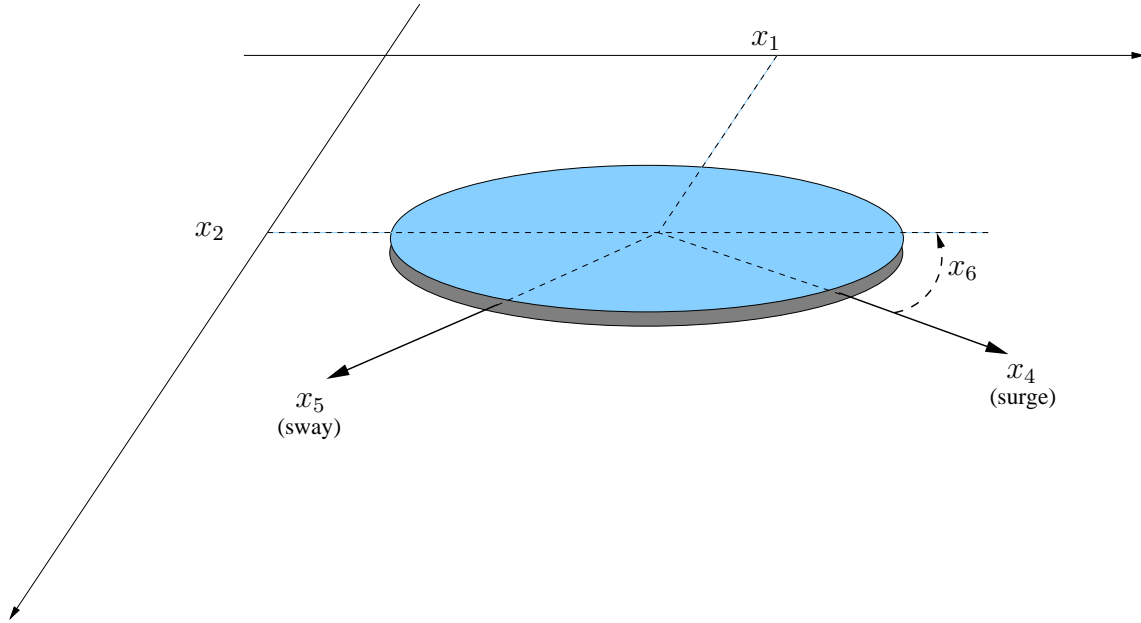


Figure 4.8: Kinematic Model of a Hovercraft.

since it can always be eliminated using a preliminary feedback. Finally, m_{33} simply acts as a scaling factor on the control input u_3 , so there is no loss of generality in setting it to 1. With these assumptions we obtain the simplified underactuated hovercraft vessel system

$$\dot{x} = \begin{bmatrix} v \cos x_3 - v \sin x_3 \\ v \sin x_3 + v \cos x_3 \\ x_4 \\ 0 \end{bmatrix} + \begin{bmatrix} 0 \\ 0 \\ 0 \\ 1 \end{bmatrix} u \quad (4.11)$$

$$y = \text{col}(x_1, x_2).$$

4.3.1 Following arbitrary paths

Consider the problem of maneuvering the output of (4.11) to an arbitrary curve $\sigma(\mathbb{D})$ satisfying Assumptions 1 and 2 with $r \geq 3$. The situation here is similar to that encountered for the car in Section 4.2. The lift of $\sigma(\mathbb{D})$ is a well defined submanifold of dimension 3 ($\Gamma = \sigma(\mathbb{D}) \times \mathbb{R}^2$). Unlike the car model, the hovercraft model, does not have

a singularity. The underactuated nature of (4.11) can be used to characterize Γ^* as

$$\Gamma^* = \{x \in \mathbb{R}^4 : x = (\sigma(t), \arctan2(\dot{\sigma}(t)) - \frac{\pi}{4}, \frac{d}{dt}(\arctan2(\dot{\sigma}(t))), t \in \mathbb{D}\}.$$

Here x_4 is constrained to be exactly the signed curvature of σ on Γ^* . We deduce that Γ^* is well defined and $n^* = 1$. Furthermore we have that $L_{f^*}h = \text{col}(v \cos x_3 - v \sin x_3, v \sin x_3 + v \cos x_3)$ is bounded away from zero. Finally, if we assume that $\|\dot{\sigma}\| = 1$, then in order for the hovercraft system to follow $\sigma(\mathbb{D})$, we have that f^* generates a flow $t \mapsto \Phi_t^{f^*} = (\sigma(vt), \arctan2(v\dot{\sigma}(vt)) - \frac{\pi}{4}, \frac{d}{dt}(\arctan2(v\dot{\sigma}(t))))$ which is well-defined for $\forall t \in \mathbb{D}$. Therefore, Assumption 3 is automatically satisfied.

Theorem 3.1.4 can be applied to the hovercraft system. Checking the transverse linear controllability condition with $n^* = 1$ and $n = 4$ we require

$$T_x\Gamma^* + \text{span}\{g, ad_f g, ad_f^2 g\} = \mathbb{R}^4.$$

In this case we have that

$$ad_f g = \frac{\partial}{\partial x_3}, \quad ad_f^2 g = (-v \sin x_3 - v \cos x_3) \frac{\partial}{\partial x_1} + (v \cos x_3 - v \sin x_3) \frac{\partial}{\partial x_2}.$$

It is easy to check that transverse linear controllability holds since $T_x\Gamma = T_x\Gamma^* + \text{span}\{g, ad_f g\}(x)$ and just as in the case of the car, $\text{span}\{ad_f^2 g\} \perp \Gamma$.

Next, we check that the desired distribution is involutive. It turns out to indeed be involutive (in fact, the vector fields commute). Therefore, by Theorem 3.1.4, we conclude that Problem 2 has a solution.

Lemma 4.3.1. *If the curve σ in (4.11) satisfies Assumption 1 with $r \geq 3$ then Corollary 3.1.2 applies to the hovercraft system (4.11).*

Proof. This proof proceeds in the same fashion as the proof of Lemma 4.1.1 and Lemma 4.2.1.

Again we require that σ be at least C^3 since Γ^* is embedded in \mathbb{R}^4 .

For the hovercraft, we obtain that the desired relative degree of 3 fails at points for which

$$\left(\frac{\partial \gamma}{\partial x_2} (\cos x_3 - \sin x_3) - \frac{\partial \gamma}{\partial x_1} (\sin x_3 + \cos x_3) \right) = 0. \quad (4.12)$$

The relative degree is ill defined when the hovercraft's heading angle is orthogonal to the desired maneuver. This cannot occur $\forall x \in \Gamma^*$. \square

4.3.2 Following paths generated by 4th order splines

Finally, we will apply the above discussion to solve the maneuver regulation problem for the hovercraft when the desired path is generated by 4th order (C^3) splines. For each segment of the spline, we can use the sole path constraint $\gamma(x)$ to generate the controller valid on the corresponding knot interval, just as was done for the car. Figure (4.9) presents various simulation results for the hovercraft following a cubic spline with 3 knots. The splines approximate the coast line of Lake Ontario near Toronto. Note, that like the car example, the hovercraft requires that the splines be at least C^3 in order to obtain bumpless switching.

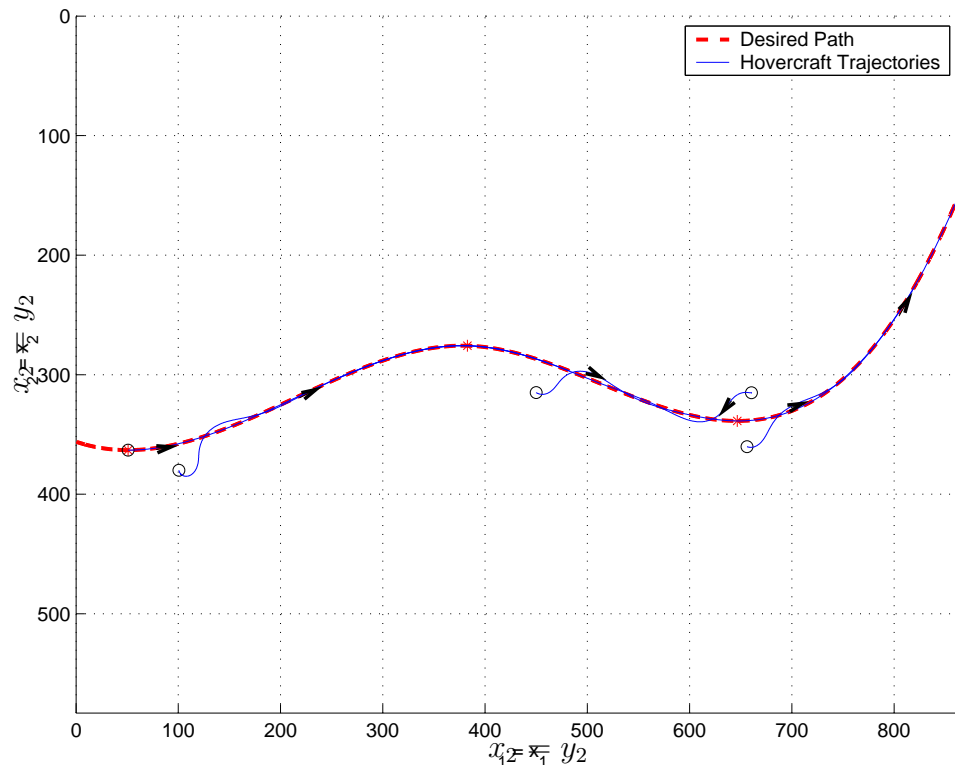


Figure 4.9: Hovercraft output trajectories following an approximation of the Lake Ontario coast line near Toronto.

4.4 1-trailer Systems

In this section we investigate the use of transverse feedback linearization on n -trailer systems with $n = 1$. We fix the translational velocity of the front vehicle to some $v \neq 0$ and then attempt to solve the maneuver regulation problem for the final trailer using solely the steering input. We will show that transverse feedback linearization cannot be applied to the 1-trailer system.

Trailer systems have garnered a lot of attention in the control systems literature on motion control. Examples of works dealing with articulated vehicles or trailer systems include [4, 5, 6, 7, 11, 18, 21, 41, 42, 43]. The literature distinguishes between two types of trailer systems, the standard trailer system and the general trailer system [4]. The standard n -trailer system is one where there is no *off axle hitching*. Each axle is hitched to the preceding trailer by means of a rigid bar. This is the trailer system investigated by Fliess et al. [21]. It is a differentially flat system and can be transformed into the chain form [43]. The general 1-trailer is one which has off axle hitching. That is, trailers are attached not exactly in the middle of the preceding axle, but at a positive distance from it. Here we consider standard trailer systems modeled with a unicycle as the tractor or lead vehicle. See figure (4.10) for an image of the trailer we consider. The kinematic model is given by

$$\dot{x} = \begin{bmatrix} v \cos x_3 \\ v \sin x_3 \\ 0 \\ \frac{v}{L} \sin(x_4 - x_5) \end{bmatrix} + \begin{bmatrix} 0 \\ 0 \\ 1 \\ 0 \end{bmatrix} u \quad (4.13)$$

$$y = \text{col}(x_1 - L \cos x_4, x_2 - L \sin x_4).$$

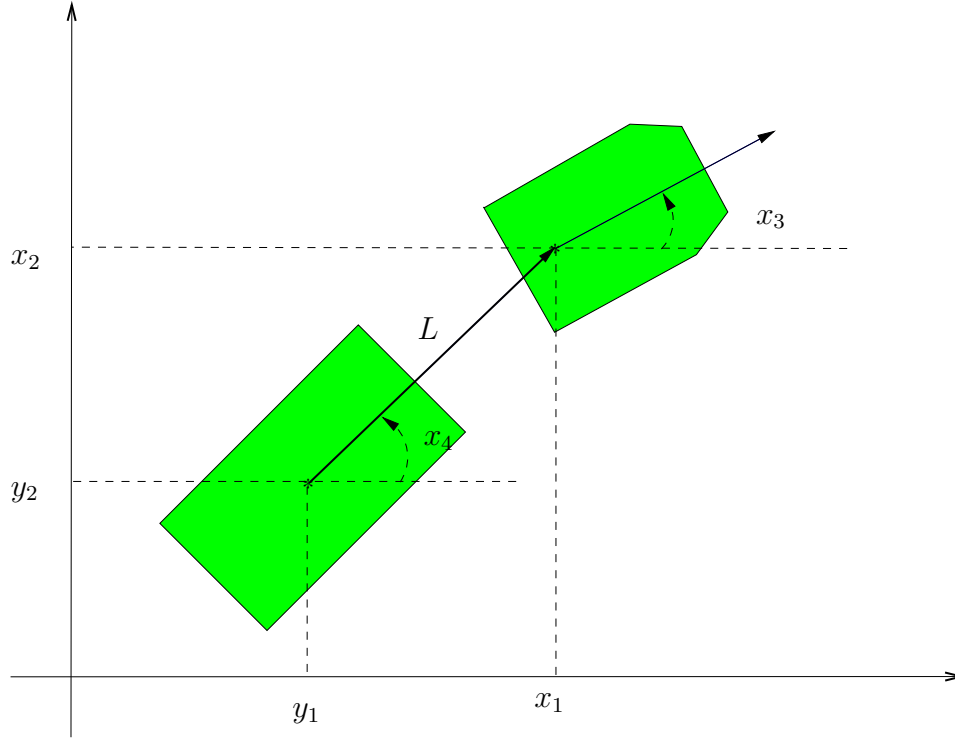


Figure 4.10: Kinematic model of the Standard 1-trailer.

4.4.1 Following a sinusoid

The goal is to force the output of system (4.13) (i.e. the position of the last trailer) to follow a sinusoid

$$\sigma : \lambda \mapsto \text{col} \left(\lambda, 100 \cos \left(\frac{\lambda}{100} \right) \right).$$

Notice, that unlike the previous examples, the output of this system is nonlinear. The curve σ satisfies Assumption 1 and the first part of Assumption 2 with

$$\sigma(\mathbb{D}) = \left\{ y \in \mathbb{R}^2 : y_2 - 100 \cos \left(\frac{y_1}{100} \right) = 0 \right\}.$$

In general, the nonlinear output means that it is not clear whether or not the path lift Γ is a submanifold of the state space. The transversality condition (2.3) is satisfied $\forall x \in \mathbb{R}^4$ since

$$\text{Im}(dh)_x = \text{Im} \begin{bmatrix} 1 & 0 & 0 & L \sin x_4 \\ 0 & 1 & 0 & -L \cos x_4 \end{bmatrix} = \mathbb{R}^2 \quad (4.14)$$

which implies

$$\Gamma = \left\{ x \in \mathbb{R}^4 : x_2 - L \sin x_4 - 100 \cos \left(\frac{1}{100} (x_1 - L \cos x_4) \right) = 0 \right\} \quad (4.15)$$

is an embedded submanifold and Assumption 2 is satisfied. In the subsequent discussion, we will require various Lie brackets associated with system (4.13).

$$ad_f g = (v \sin x_3) \frac{\partial}{\partial x_1} + (-v \cos x_3) \frac{\partial}{\partial x_2} + \left(-\frac{v}{L} \cos(x_3 - x_4) \right) \frac{\partial}{\partial x_4} \quad (4.16)$$

$$ad_f^2 g = -\frac{v^2}{L^2} (\sin^2(x_3 - x_4) + \cos^2(x_3 - x_4)) \frac{\partial}{\partial x_4} \quad (4.17)$$

4.4.2 Characterizing Γ^*

To check if Assumption 3 is satisfied, we must first characterize Γ^* . Note that this system is kinematically equivalent to a unicycle with a trailer. From the discussion in Section 4.1 we know that if we desired that the front vehicle follow a path (i.e. $y = \text{col}(x_1, x_2)$), then by Lemma 4.1.1, a controller which accomplishes this task can be designed using Corollary 3.1.2. For the case $y = \text{col}(x_1, x_2)$, we would find that

$$\Gamma = \left\{ x \in \mathbb{R}^4 : x_2 - 100 \cos \left(\frac{x_1}{100} \right) = 0 \right\}.$$

and

$$\Gamma^* = \left\{ x \in \Gamma : \sin \left(\frac{x_1}{100} \right) \cos x_3 + \sin x_3 = 0 \right\}$$

We would conclude that for the case when $y = \text{col}(x_1, x_2)$, $n^* = 2$. This shows that $\dim \Gamma^*$ depends on the degrees of freedom, or redundant dynamics available in a system. The trailer position, a function of the x_4 dynamics in (4.13), is irrelevant to the problem of making the tractor follow a path. Thus the extra degree of freedom in the dynamics are reflected in the dimension of Γ^* .

Returning to the case $y = \text{col}(x_1 - L \cos x_4, x_2 - L \sin x_4)$, the above discussion leads to the strong suspicion that $n^* = 1$. The standard n-trailer system is flat [21]. Specifying

a path for the final vehicle completely determines the state of the system. This implies that $n^* = 1$ for this system and so we seek to characterize Γ^* as the zero level set of 3 functions. A natural tool for accomplishing the goal of characterizing Γ^* is the zero dynamics algorithm of Isidori and Moog [26, 27] (see Section 2.4). We can apply the zero dynamics algorithm by choosing our initial point as any $x_0 \in \Gamma^*$ and some $u_0 \in \mathbb{R}$ such that $f(x_0) + g(x_0)u_0 \in T_x\Gamma^*$. This illustrates a drawback of our definition of a regular point. We do not have, a priori, a point x^0 and real number u_0 such that $f(x^0) + g(x^0)u_0 \in T_x\Gamma^*$. However, as we now show, this problem can be overcome. Let us go through, in detail, the zero dynamics algorithm applied at some $x \in \mathbb{R}^n$ for the trailer system.

$$M_0 = \Gamma = (\gamma \circ h)^{-1}(0) = M_0^c.$$

Recall from the discussion of Section 2.4, that $U_0 = \mathbb{R}^4$ and so by transversality, $M_0 = M_0^c$. Let $H_0(x) := (\gamma \circ h)(x)$, i.e.,

$$M_0^c = \left\{ x \in \mathbb{R}^4 : H_0(x) = 0 \right\}$$

The next step of the algorithm yields

$$M_1 = \left\{ x \in M_0^c : f(x) \in \text{span} \{g\}(x) + T_x M_0^c \right\}$$

where $T_x M_0^c = \ker(dH_0)$. Then M_1 can be written as

$$M_1 = \left\{ x \in M_0^c : \langle dH_0, f(x) \rangle + \langle dH_0, g(x) \rangle u = 0 \right\}.$$

At this step, $L_g H_0 \equiv 0$ and $L_f H_0 \not\equiv 0$, so M_1 is not invariant. We must add another constraint, namely $L_f H_0 = 0$. Let $H_1 = \text{col}(H_0, L_f H_0)$ then we have that

$$M_1 = \left\{ x \in \mathbb{R}^4 : H_1(x) = 0 \right\}$$

where

$$H_1 = \begin{bmatrix} (\gamma \circ h) \\ L_f H_0 \end{bmatrix} = \begin{bmatrix} x_2 - 100 \cos\left(\frac{x_1}{100}\right) \\ \sin\left(\frac{1}{100}(x_1 - L \cos x_4)\right) \cos x_3 + \sin x_3 - \sin(x_3 - x_4) \cos x_4 \\ + \sin(x_3 - x_4) \sin\left(\frac{1}{100}(x_1 - L \cos x_4)\right) \sin x_4 \end{bmatrix}.$$

M_1^c is the connected component of $M_1 \cap U_1$, where U_1 is the neighborhood of x in which M_1 is a smooth manifold. In this case $M_1 = M_1^c$ since dH_1 is full rank for all $x \in \mathbb{R}^4$. The next iteration yields

$$M_2 = \left\{ x \in M_1^c : \langle dH_1, f(x) \rangle + \langle dH_1, g(x) \rangle u = 0 \right\}. \quad (4.18)$$

$$L_g H_1 = \begin{bmatrix} 0 \\ L_g L_f H_0 \end{bmatrix} = \begin{bmatrix} 0 \\ v \left(\cos x_3 - \sin\left(\frac{1}{100}(x_1 - L \cos x_4)\right) \sin x_3 + -\cos(x_3 - x_4) \cos x_4 \right. \\ \left. + \cos(x_3 - x_4) \sin\left(\frac{1}{100}(x_1 - L \cos x_4)\right) \sin x_4 \right) \end{bmatrix}.$$

so it is not immediately clear whether $L_g H_1 = 0$ on M_1^c . If $L_g L_f H_0$ is nonzero on M_1^c then it would follow that (4.18) can be solved for u leading to the conclusion that $M_2 = M_1^c$ and the algorithm terminates yielding $n^* = 2$. Otherwise, the algorithm continues.

Suspecting that $n^* = 1$, we continue the algorithm under the assumption that $L_g L_f H_0(x) = 0$ on M_1^c , later, we verify that this assumption is valid. Let $H_2 = \text{col}(H_1, L_f H_1) = \text{col}(H_1, L_f^2 H_0)$. The next iteration in the algorithm yields

$$M_3 = \left\{ x \in M_2^c : \langle dH_2, f(x) \rangle + \langle dH_2, g(x) \rangle u = 0 \right\}.$$

Again, we find that due to the complexity of the expression for $\langle dH_2, g(x) \rangle$, it is unclear whether or not $M_3 = M_2^c$.

We are now set to show, numerically, the following two facts

$$(1) (\forall x \in M_1^c \cap U) L_g L_f H_0(x) = 0$$

$$(2) (\forall x \in M_2^c \cap U) L_g L_f^2 H_0 \neq 0$$

(where U is some open set) which allow us to conclude that the assumption above is in fact correct and that the algorithm terminates with $n^* = 1$ and $\Gamma^* \cap U = H_2^{-1}(0) \cap U$. We do that by numerically generating a uniform orthogonal grid of M_1^c (a two dimensional manifold) and M_2^c (a one dimensional manifold) and checking whether properties (1) and (2) hold at the resulting grid points. To this end, given an n -dimensional submanifold M in \mathbb{R}^m , expressed as $M = H^{-1}(0)$, where $H = \text{col}(H_1, \dots, H_{m-n}) : \mathbb{R}^m \rightarrow \mathbb{R}^{m-n}$, we introduce the following

Numerical procedure to generate a uniform grid of M

1. Find a basis $\{v_1, \dots, v_n\}$ for $T_x M = \ker(dH_x)$.
2. Apply Gram - Schmidt orthonormalization to get $\{\tilde{v}_1, \dots, \tilde{v}_n\}$
3. Let $G = \sum_{i=1}^{m-n} H_i^2$ and let

$$\hat{v}_i = \begin{cases} \tilde{v}_i - \mu \frac{\nabla G}{\|\nabla G\|} & \text{if } \|\nabla G\| \geq \epsilon \\ \tilde{v}_i - \mu \frac{\nabla G}{\epsilon} & \text{if } \|\nabla G\| < \epsilon. \end{cases}$$

where $\mu, \epsilon > 0$.

4. Choose an $x^0 \in M$ and integrate the \hat{v}_i to generate an orthogonal uniform grid.

The procedure above uses a continuous approximation to the gradient vector field ∇G to make M attractive [29]. The parameter μ can be used to control the speed of

convergence, in this work we set $\mu = 1$. The value of ϵ should be significantly larger than the integration tolerance used in step 4. We use a tolerance of 10^{-12} and $\epsilon = 10^{-3}$. Figure 4.11 illustrates the concept of gridding for the case $\dim M = 2$.

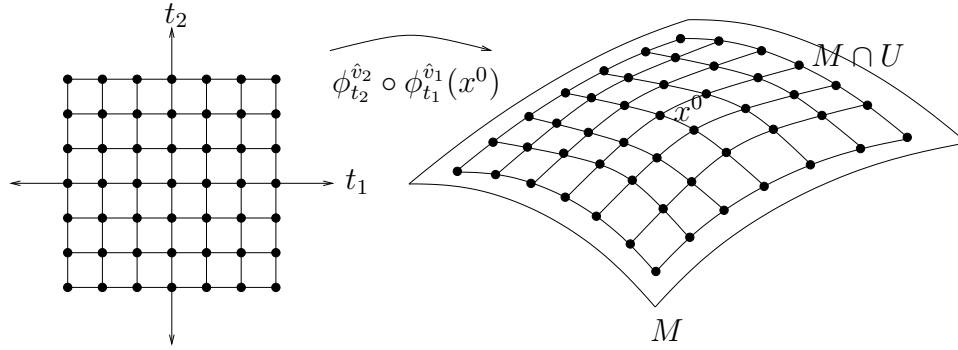


Figure 4.11: Gridding a two dimensional manifold.

Remark 4.4.1. The map generated by the gridding algorithm is isometric, i.e., unit time intervals are mapped to unit length intervals in the grid. The vector fields \hat{v}_i are continuous and the manifold M is attractive for each of them. This is useful for numerical stability of the procedure: if the algorithm is initialized at a point x^0 which is not exactly on M , the procedure generates grid points that get closer and closer to M . Finally, the flows associated to the vector fields \hat{v}_i commute, i.e., starting from a point $x \in M$, $\phi_{t_j}^{\hat{v}_j} \circ \phi_{t_i}^{\hat{v}_i}(x) = \phi_{t_i}^{\hat{v}_i} \circ \phi_{t_j}^{\hat{v}_j}(x)$.

Initialize the procedure at a point x^0 found using an unconstrained nonlinear minimization on the sum of squares

$$G(x) = \sum_{i=0}^2 (L_f^i H_0(x))^2. \quad (4.19)$$

to obtain

$$x^0 = [471.19040123 \quad -0.060442363014 \quad 0.78665447694 \quad 0.78412668186]$$

$$G(x^0) = 5.7281 \times 10^{-21}.$$

We have now obtained a point $x^0 \in M_2^c \subset M_1^c$. We first address item (1), the assumption that $(\forall x \in M_1^c \cap U) L_g H_1 = 0$. Using symbolic mathematical software, solve for two independent solutions, v_1 and v_2 , spanning $\ker(dH_1)$. These solutions are valid in a neighborhood of x^0 . Apply Gram-Schmidt orthonormalization [22] to v_1 and v_2 to obtain

$$\tilde{v}_1 = \frac{v_1}{\|v_1\|}$$

and

$$\tilde{v}_2 = \frac{v_2 - (v_2 \cdot \tilde{v}_1)\tilde{v}_1}{\|v_2 - (v_2 \cdot \tilde{v}_1)\tilde{v}_1\|}.$$

In this case, we use (4.19) with $i = 0, 1$ to generate a gradient vector field and obtain the vector fields \hat{v}_1 and \hat{v}_2 . Generate a uniform grid centered at x^0 . In order to determine if $L_g L_f H_0 = 0$, we check its value at each point of the grid. A plot of this is shown in Figure 4.12. Figure 4.12 shows that $|L_g L_f H_0| < 10^{-11}$, which close to the accuracy of

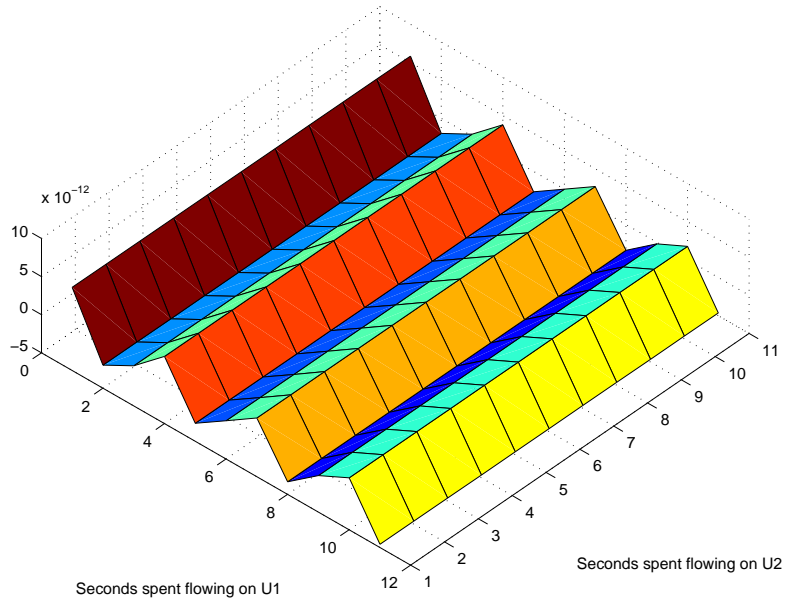


Figure 4.12: The value of $L_g L_f H_0$ over a uniform 2-dimensional grid of M_1^c .

the numerical integration used to generate the gridding. We conclude that $L_g L_f H_0 \cong 0$ on M_1^c .

Finally, we address item (2) by applying the gridding algorithm to M_2^c . Again, using symbolic mathematical software, we solve for v_1 , spanning $\ker(dH_2)$ which we normalize

to obtain \tilde{v}_1 . Here we use (4.19) directly to generate a gradient vector and obtain \hat{v}_1 . We generate a uniform gridding of M_2^c starting from x^0 .

Figure 4.13 shows the value of the functions defining $H_2(x)$ along the gridding. After

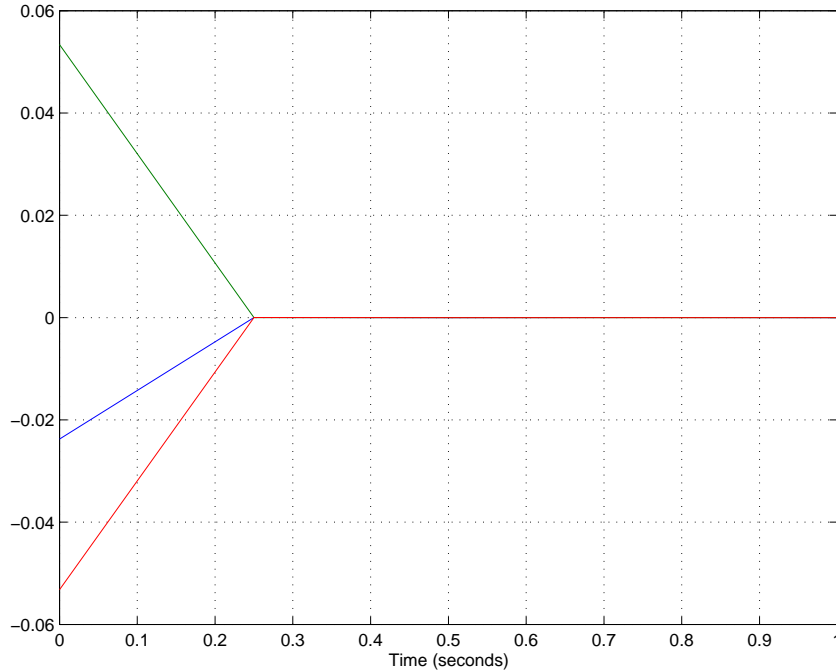


Figure 4.13: The value of the functions defining $H_2(x)$ generated by a uniform gridding of Γ^* .

0.3 seconds the function H_2 , evaluated at the grid points is essentially zero. This illustrates the numerical stability of the procedure: the point x^0 found using an unconstrained optimization algorithm is not exactly on M_2^c because $H_2(x^0)$ is not exactly zero. The procedure generates grid points that get closer and closer to M_2^c because H_2 gets closer and closer to zero. Next, Figure 4.14 shows that $L_g L_f^2 H_0 \neq 0$ on M_2^c . These plots confirm that $M_2^c = \Gamma^*$ has been properly characterized. Figure 4.15 shows that the output the trailer system (4.13) along the gridding of $M_2^c = \Gamma^*$ perfectly follows the prescribed path. This is a further evidence of the fact that the procedure generates points on Γ^* .

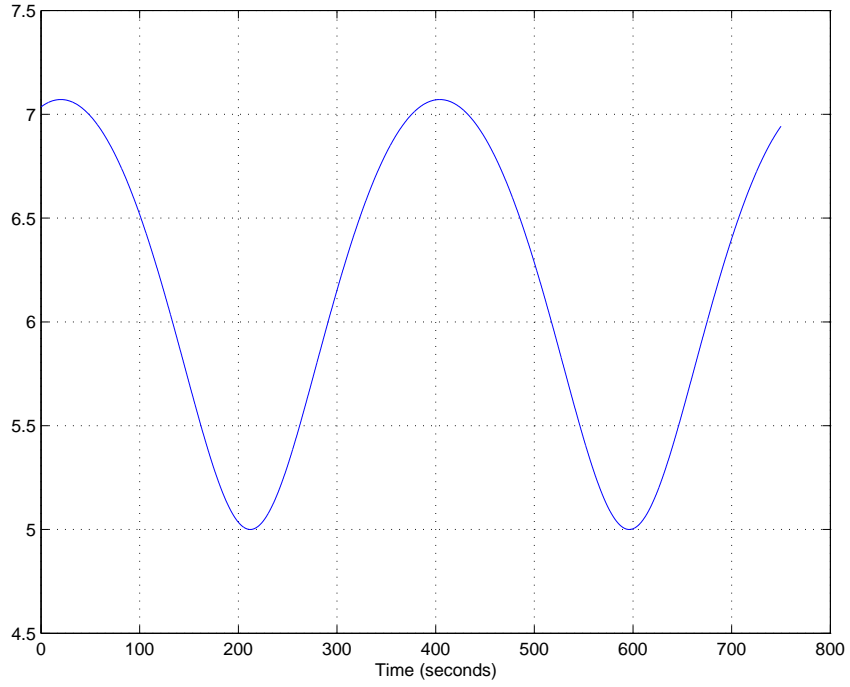


Figure 4.14: The value of $L_g L_f^2 h$ along a uniform gridding of Γ^* .

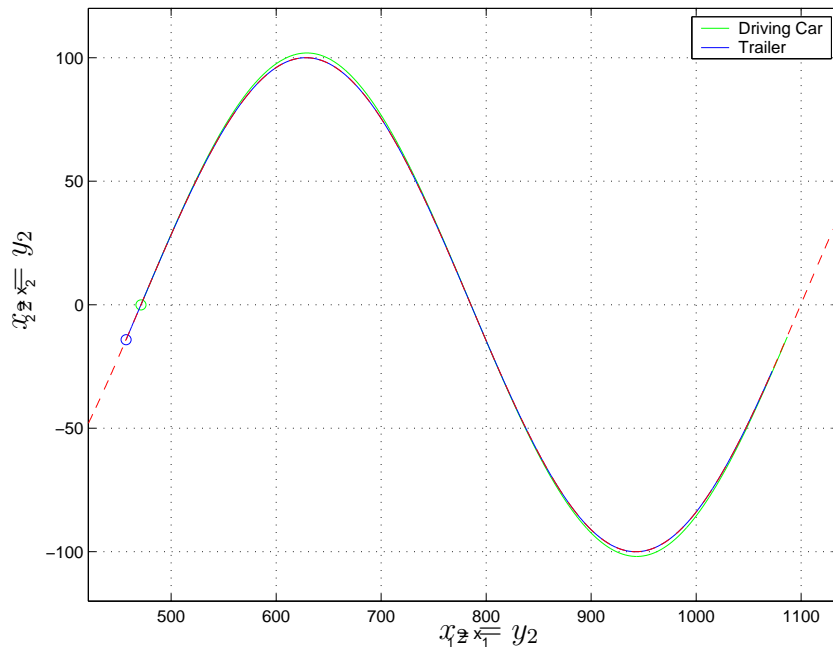


Figure 4.15: Output of the trailer system (4.13) generated by a uniform gridding of Γ^* .

4.4.3 Checking Relative Degree

In order to apply Theorem 3.1.1 to the trailer (4.13), we require a function which yields a relative degree of $n - n^* = 3$. Specifically, if Corollary 3.1.2 is to be applied, we must have that $L_g(\gamma \circ h)(x) = L_g L_f^i(\gamma \circ h)(x) = 0$, and $L_g L_f^2(\gamma \circ h)(x) \neq 0$ for all x in a neighborhood of Γ^* . We have already shown that $L_g(\gamma \circ h)(x) \equiv 0$ and $L_g L_f^2(\gamma \circ h)(x) \neq 0$. Furthermore, we have shown that $L_g L_f(\gamma \circ h)(x) = 0 \forall x \in \Gamma^*$, so we only need to check the value of $L_g L_f(\gamma \circ h)(x) = 0$ for points near Γ^* . By doing so, one immediately finds that $L_g L_f(\gamma \circ h)$ changes sign in a neighborhood of Γ^* . Thus we conclude that the path constraint does not yield a well defined relative degree and Corollary 3.1.2 does not apply.

Remark 4.4.2. The lone path constraint does not yield a uniform relative degree. If we ignore this fact and implement the controller generated from Corollary 3.1.2, we will find that numerical simulations suggest the controller solves the maneuver regulation problem. The reason for this is that $L_g L_f(\gamma \circ h)(x)$, although nonzero, is small for x sufficiently close to Γ^* .

4.4.4 Involutivity

Next we attempt to apply the results of Theorem 3.1.4. We again rely on numerical analysis to check for transverse linear controllability. We randomly select 100 points in a closed cube of each point along Γ^* . That is, at each point $x \in \Gamma^*$ generated from the gridding above, we randomly select 100 uniformly distributed points in the region

$$C_\epsilon(x) = \left\{ z \in \mathbb{R}^4 : |x_i - z_i| \leq \epsilon, i = 1, \dots, 4 \right\}$$

where $\epsilon = 0.1$. Pointwise we check that transverse linear controllability holds.

$$T_x \Gamma^* + \text{span} \{g, ad_f g, ad_f^2 g\}(x) = \text{span} \{v, g, ad_f g, ad_f^2 g\}(x) = \mathbb{R}^4.$$

Pointwise, the above distribution is the image of a matrix. Since this analysis is numerical, we check the condition number of the transverse linear controllability matrix. In other

words, numerical errors will mean that the determinant will rarely be identically zero. Instead we check that the condition number (i.e the ratio of the largest singular value to the smallest), is sufficiently small.

Figure 4.16 shows the result of the analysis. In Figure 4.16, the abscissa is the point along Γ^* . The ordinate is the number of well conditioned points obtained in the random sample. The constant line at 100 indicates that every point tested yields a well conditioned matrix. We conclude that transverse linear controllability holds in a neighborhood of Γ^* . Next we check for involutivity of the distribution span $\{g, ad_f g\}$.

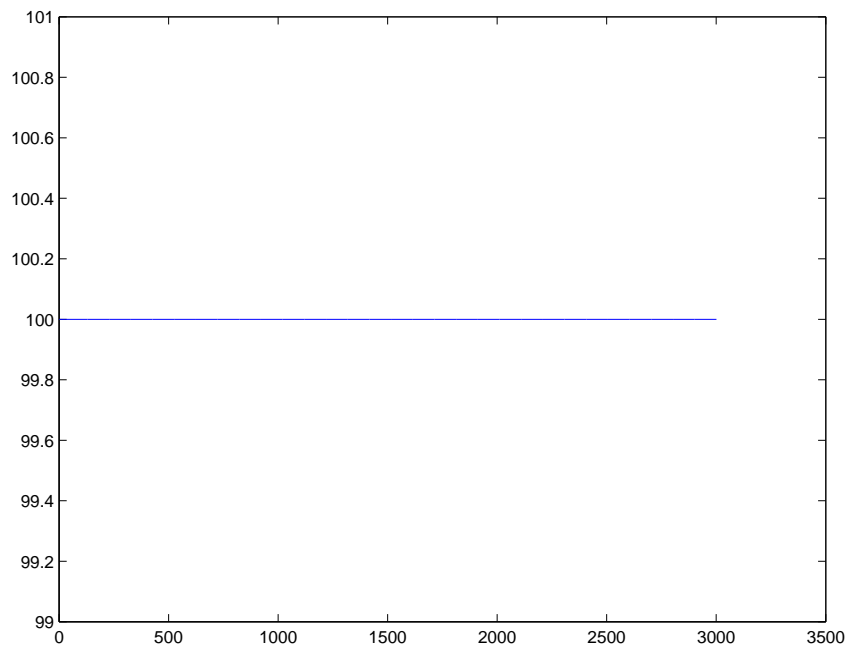


Figure 4.16: Numerically checking transverse linear controllability in a neighborhood of Γ^* .

We find that

$$[g, ad_f g] = (v \cos x_3) \frac{\partial}{\partial x_1} + (v \sin x_3) \frac{\partial}{\partial x_2} + \left(\frac{v \sin(x_3 - x_4)}{L} \right) \frac{\partial}{\partial x_4}. \quad (4.20)$$

Since (4.20) cannot be written as a linear combination of (4.16) and (4.17), we conclude that involutivity fails. Thus, the sufficient conditions of Theorem 3.1.4 do not hold

and we cannot construct a function α based on vector field flows. In light of this, a natural thing to do is to show that Problems 2 and 3 are not solvable for the 1-trailer system. To this end, we employ Corollary 3.3.5 and check the involutive closure of $D = \text{span}\{g, ad_f g, ad_f^2 g\}$. A semi-constructive procedure for finding the involutive closure of a distribution can be found in [26, Theorem 1.4.1] in the proof of sufficiency. Here we use symbolic mathematics software to find $\text{inv } D$ [31]. It turns out that

$$\text{inv } D = \text{span}\{g, ad_f g, v_3, v_4\} \quad (4.21)$$

where

$$v_3 = (-v \cos x_3) \frac{\partial}{\partial x_1} + (-v \sin x_3) \frac{\partial}{\partial x_2} + \left(-\frac{v}{L} \sin(x_3 - x_4)\right) \frac{\partial}{\partial x_4}$$

$$v_4 = \left(\frac{v^2}{L^2} (\sin^2(x_3 - x_4) + \cos^2(x_3 - x_4))\right) \frac{\partial}{\partial x_4}.$$

In matrix form

$$\text{inv } D = \begin{bmatrix} 0 & v \sin x_3 & -v \cos x_3 & 0 \\ 0 & -v \cos x_3 & -v \sin x_3 & 0 \\ 1 & 0 & 0 & 0 \\ 0 & -\frac{v}{L} \cos(x_3 - x_4) & -\frac{v}{L} \sin(x_3 - x_4) & \frac{v^2}{L^2} (\sin^2(x_3 - x_4) + \cos^2(x_3 - x_4)) \end{bmatrix}$$

and since $ad_f^2 g = -v_4$, we conclude that the conditions of Theorem 3.3.3 do not hold and by Corollary 3.3.5, Problems 2 and 3 are unsolvable. This shows that even though a solution to the general maneuver regulation problem, Problem 1, exists (recall that the trailer is differentially flat), the approach used here does not yield a solution.

Conclusions and Future Research

Conclusions

This thesis has investigated the maneuver regulation problem from a general perspective. Solutions were presented for Problems 2 and 3. The solutions to these problems solve an output stabilization problem, but under the special conditions imposed in Chapter 2, the maneuver regulation problem can also be solved.

In Chapter 3, a semi-constructive procedure for designing maneuver regulation controllers was introduced. The drawback of these procedures is that they rely on the knowledge of the flow of vector fields, which may not be amenable to closed form solutions. It was shown that when specialized to the LTI case, the work presented here recovers a well known result on output stabilization. The approach presented was then applied to various kinematic systems in Chapter 4.

In conclusion, the main contribution to the path following problem lies in the sufficient checkable conditions of Theorem 3.1.4 and the necessary and sufficient conditions of Theorem 3.3.3. In particular, we were able to extend the concept of transverse feedback linearization from the results of Banaszuk and Hauser [8] and apply it to a more general problem. We quantified the role which unstable zero dynamics play in this approach to path following. We also showed that in certain applications, this approach leaves a degree of control freedom for assigning the zero dynamics. Most importantly, we showed that even if a system is not input - output linearizable, we may be able to construct a function suitable for output stabilization, which under the right conditions, also solves a

maneuver regulation problem.

Future Research

Thanks in large part to the generality of the approach, this topic has opened many doors for possible future research. Some obvious directions in which this work can be extended include output feedback systems, robustification of the controller and hybrid controllers to switch through singularities [46]. Approximate solutions to the differential equations can be generated using power series. The use of approximate vector field flows for generating virtual output functions is a viable topic for future research. In order to further generalize the results presented here, the multi input-input multi-output case should also be investigated.

In view of the connection between this thesis and output stabilization, the results here may be relevant to output synchronization [38]. Finally, in connection with the MIMO case, it would prove to be of practical interest to be able to quantify the degrees of control freedom available for assigning zero dynamics. That is, to be able to quantify the minimum number of controls needed to solve the geometric task. This test would presumably generate checkable conditions which tell the designer, a priori, whether or not they will have any degree of freedom for the dynamic task.

Appendix A

Basic Concepts

This appendix reviews some of the basic concepts and terms used in this thesis. The purpose of this appendix is to give an informal, intuitive review of some tools used throughout this work. These concepts can be found in [12, 26, 29, 36].

Manifold Differentiable manifolds generalize the notion of a hypersurface to abstract sets. A differentiable manifold M (a smooth manifold) is a set equipped with a differentiable structure, that is, an atlas equipped with C^∞ -compatible coordinate charts. A coordinate chart is a pair (V, ϕ) , where $V \subset M$ and $\phi : V \rightarrow \mathbb{R}^m$ ($m := \dim M$) is a bijection. A pair of coordinate charts, (V_1, ϕ_1) and (V_2, ϕ_2) , are C^∞ compatible if $V_1 \cap V_2 \neq \emptyset$ implies that $\phi_2 \circ \phi_1^{-1}$ is a diffeomorphism. The atlas is a collection of C^∞ compatible coordinate charts which cover M . In this work all manifolds are smooth.

Submanifold A subset N of an m -dimensional manifold M is called an embedded or regular submanifold of dimension $n < m$, if N can locally be represented as a slice of M , $(\forall p \in N)(\exists (U, \phi), p \in U) \phi(U \cap N) = \{q \in U \cap N : \phi_{n+1}(q) = \dots = \phi_m(q) = 0\}$. In this work, it is understood that the term submanifold implies embedded or regular submanifold. See Figure A.1.

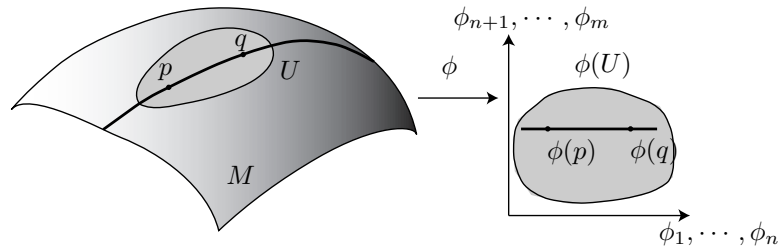


Figure A.1: An n -dimensional slice of $U \subset M$.

T_pM This refers to the tangent space to a manifold M at $p \in M$. The tangent space, T_pM , can be given the structure of an m -dimensional vector space, where $m = \dim M$. There are several ways of doing this. One of them is to define T_pM as the collection of *all* operators $X_p : C^\infty(p) \rightarrow \mathbb{R}$ which satisfy the linearity property and the Leibniz rule. See Figure A.2. Alternatively, T_pM is the set of all tangent vectors to M at p .

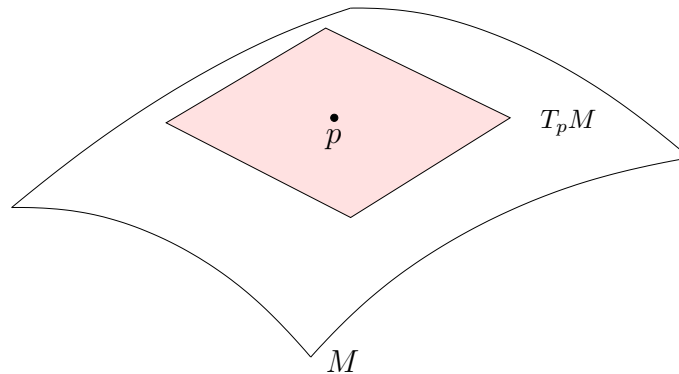


Figure A.2: An example of the tangent space at a point $p \in M$.

$\frac{\partial}{\partial \phi_i}$ This is the notation used to indicate the natural basis of T_pM . Since T_pM is defined as a space of operators (see above), this notation indicates that the basis for T_pM is also generated by operators.

Vector Field A smooth vector field f , on a manifold N , is a mapping which assigns to each $p \in N$ a tangent vector $f(p)$ in T_pN . The following demonstrates the notation

for vector fields used interchangeably in this thesis.

$$f(x) = \begin{bmatrix} x_3 \\ 0 \\ 1 + x_1^2 \end{bmatrix} = x_3 \frac{\partial}{\partial x_1} + (1 + x_1^2) \frac{\partial}{\partial x_3}.$$

Parallelizable An m -dimensional manifold M is *parallelizable* if m vector fields *on* M , s_1, \dots, s_m , can be defined such that $\forall p \in M$, $s_1(p), \dots, s_m(p)$ are linearly independent.

(dh) $_x$ Denotes the Jacobian matrix of a differentiable mapping $h : \mathbb{R}^m \rightarrow \mathbb{R}^n$ evaluated at the point $x \in \mathbb{R}^m$.

Regular Value Given a mapping between manifolds $F : M \rightarrow N$, a point $q \in F(M)$ is said to be a *regular value* of F if $(\forall p \in M)$ such that $F(p) = q$, $\text{rank}(dF)_p = \dim N$.

$L_f \lambda$ The directional or *Lie* derivative of a real valued function λ in the direction of the vector field f

$$(L_f \lambda)(p) = \langle (d\lambda)_p, f(p) \rangle = \left(\frac{\partial \lambda}{\partial x} f(x) \right)_{x=p}.$$

$L_f^k \lambda$ Repeated Lie derivatives

$$(L_f^k \lambda)(p) = \langle (dL_f^{k-1} \lambda)_p, f(p) \rangle = \left(\frac{\partial L_f^{k-1} \lambda}{\partial x} f(x) \right)_{x=p}.$$

$L_g L_f \lambda$ Lie derivative of λ along the vector field f and then along the vector field g

$$(L_g L_f \lambda)(p) = \langle (dL_f \lambda)_p, g(p) \rangle = \left(\frac{\partial L_f \lambda}{\partial x} g(x) \right)_{x=p}.$$

$[f, g]$ The *Lie product* or *bracket* of the smooth vector fields f and g . The result is a new smooth vector field given by

$$[f, g](x) = \frac{\partial g}{\partial x} f(x) - \frac{\partial f}{\partial x} g(x).$$

The Lie bracket can be used to give the space of vector fields on a manifold the structure of a *Lie algebra*.

$ad_f^k g$ Notation used to simplify the representation of repeated Lie bracketing

$$ad_f^0 g = g, \quad ad_f^k g = [f, ad_f^{k-1} g].$$

$\Phi_t^f(x^0)$ Denotes the flow associated to a vector field f from the initial condition $x(0) = x^0$. In other words, $x(t) = \Phi_t^f(x^0)$ solves the ordinary differential equation

$$\dot{x}(t) = f(x), \quad x(0) = x^0.$$

Complete Vector Field A vector field f defined on a manifold N is complete if $(\forall p \in N) \Phi_t^f(p)$ is defined $\forall t \in \mathbb{R}$.

S^1 (**Unit Circle**) The unit circle in \mathbb{R}^2 . The simplest 1 dimensional space that isn't just \mathbb{R} . May be defined to be all points in \mathbb{R}^2 unit distance from a fixed point. Equivalently

$$S^1 = \{z \in \mathbb{C} : |z| = 1\}$$

Controlled Invariant Consider a control system defined in \mathbb{R}^n . Let M be a smooth connected submanifold of \mathbb{R}^n containing the point x^0 . The manifold M is said to be (locally) controlled invariant at x^0 if there exists a smooth mapping $u : M \rightarrow \mathbb{R}^m$ (and a neighborhood U_0 of x^0), such that the vector field of the resulting closed loop system is tangent to M for all x in M (in $M \cap U_0$).

Distribution A distribution Δ on a manifold M is a mapping which assigns to each $p \in M$ a subspace, $\Delta(p)$, of $T_p M$. A smooth distribution is one which can be written as the span of smooth vector fields.

Regular at x^0 A distribution Δ , defined on an open set U , is said to be nonsingular if $(\exists d \in \mathbb{Z})(\forall x \in U) \dim \Delta(x) = d$. A distribution Δ is *regular at a point x^0* if there exists a neighborhood U_0 of x^0 in which Δ is nonsingular.

Involutivity A distribution Δ is involutive (it has the property of *involutivity*) if the Lie bracket $[\tau_1, \tau_2]$ of any pair vector fields τ_1 and τ_2 belonging to Δ also belongs to Δ .

$$\tau_1(x), \tau_2(x) \in \Delta(x) \Rightarrow [\tau_1, \tau_2](x) \in \Delta(x).$$

Involutive Closure Given a distribution Δ , the *involutive closure* of Δ , denoted $\text{inv } \Delta$, is the *smallest* (with respect to distributions inclusion) involutive distribution containing Δ .

Integral Manifold Given a distribution Δ defined on a manifold M . A submanifold S_p of M is an *integral submanifold* of Δ passing through p if $(\forall q \in S_p) T_q S_p = \Delta(q)$. So, an integral manifold of Δ is a submanifold whose tangent space, pointwise, coincides with Δ . See Figure A.3.

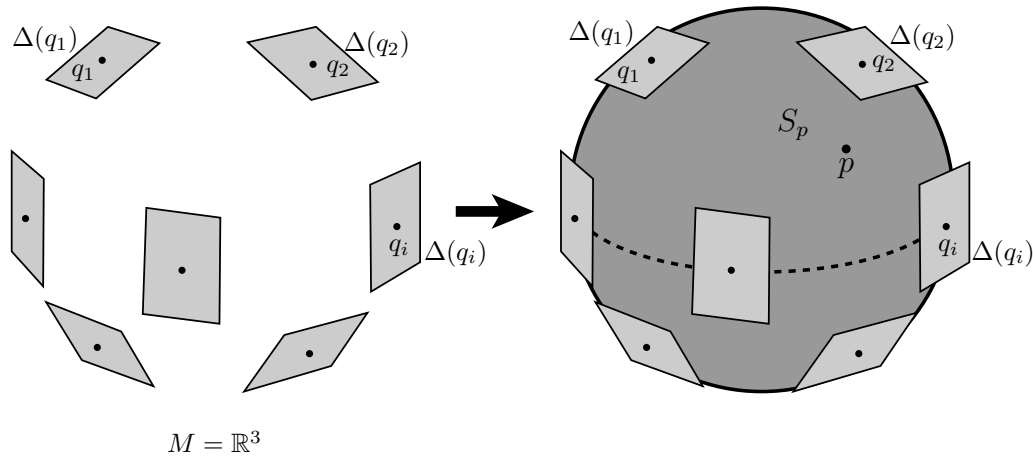


Figure A.3: Example of an integral manifold in \mathbb{R}^3 .

Complete Integrability A distribution Δ on M is said to be *completely integrable* if through each point $p \in M$ there passes an integral submanifold of Δ .

Frobenius Theorem A nonsingular distribution is completely integrable if and only if it is involutive.

Foliation A foliation of M is a partition of M by submanifolds, all having equal dimension. Frobenius Theorem implies that a nonsingular and involutive distribution defines a foliation of an open set $U^0 \subset M$ by integral submanifolds of Δ (called *leaves* of the foliation). See Figure A.4.

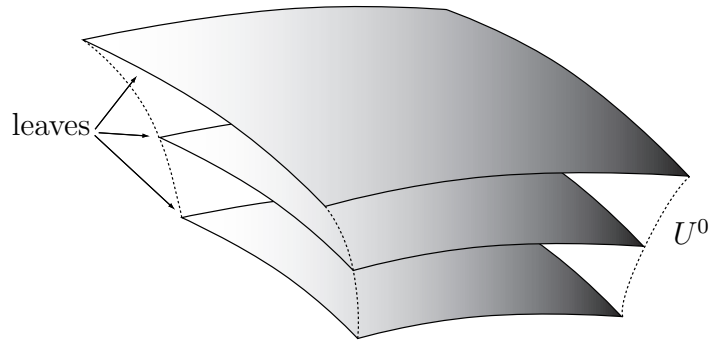


Figure A.4: A foliation by integral submanifolds.

(Uniform) Relative Degree A single input, single output system

$$\dot{x} = f(x) + g(x)u$$

$$y = h(x)$$

defined on \mathbb{R}^n is said to have relative degree r at a point x^0 if

- (i) $L_g L_f^k h(x) = 0$ for all x in a neighborhood of x^0 and $k < r - 1$
- (ii) $L_g L_f^{r-1} h(x^0) \neq 0$.

The system is said to have *uniform* relative degree if (i) and (ii) hold $\forall x \in \mathbb{R}^n$.

Zero Dynamics Manifold The zero dynamics manifold is the largest controlled invariant submanifold, Z^* , contained in $h^{-1}(0)$ (i.e. output zeroing). If the system has a well defined relative degree, then

$$Z^* = \{x \in \mathbb{R}^n : h(x) = L_f h(x) = \dots = L_f^{r-1} h(x) = 0\}.$$

Bibliography

- [1] R. Abraham and J. Robbin. *Transversal Mappings and Flows*. W.A. Benjamin Inc., New York, 1967. [2.1](#)

- [2] M. Aicardi, G. Casalino, A. Bicchi, and A. Balestrino. Closed loop steering of unicycle-like vehicles via lyapunov techniques. *IEEE Robotics and Automation Magazine*, 2(1):27–35, Mar. 1995. [1.1](#), [1.5](#)

- [3] A. Al-Hiddabi and N.H. McClamroch. Tracking and maneuver regulation control for nonlinear nonminimum phase systems: application to flight control. *IEEE Transactions on Control Systems Technology*, 10(6):780–792, Nov. 2002. [1.3](#)

- [4] C. Altafini. Some properties of the general n-trailer. *Intl. Journal of Control*, 74(4):409–424, 2001. [4.4](#)

- [5] C. Altafini. Following a path of varying curvature as an output regulation problem. *IEEE Trans. on Automatic Control*, 47(9):1551–1556, 2002. [1.4](#), [4.4](#)

- [6] C. Altafini. Path following with reduced off-tracking for multibody wheeled vehicles. *IEEE Trans. on Control Systems Technology*, 11(4):598–605, 2003. [1.4](#), [4.4](#)

- [7] A. Astolfi, P. Bolzern, and A. Locatelli. Path-tracking of a tractor-trailer vehicle along rectilinear and circular paths: A Lyapunov-based approach.. *IEEE Transactions on Robotics and Automation*, 20(4):154–160, Feb. 2004. [1.2](#), [4.4](#)

- [8] A. Banaszuk and J. Hauser. Feedback linearization of transverse dynamics for periodic orbits. *Systems and Control Letters*, 26(2):95–105, Sept. 1995. (document), 1.4, 2, 2.1, 2.2, 2.2, 3, 3.1, 3.1.2, 3.3, 3.4, 3.4, 3.4, 3.4, 3.5.2, 4.4.4
- [9] A. Banaszuk and J. Hauser. Feedback linearization of transverse dynamics for periodic orbits in \mathbb{R}^3 with points of transverse controllability loss. *Systems and Control Letters*, 26(3):185–193, Oct. 1995. 1.4
- [10] R. H. Bartels, editor. *An introduction to splines for use in computer graphics and computer modelling*. Morgan Kaufmann Publishers Inc., Los Angeles, 1st edition, 1987. 4.2.2
- [11] P. Bolzern, R.M. DeSantis, and A. Locatelli. An input - output linearization approach to the control of an n-body articulated vehicle. *Journal of Dynamic Systems, Measurement, and Control*, 123(3):309–316, 2001. 1.4, 4.4
- [12] W.M. Boothby. *An Introduction to Differentiable Manifolds and Riemannian Geometry*. Academic Press, London, 2nd, revised. edition, 2003. 1.4, 2.1, 2.1, 3.1.3, A
- [13] C. Chevallereau, G. Abba, Y. Aoustin, F. Plestan, E.R. Westervelt, C. Canudas-De-Wit, and J.W. Grizzle. Rabbit: a testbed for advanced control theory. *IEEE Control Systems Magazine*, 23(5):57–79, Oct. 2003. 1.5
- [14] P. Coelho and U. Nunes. Lie algebra application to mobile robot control: a tutorial. *Robotica*, 21(5):483–493, 2003. 1.4
- [15] L. Consolini and M. Tosques. Local path following problem for time-varying nonlinear control affine systems. In *Proc. of the American Control Conference*, pages 3531 – 3526, Denver, CO, USA, June 2003. 1.1, 2.1, 2.4

- [16] L. Consolini, M. Tosques, and A. Piazzzi. Dynamic path inversion for a class of nonlinear systems. In *Proc. of the 41st IEEE Conference on Decision & Control*, pages 3831 – 3836, Las Vegas, NV, USA, December 2002. [1.1](#)
- [17] C. Canudas de Wit *et al.* *Recent trends in mobile robots (editor, Yuan F. Zheng)*, chapter 5. World Scientific, New York, 1st edition, 1993. [1.2](#)
- [18] R.M. DeSantis. Path-tracking for a tractor trailer-like robot. *International Journal of Robotics Research*, 13(6):533–544, Dec. 1994. [1.2](#), [4.4](#)
- [19] P. Encarnaç o and A. Pascoal. 3-d path following for autonomous underwater vehicle. In *Proc. of the 39th IEEE Conference on Decision and Control.*, pages 2977 – 2982, Sydney, AUS, Dec. 2000. [1.2](#)
- [20] P. Encarnaç o and A. Pascoal. Combined trajectory tracking and path following: an application to the coordinated control of autonomous marine craft. In *Proc. of the 40th IEEE Conference on Decision and Control.*, pages 964 – 969, Orlando, FL, USA, Dec. 2001. [1.3](#)
- [21] M. Fliess, J. L evine, P. Martin, and P. Rouchon. Flatness and defect of nonlinear systems: introductory theory and examples. *International. Journal of Control*, 61(6):1327 – 1361, 1995. [1.1](#), [1.4](#), [4.4](#), [4.4.2](#)
- [22] S. I. Grossman. *Elementary Linear Algebra*. Saunders College Publishing, Toronto, 5th edition, 1994. [4.4.2](#)
- [23] V. Guillemin and A. Pollack. *Differential Topology*. Prentice Hall, New Jersey, 1974. [2.1](#), [2.1](#)
- [24] J. Hauser and R. Hindman. Maneuver regulation from trajectory tracking: Feedback linearizable systems. In *Proc. of the IFAC symposium on Nonlinear Control Systems Design*, pages 595 – 600, Tahoe City, CA, USA, June 1995. [\(document\)](#), [1.3](#), [1.5](#)

- [25] J. Hauser and R. Hindman. Aggressive flight maneuvers. In *Proc. of the 36th IEEE Conference on Decision & Control*, pages 4186 – 4191, San Diego, CA, USA, December 1997. [1.1](#)
- [26] A. Isidori. *Nonlinear Control Systems*. Springer, New York, 3rd edition, 1995. [1.1](#), [1.4](#), [2.1.1](#), [2.4](#), [2.4.1](#), [3.1](#), [1](#), [3.1.3](#), [3.3](#), [4.1.2](#), [4.4.2](#), [4.4.4](#), [A](#)
- [27] A. Isidori and C. H. Moog. On the nonlinear equivalent of the notion of transmission zeros. In C.I. Byrnes and A. Kurzhanski, editors, *Modelling and Adaptive Control*, volume 105 of *Lect. Notes Contr. Inf. Sci.*, pages 146–158. Springer Verlag, 1988. [2.1.1](#), [4.4.2](#)
- [28] J.Pan K.D. Do, Z.P. Jiang and H. Nijmeijer. A global output-feedback controller for stabilization and tracking of underactuated odin: A spherical underwater vehicle. *Automatica*, 40(1):117–124, 2004. [4.3](#)
- [29] H. K. Khalil. *Nonlinear Systems*. Prentice Hall, Upper Saddle River, NJ, 3rd edition, 2002. [4.4.2](#), [A](#)
- [30] I. Kolmanovsky and N.H. McClamroch. Developments in nonholonomic control problems. *IEEE Control Systems Magazine*, 15(6):20–36, Dec. 1995. [1](#)
- [31] A. Kugi, K. Schlacher, and R. Novak. *Affine Input Systems Package for Maple*. Department of Automatic Control and Control Systems Technology at the Johannes Kepler University, Linz, Austria, 2nd edition, 2003. [4.4.4](#)
- [32] A. De Luca, G. Oriolo, and C.Samson. *Robot Motion and Planning and Control* (ed. J.P. Laumond). Springer, New York, 1st edition, 1998. [1.1](#)
- [33] K. Nam and A. Arapostathis. A sufficient condition for local controllability of nonlinear systems along closed orbits. *IEEE Transactions on Automatic Control*, 37(3):378–380, March 1992. [3.1.2](#)

- [34] W.L. Nelson and I.J. Cox. Local path control for an autonomous vehicle. In *Proc. IEEE International Conference on Robotics and Automation*, pages 1504 – 1510, Philadelphia, PA, USA, April 1988. [1.5](#)
- [35] H. Nijmeijer and G. Campion. Feedback linearization of parametrized nonlinear time-varying systems. In *Proceedings of the 2nd European Control Conference*, pages 31 –36, Groningen, NLD, June 1993. [3.4](#)
- [36] H. Nijmeijer and A. van der Schaft. *Nonlinear Dynamical Control Systems*. Springer - Verlag, New York, 1990. [2.1.1](#), [3.1.3](#), [A](#)
- [37] F. Plestan, J.W. Grizzle, E.R. Westervelt, and G. Abba. Stable walking of a 7-dof biped robot. *IEEE Transactions on Robotics and Automation*, 19(54):653–668, Aug. 2003. [1.5](#)
- [38] A. Pogromsky, G. Santoboni, and H. Nijmeijer. Partial synchronization: from symmetry towards stability. *Physica D*, 172(1-4):65–87, Nov. 2002. [4.4.4](#)
- [39] H.S. Ramírez and C.A. Ibáñez. On the control of the hovercraft system. *Dynamics and Control*, 10(2):151–163, 2000. [4.3](#), [4.3](#)
- [40] O.J. Sørдалen and C. Canudas de Wit. Exponential control law for a mobile robot: extension to path following. *IEEE Transactions on Robotics and Automation*, 9(6):837–842, 1993. [1.1](#), [1.5](#)
- [41] P. Ridley and P. Corke. Load haul dump vehicle kinematics and control. *Journal of Dynamics Systems, Measurement and Control*, 125(1):54–59, March 2003. [4.4](#)
- [42] M. Sampei, T. Tamura, T. Itoh, and M. Nakamichi. Path tracking control of trailer-like mobile robot. In *Proceedings of the International Workshop on Intelligent Robots and Systems*, pages 193 – 198, Osaka, JPN, Nov. 1991. [1.5](#), [4.4](#)

- [43] C. Samson. Control of chained systems application to path following and time-varying point-stabilization of mobile robots. *IEEE Transactions on Automatic Control*, 40(1):64–77, Jan. 1995. [1.2](#), [4.4](#)
- [44] R. Skjente, T.I. Fossen, and P.V. Kokotović. Robust output maneuvering for a class of nonlinear systems. *Automatica*, 40(3):373–383, March 2004. [1.3](#)
- [45] R. Su and L.R. Hunt. A canonical expansion for nonlinear systems. *IEEE Transactions on Automatic Control*, 31(7):670–673, 1986. [3.1](#), [3.1](#), [3.3](#)
- [46] C. Tomlinson and S.S. Sastry. Switching through singularities. *Systems and Control Letters*, 35(3):145–154, Oct. 1998. [4.4.4](#)
- [47] W.M. Wonham. *Linear Multivariable Control: A Geometric Approach*. Springer-Verlag, New York, 3rd edition, 1985. [3](#), [3.2](#), [3.2](#)